Title
Identification of yeast proteins necessary for cell surface function of a potassium channel

Author
Haass, Friederike Antigone

Publication Date
2007-10-15

Peer reviewed|Thesis/dissertation

Identification of yeast proteins necessary for cell surface function of a potassium channel

by

Friederike A. Haass

DISSERTATION

Submitted in partial satisfaction of the requirements for the degree of

DOCTOR OF PHILOSOPHY

in

Neuroscience

in the

GRADUATE DIVISION

of the

Acknowledgements

“Dear Friederike:
Hi, I'm very happy to hear that you are interested in our lab. You are most welcome to join our group. Those times next week are fine, except for Tuesday morning (development group meeting; Tuesday afternoon is good).
We can talk about projects that interest you--generally I think it's good for you to choose your own project and I'll just do my best to support what you do. With typical UCSF space it may be a bit crowded, but then everyone gets to have their own station even though sometimes they need to start with temporary space.
See you soon,
Lily”

What better welcome could one expect as a first year student trying to decide on a lab to join? And what better PhD advisor could one imagine than one who, for the past five years, has provided unwavering support for all the projects I chose to explore? Indeed, it was initially crowded when I started out in U240 on a low bench, which was only slightly enlarged by covering a sink with a piece of plywood. However, I soon moved to my own bench in U212 and started exploring. Lily’s door was always open to me and she always took time to talk about new ideas, exciting results, or failed experiments. Her kind smile and sharp mind have taught me to structure my own thinking better and to not lose sight of the big picture and where things are going. I frequently walked into Lily’s office confused about an article I had read, an experimental result, a seminar, etc. Lily would carefully listen to my arguments and, in a manner that is still somewhat mysterious to me to this day, guide my thoughts in a way that clarified the confusion. Although I know her guidance led me to the new insights, it would still feel like they came from my own thoughts. In this manner, discussions with Lily provided me with continuing motivation to explore new ideas, try the next set of

experiments, or approach a new project. I thank Lily for all her patience and her dedication to my training as a scientist.

Of course life as a graduate student involves not only the PhD advisor and student. The Jan lab has provided an amazing training environment due to all its highly motivated, successful, and friendly members. I would like to especially thank Delphine, who has taught me the basics of lab life and continues to be a mentor to me. Helen and Toral became close friends of mine and provide guidance from their perspectives as fellow graduate students, and now post-doc and resident, respectively, after they moved on from the lab. I would also like to thank the other graduate students who overlapped with me in the Jan lab, Cindy, Alex, Patrick, Michelle, Ye, David, and Wendy, for the energy they brought to the lab and the many fun times we had together. The Jan lab would stop working without the support of Sandra, Sunny, Lani, Cecilia, Monika, and Jacqueline. I especially thank Lani for patiently waiting for the many bottles of media she autoclaved for me. I would also like to thank Monika Jain for her hard work on the RNAi project and yeast follow-up studies.

The UCSF Neuroscience program has provided a supportive training environment for me. The course work, seminars, exams, etc. challenged me to the right extent to foster learning, a balance that is not easy to achieve. Pat, Deborah, and Carrie provide outstanding administrative support and ensure that everything runs smoothly. I thank my oral exam and thesis committee members Mark von Zastrow, Ulrike Heberlein, Herwig Baier, Louis Ptacek, Peter Walter, Eitan Reuveny and Jonathan Weissman for their feedback and suggestions.

Special thanks go to Maya. She taught me a new approach to experiments and science, and without her mentorship and friendship, many of the most rewarding moments during my dissertation work would not have happened.

A big hug for Alo, without whom there would be no formatting, commas or references in this thesis. Alo's sense of humor and the way she brings perspective to life has shaped my view of the world, provided me with many great experiences, and helped me through many crises.

I thank my parents, Anton and Liselotte, and my sister, Annette, for the emotional warmth they have provided me with over the years and for reminding me that there is life outside the lab.

Chapter 2 of this dissertation/thesis is a reprint of the material as it appears in a preprint for the Proceedings of the National Academy of Sciences. PNAS authors retain the right to include articles in a thesis or dissertation (PNAS, August 24, 2004; Vol. 101, No. 34, p. 12399). The co-authors listed in the PNAS paper contributed to the work as follows. Lily Y. Jan directed and supervised the research that forms the basis for the dissertation/thesis. Maya Schuldiner contributed to the experimental design, data analysis and writing of the paper. She also designed, performed, and analyzed the experiments for the E-MAP of early secretory pathway genes (Figure 2-5 A). Martin Jonikas and Peter Walter designed, conducted and analyzed the experiments on UPR induction (Figure 2-5 B). Jonathan Weissman and Yuh Nung Jan contributed new reagents and analytic tools. All of the experiments besides the E-MAP and UPR data have been designed and carried out by Friederike Haass; this work is comparable to work for a standard thesis awarded by the University of California San Francisco.

Lily Jan

Abstract

Electrical signals generated by the flow of ions across cellular membranes serve many physiological purposes. For example, neurons convey information in the form of action potentials, skeletal muscle contracts upon receiving electrical inputs, and hormones are released in response to depolarization. The currents that underlie these signals flow through ion channels. Appropriate abundance, localization, and activity of ion channels are crucial to ensure coordinated signaling and normal cellular function. Structure-function studies have revealed many sequence motifs in ion channels that are important for their biosynthesis, trafficking, and function. Less is known about the cellular machinery that interacts with ion channels during their biosynthesis and trafficking, and that regulates channel function at the plasma membrane. For my thesis project, I designed and implemented a screen to identify basic cellular machinery necessary for the functional expression of an inwardly rectifying K^+ (Kir) channel.

The screen took advantage of previous knowledge gained from structure-function studies, and of the powerful genetic tools available in the yeast *Saccharomyces cerevisiae*. By assaying 374 yeast strains, each lacking one gene, for functional expression of the Kir channel, we identified seven yeast deletion strains (*sur4*Δ, *csg2*Δ, *erv14*Δ, *emp24*Δ, *erv25*Δ, *bst1*Δ, and *yil039w*/*ted1*Δ) in which functional expression of the Kir channel was disrupted. The seven strains lack proteins with conserved cellular functions in quality control in, and vesicle budding from the endoplasmic reticulum (ER), and in lipid biosynthesis.

The identification of these seven proteins as players in Kir channel biosynthesis, trafficking, and/or function, opens new avenues of research. Future studies will address the role of the mammalian homologs of the seven yeast genes in Kir channel ontogenesis. In addition to pointing toward specific genes, the results of our screen highlight the importance of protein-lipid interactions in trafficking and function of Kir channels. Last but not least, we propose that the previously uncharacterized protein Yil039wp, which we named Ted1p (**T**rafficking of **E**mp24p/Erv25p dependent cargo **D**isrupted), regulates the function of p24 proteins, possibly through dephosphorylation of a yet unknown target.

Table of contents

List of Tables

CHAPTER 1

CHAPTER 2

APPENDIX

List of Figures

CHAPTER 1

CHAPTER 2

APPENDIX

Chapter 1: Introduction

1 Kir channel ontogenesis

1.1 Kir channels

Inwardly rectifying potassium (Kir) channels form pores that allow regulated flow of potassium (K^+) ions across cellular membranes. The pores are formed by the assembly of four Kir channel subunits, each with two transmembrane segments, into tetrameric channels (Figure 1-1). Kir channels are named for their characteristic current-voltage relationship: in extracellular solutions with high K^+ content, it results in prominent inward currents at potentials below the equilibrium potential for K^+, but only small outward currents at more depolarized potentials. Outward currents are blocked by the entry of Mg^{2+} ions and polyamines into the cytoplasmic pore of the channels (Lopatin et al., 1994).

There are seven subfamilies of Kir channels, Kir1.x through Kir7.x (Figure 1-2). The rectification and gating properties of the different subfamilies differ substantially (Hille, 2001, p. 152-153). For example, Kir2.x channels are strongly rectifying and constitutively active. Kir3.x channels are also strongly rectifying, but require G-protein signaling (specifically binding of $G\beta\gamma$ to the channel) for activation. Kir6.x channels show mild inward rectification and their gating is regulated by the intracellular ATP/ADP ratio.

The electrophysiological properties of Kir channels make them important players in regulating the cellular membrane potential (Hille, 2001, p. 151-154). Small depolarizations from the K^+ equilibrium potential (E_K) lead to K^+ efflux through Kir channels, which hyperpolarizes the cell back towards E_K. During

large depolarizations above E_K, Kir channels are blocked, thus preserving K^+ during the firing of action potentials. In most animal cell types, Kir channels do not conduct inward currents, because the resting membrane potential usually does not fall below E_K. Glial cells are an important exception to this rule, in that they regulate the extracellular K^+ concentration in the brain by taking up K^+ via Kir channels (Butt and Kalsi, 2006).

In addition to their general role in stabilizing the resting membrane potential, the specific properties of each Kir channel subfamily allow them to fulfill specialized physiological functions (Table 1-1). For example: Kir1.x family members regulate K^+ homeostasis in the kidney (Giebisch, 1998). Inhibition of K_{ATP} channels, which are octamers composed of four Kir6.2 subunits and four sulfonylurea receptor 1 (SUR1) subunits, depolarizes pancreatic β-cells, thereby causing insulin release (Ashcroft, 2000). In midbrain dopaminergic neurons, Kir3.2 channels mediate inhibitory postsynaptic potentials, and activation of Kir3.1/Kir3.4 heterotetramers slows the heart rate upon vagal stimulation (Mark and Herlitze, 2000).

Human diseases that arise due to lack or misregulation of Kir channel function also attest to the physiological importance of Kir channels (Abraham et al., 1999; Neusch et al., 2003). Mutations in Kir1.1 channels underlie some cases of Bartter's syndrome, which is characterized by increased loss of K^+ and other ions from the body as well as dehydration (Kleta and Bockenhauer, 2006). Mutations in both subunits of the pancreatic K_{ATP} channel, Kir6.2 and SUR1, have been identified in patients with persistent hyperinsulinemic hypoglycemia of

infancy (PHHI) (Aguilar-Bryan and Bryan, 1999). In PHHI patients, insulin secretion from pancreatic β-cells continues even during hypoglycemia, because the hyperpolarizing activity of K_{ATP} channels in β-cells is lacking. Based on altered channel properties of Kir6.2 carrying the amino acid change E23K, it has been proposed that this common polymorphism predisposes to type 2 diabetes (Schwanstecher et al., 2002; Koster et al., 2005). Andersen's syndrome, which is characterized by periodic paralysis of skeletal muscle, cardiac arrhythmias, and dysmorphic features, arises from mutations in Kir2.1 (Plaster et al., 2001). A spontaneous mutation in mice in the K^+ channel signature sequence of Kir3.2 underlies the *weaver* phenotype, which is characterized by ataxia, tremor, and male sterility (Patil et al., 1995).

In light of the human diseases caused by Kir channel malfunction, and also from a basic science point of view, it is important to understand the ontogenesis of Kir channels. Kir channel ontogenesis begins with transcription and its regulation via signaling cascades that induce or repress transcription of channel genes. Transcription is followed by Kir channel biosynthesis, which includes translation of the messenger ribonucleic acid (mRNA) by ribosomes, translocation of the nascent channel protein into the membrane of the endoplasmic reticulum (ER), folding of the channel protein to attain its secondary and tertiary structures, and assembly of channel subunits into a tetrameric (or octameric) channel. Exit of the quality-controlled channel from the ER is the first step in Kir channel trafficking. Since the most well understood functions of Kir channels are at the plasma membrane, trafficking is understood as the journey

the channel takes to and from the plasma membrane, through the secretory and endocytic pathways, respectively. During their lifetime at the plasma membrane, many players influence channel function, including the lipid environment, activating or inhibiting protein-protein interactions, small molecules, and phosphorylation.

As the following review highlights, a growing body of literature provides insights into “how Kir channels are made.” However, the review will also point out many areas where our understanding is still rudimentary. For my thesis project, I focused on one of these less well-understood areas, namely the identification of cellular proteins and machinery that are necessary for functional expression of a Kir channel at the plasma membrane.

1.2 Kir channel transcription

With the sequencing of several mammalian genomes completed, the genomic localization and organization of Kir channel genes can be accessed in databases. Some Kir channel genes have been studied in more detail to confirm intron-exon boundaries, determine transcription start sites, and analyze the promoter regions. For example, human Kir3.1 is encoded by three exons, has two transcription start sites (nt C -196 and G -198), and does not possess a traditional transcription initiation site (no TATA or CAAT box), but a 5’ region of high GC content (Schoots et al., 1997). A similar analysis of the promoters of Kir6.2 and SUR1 showed that the Kir6.2 gene also lacks TATA and CCAAT boxes, but is preceded by a 5’ GC-rich region, features that were originally

thought to be associated with “housekeeping” genes, but have since been found for other genes as well (Ashfield and Ashcroft, 1998).

Kir channels show characteristic expression patterns in different tissues of the body. However, little is known about the transcription factors that activate Kir channel expression in certain tissues, but not others. The promoter of Kir3.1, which contains predicted transcription factor binding sites for AP-2, Sp1, Krox24, and glucocorticoid receptor, drives expression of luciferase in a pituitary cell line that expresses Kir3.1, but not in CHO cells, which do not express Kir3.1 (Schoots et al., 1997). The Kir6.2 and SUR1 promoter regions contain binding sites for several transcription factors thought to drive expression in pancreatic β-cells, and sequences from the Kir6.2 and SUR1 promoter regions drove expression of luciferase in a somewhat tissue specific manner (Ashfield and Ashcroft, 1998).

Several Kir channels are alternatively spliced. For example Kir1.1 has five alternative transcripts (Shuck et al., 1994) and Kir3.2 has six (Wei et al., 1998). Although little is known about the expression patterns of the different isoforms and their role in channel function, it will be important to take potential differences into account to understand the physiological functions of Kir channels. For example, the different Kir3.2 isoforms contain or lack amino acids motifs that have been shown to regulate channel trafficking (Mirshahi and Logothetis, 2002). Differences in the untranslated regions of the isoforms may also affect mRNA stability and targeting. The burgeoning field of mRNA regulation by RNA-binding proteins (Nicchitta, 2002; Hieronymus and Silver, 2004; Keene and Lager, 2005) may hold answers to many long-standing questions regarding Kir channels, such

as channel targeting to dendrites or axons of neurons, and even channel assembly, as discussed below.

Yet another intriguing, but little understood question concerns the coordinated expression of Kir channel subunits that form heteromers. Presumably, equal amounts of each subunit are transcribed to allow 1:1 assembly of the channel subunits into heteromeric tetramers or octamers. In this regard, it is interesting to note that the genes for Kir6.1 and SUR2 are located in tandem; so are the genes for Kir6.2 and SUR1 and those for Kir2.1 and Kir5.1 (AceView, http://www.ncbi.nlm.nih.gov/IEB/Research/Acembly/index.html). In the case of the K_{ATP} channel subunits, one may speculate that the tandem arrangement is part of the mechanism that coordinates subunit expression. Kir2.1 and Kir5.1 are expressed together in some tissues, but not in others (Derst et al., 2001). Evidence with regard to heteromerization of Kir2.1 and Kir5.1 is conflicting, with one study reporting suppression of Kir2.1 currents by Kir5.1 (Derst et al., 2001) and a different study reporting lack of assembly between Kir2.1 and Kir5.1 (Konstas et al., 2003). The close proximity of the Kir2.1 and Kir5.1 genes may suggest a recent gene duplication event rather than common transcriptional regulation. The tandem arrangement of Kir2.1 and Kir5.1 is conserved in human, chimpanzee, dog, mouse, rat, and chicken (HomoloGene, http://www.ncbi.nlm.nih.gov/sites/entrez?db=homologene).

Apart from determining tissue localization of Kir channels, transcriptional regulation may also influence Kir channel expression levels in response to environmental stimuli and cellular signaling events. For example, Pei and

colleagues (Pei et al., 1999) observed that Kir3.1 and Kir3.2 mRNA and protein levels in the dentate gyrus were altered following electroconvulsive shock in rats. Jiang et al. (Jiang et al., 2004) found that Kir6.1, Kir6.2, SUR1, and SUR2B mRNA levels and Kir6.2 and SUR1 proteins levels changed in rat brains after picrotoxin-induced kindling. K_{ATP} channel mRNA levels in the pancreas were regulated by extracellular glucose levels (Moritz et al., 2001), but not by application of K_{ATP} channel blockers (Ball et al., 2004). Although these studies show that Kir channel expression is regulated at the transcriptional level, we do not know the physiological significance, especially in relation to modulation of channel expression levels at the translational and post-translational level. Imaging of cultured cells overexpressing Kir channels indicated that large proportions of Kir channels are located in the ER, not at the cell surface (Ma et al., 2002; Yoo et al., 2003; Hofherr et al., 2005). Cell surface biotinylation experiments with cultured hippocampal neurons showed that ~80% of total Kir3.2 and ~90% of total Kir3.1 channel protein was localized intracellularly (Hee Jung Chung, Xiang Qian, Ofer Wiser, Melissa Ehlers, Yuh Nung Jan, and Lily Jan, submitted paper: Neuronal activity regulates surface density of G-protein activated inwardly rectifying potassium channels via a phosphorylation-dependent endocytic pathway). If the predominant ER localization of Kir channels is confirmed in other native cell types (if possible *in vivo*) changes in mRNA levels may be considered less important to the regulation of Kir channel expression levels, which would be buffered by the high levels of already existing protein.

1.3 Kir channel biosynthesis: translation, translocation, folding, and assembly

Translation, translocation, and topogenesis

Following transcription, splicing, and nuclear export, mRNAs are translated into proteins at the ribosome. Kir channels contain an internal signal sequence, which is recognized by the signal recognition particle, which in turn targets the ribosome-nascent chain complex to the translocon in the ER membrane. The exact location of the first signal sequence, which pauses translation until the ribosome-nascent chain complex interacts with the translocon, in Kir channels is not known. Consequently, we have no information about how long the Kir channel nascent chain is before it is targeted to the ER, or what the conformation of this nascent Kir channel would be. Studies addressing these questions in voltage gated K^+ channels (Kosolapov et al., 2004; Lu and Deutsch, 2005a, 2005b; Robinson and Deutsch, 2005) may serve as a guide for future research on Kir channels.

As transmembrane segments in the nascent chain exit the ribosome and are threaded through the translocon, they have to obtain their correct orientation in the membrane. Umigai et al. (Umigai et al., 2003) studied the topogensis of Kir2.1 by synthesizing peptide fragments corresponding to the transmembrane segments (M1 and M2) *in vitro* and assaying the orientation of the peptides in microsomal membranes using glycosylation and protease sensitivity. Both M1 and M2 of Kir2.1 integrated into ER membranes, albeit with relatively low efficiency. Surprisingly, M1 preferentially integrated with its N-terminus facing the ER lumen, which is opposite to its orientation in the full-length channel. *In vitro*

translation of the entire N-terminus plus M1 resulted in a higher proportion of correctly inserted protein (C-terminus in ER lumen), suggesting that the N-terminus contributes to establishing the correct topology of M1. To explain how M1 achieves its correct membrane insertion given its relatively weak signal anchor function, the authors showed that M1 possessed a strong translocation initiation function and inserted correctly into the membrane if the sequence located N-terminally to it was anchored in the membrane. The authors also found that the N-terminus of Kir2.1 is N-acetylated when attached to a fusion protein, raising the intriguing question of whether N-acetylation anchors the N-terminus of Kir2.1 in the cytoplasmic face of the membrane, thereby establishing the correct orientation of M1. The M2 fragment inserted correctly (N-terminus in ER lumen) into the membrane. It contained a strong stop-transfer function, suggesting that once the N-terminus and M1 have obtained their correct topology, M2 will insert in its correct orientation as well.

Correctly oriented transmembrane segments integrate laterally into the lipid bilayer of the ER. Whereas some transmembrane segments integrate individually into the lipid bilayer immediately following their translocation, others remain in contact with the translocon for extended periods of time and assemble with other transmembrane segments before integrating into the ER membrane as a biogenic unit (Alder and Johnson, 2004). The integration of transmembrane segments as biogenic units has been observed for voltage gated K^+ channels (Tu et al., 2000; Sato et al., 2002). The biogenic unit model is appealing for K^+ channels, because their transmembrane helices contain lipid-, protein-, and pore-

lining faces (Choe et al., 1995; Minor et al., 1999). Prolonged interactions with the translocon could stabilize the transmembrane segments until they have made proper protein-protein contacts. However, this model does not resolve the question of how the pore-lining, hydrophilic face of K^+ channel monomers is stabilized. One speculative idea is that monomers are stabilized by the translocon until tetramers assemble. To take the speculation a step further, assembly of tetrameric channels inside the same translocon could follow translation of a single mRNA by multiple ribosomes (polysomes). To account for the occurrence of heteromeric channels, it has been postulated that translation of mRNAs for different subunits is coordinated by binding of these mRNAs to common sets of RNA-binding proteins (Deutsch, 2003). Although appealing as a model, the role of “posttranscriptional operons” in coordinating gene expression as proposed by Keene and colleagues (Keene and Tenenbaum, 2002) (Keene and Lager, 2005) is not well understood in general, and any extension of the hypothesis to K^+ channels has, at the present time, no experimental basis. As our understanding of RNA-binding proteins and their role in localizing mRNAs and coordinating their translation increases, a putative bundling of mRNAs that encode proteins that form a complex should be kept in mind. At the same time, an alternative model, in which channel subunit monomers are stabilized by interactions with transmembrane chaperones until they encounter other subunits or partially assembled channels, deserves further attention.

Folding of the pore loop

As the transmembrane segments of Kir channels fold and integrate into the membrane, possibly in connection with the first steps of tetramer assembly, a folding problem particular to K^+ channels is posed by the pore loop (also referred to as P-loop). In native, tetrameric channels, the P-loops are thought to partially dip into the membrane where they form a narrow part of the ion permeation pathway and the selectivity filter. This arrangement is seen in X-ray crystal structures of several K^+ channels (Figure 1-3 A) (Bichet et al., 2003). It is unclear how the four loops that are tucked into the center of the tetrameric channel arrive at their final conformation. Although the P-loop is hydrophobic (Figure 1-3 B), it does not integrate into the membrane on its own (Umigai et al., 2003).

Artificial glycosylation sites in the P-loops of Kir1.1 (Y144N F146S) or Kir2.1 (Q140N, I143N Y145T, F147N C149T) can be modified with sugar moieties (Schwalbe et al., 1997; Schwalbe et al., 2002; Umigai et al., 2003), suggesting that the P-loop is accessible to ER luminal glycosylation enzymes. Although Schwalbe et al. (Schwalbe et al., 1997; Schwalbe et al., 2002) proposed a revised model of Kir topology that places the P-loop of functional, tetrameric Kir channels extracellularly, it seems more likely that the glycosylation tagging method samples a transient folding state during which the P-loop is exposed to the ER lumen. Umigai et al. (Umigai et al., 2003) observed that an artificial glycosylation site at the C-terminal end of the pore helix (Q140N) abolished Kir2.1 function. If the P-loop is exposed to the ER lumen after its synthesis, when does it attain its conformation in the membrane? One model passed on as part of

the oral history of the Jan lab, and attributed to Tom Schwarz, is that the four P-loops tuck into the membrane only after assembly of the tetrameric channel, which would allow stabilization of the P-loops by neighboring subunits.

Two features that contribute to the stabilization of the P loop have been identified: First, a salt bridge between glutamate 138 (E138) and arginine 148 (R148) of Kir2.1 (Yang et al., 1997), and second, a disulfide bond between C122 and C154 of Kir2.1 (Cho et al., 2000). The residues forming the salt bridge and disulfide bond are conserved in all Kir channels (except for Kir7.1, which lacks the arginine of the salt bridge). Although mutations that disrupt the salt bridge or disulfide bond clearly abolish channel function, further experiments are needed to establish at what stage of Kir channel folding the salt bridge and disulfide bond form, and what their contributions are to stabilizing the immature channel while it folds versus the mature channel as it functions at the plasma membrane. Although a negative result, the observation that application of reducing agents while recording from *Xenopus* oocytes expressing Kir2.1 did not alter whole cell current properties may indicate that the disulfide bond is necessary for channel folding, but not for function of the mature channel (Cho et al., 2000).

Glycosylation

N-linked glycosylation, which is the attachment of sugar moieties to ER luminal/extracellular asparagine residues, promotes folding of the modified proteins by directly stabilizing their structures and by facilitating interactions with chaperones, such as calnexin and calreticulin (Helenius and Aebi, 2004). Two Kir

channels, Kir1.1 and Kir3.1, contain extracellular glycosylation consensus sequences (NXS/T), and have been shown to be glycosylated *in vivo* (Ho et al., 1993; Krapivinsky et al., 1995). SUR1 (sulfonylurea receptor 1), the non-Kir channel component of K_{ATP} channels, is also glycosylated (Clement et al., 1997).

The role of glycosylation in Kir channel biosynthesis or function is not clear. Schwalbe et al. (Schwalbe et al., 1995) reported that removal of glycosylation from Kir1.1 by mutating the glycosylation consensus sequence or by application of tunicamycin, which inhibits glycosylation, reduced whole cell currents in Sf9 cells. Surprisingly, the authors observed differences in the single channel properties of channels with and without glycosylation, but based on the frequency of successful patches and the number of channels per patch, did not detect differences in the level of cell surface expression. Pabon et al. (Pabon et al., 2000) studied the role of glycosylation of Kir3.1 channels. The authors found that non-glycosylated Kir3.1N119Q still assembled into heteromers with Kir3.4, and that current levels in oocytes co-expressing Kir3.4 and Kir3.1 with or without glycosylation showed comparable current levels and single channel properties. Given that these studies conflict with each other and contradict the general view of the role of glycosylation in protein folding, future studies may revisit the question of whether Kir1.1 and Kir3.1 glycosylation affects channel biosynthesis and surface expression by employing more direct measures such as immunostaining and cell surface biotinylation, and possibly by looking at channel turnover, which may be altered if folding is delayed. However, given that Kir1.1

and Kir3.1 are the only glycosylated Kir channels, it may be that other features in the channels are sufficient to promote folding.

The glycosylation state of SUR1 has been shown to affect cell surface expression of K_{ATP} channels (Conti et al., 2002). Using electrophysiology, surface biotinylation, and immunostaining, the authors demonstrated that SUR1 carrying mutations in one or both of its glycosylation sites did not reach the cell surface efficiently, but was retained in the ER. Interestingly, the authors also observed that assembly of SUR1 with Kir6.2 decreases the complexity of the sugar moieties added to SUR1. Two hypotheses to explain this observation were put forth: (i) access to the sugar modifications may be blocked after assembly of the octameric channel, thereby preventing remodeling in the Golgi, or (ii) the octoameric channel may have a shorter residence time in the Golgi, and therefore not accumulate extensive sugar modifications.

Kir channel assembly

Mature, functional Kir channels are tetramers (Raab-Graham and Vandenberg, 1998) or octamers in the case of K_{ATP} channels (Clement et al., 1997). Many studies have been conducted to identify Kir channel regions involved in tetramer formation (Tinker, 2002; Neagoe and Schwappach, 2005). In thinking about Kir channel assembly, three types of domains have to be taken into account. First, assembly domains (also called recognition domains) are the initial points of contact between subunits that are necessary for the formation of tetrameric channels. Second, interaction domains (also called stabilization

domains) are the points of contact that exist between subunits in the fully assembled channel. Interaction domains may or may not overlap with assembly domains. Although it may appear straightforward to identify interaction domains based on X-ray crystal structures, it is important to note that the location of interaction domains may change with channel gating. Third, heteromerization domains are regions of the channel that determine compatibility of different subfamily members for assembly into tetramers.

Although clear-cut in principle, it is often not easy to make these distinctions experimentally, especially since a commonly used technique for the identification of assembly domains involves construction of chimeric proteins pieced together from parts of incompatible Kir subfamily members. In addition, the distinctions may not be as clear for Kir channels as they are for voltage gated K^+ (K_V) channels (Deutsch, 2003). The N-terminal T1 domain of K_V channels guides the initial assembly of tetrameric complexes, an event that occurs even before translation of the entire subunit is complete (Lu et al., 2001a). In addition to their role as assembly domains, T1 domains also determine subunit compatibility. The transmembrane domains of K_V channels are interaction domains that stabilize the tetrameric channel, but are inefficient and promiscuous in tetramer assembly (Deutsch, 2003).

Based on suppression of Kir2.3 currents by Kir2.3-Kir3.2 chimeric channels, Fink et al. (Fink et al., 1996) proposed that the N-terminus is important in mediating channel assembly. Tucker et al. (Tucker et al., 1996) found that Kir3.4 suppressed currents carried by Kir4.1 and that this inhibitory interaction was

mediated by the transmembrane domains. Experiments involving coimmunoprecipitation and suppression of currents by truncated or chimeric channels led Tinker et al. (Tinker et al., 1996) to the conclusion that the proximal C-terminus and the transmembrane segment M2 of Kir2.1 and Kir2.3 channels mediate homomultimerization and determine subunit compatibility. Woodward et al. (Woodward et al., 1997) employed truncated constructs in coimmunoprecipitation, current suppression, and cell surface localization experiments, and concluded that the C-terminal domains of Kir3 channels interact. Using similar techniques, Koster et al. (Koster et al., 1998) proposed that multiple interaction sites between Kir1.1 subunits exist in the transmembrane and cytoplasmic regions. Schwappach et al. (Schwappach et al., 2000) developed assays based on K_{ATP} channel forward trafficking (trafficking enhancement assay) and ER retention (trafficking trap assay) to assay Kir channel assembly. They confirmed the result of Tinker et al. (Tinker et al., 1996) implicating the proximal C-terminus and M2 in Kir2.1 and Kir6.2 homotetramer formation. With regard to KATP assembly, the authors conclude that M1 and the N-terminus of Kir6.2 interact with SUR1. Konstas et al. (Konstas et al., 2003) tested the ability of Kir1.1-Kir4.1 chimeras to assemble with Kir5.1 in a trafficking trap assay and concluded that the proximal C-terminus of Kir4.1 was sufficient to mediate assembly of Kir4.1 and Kir5.1.

The incoherent picture that arises from these studies may partially be due to the fact that different techniques assay different kinds of interactions, and that it is sometimes not clear what kind of interaction is being assayed. For example,

coimmunoprecipitation will yield positive results for any type of interaction that has high enough affinity in cell lysates to remain in place during the wash process. Coimmunoprecipitation does not address whether or not an interaction can occur in the native channel protein. Experiments testing whether or not a truncated or chimeric construct suppresses currents conducted by a full-length channel are ambiguous unless the method of Tinker et al. (Tinker et al., 1996), which introduces a mutation into the channel pore of the deletion or chimeric protein, is used. Expression of a deletion or chimeric protein with a full-length channel can have three outcomes: First, the two constructs assemble and form a functional channel. Second, the two constructs assemble and form a non-functional channel. Third, the two constructs do not interact and the full-length channel forms a homotetrameric channel. The ambiguity arises because both the first and third outcome yield measurable currents, even though they reflect assembly versus no assembly. Mutating the pore region of the deletion or chimeric channel construct ensures that assembly will lead to no current, be it due to the pore mutation or due to incompatibility within the heteromeric channel.

However, even with these caveats in mind, it seems likely that a conserved and strong assembly and/or heteromerization domain such as the T1 domain of K_V channels would have been detected in the course of the many studies that have been conducted over the years. Although the proximal C-terminus and possibly M2 are tentative consensus candidates for an assembly domain, we may have to revisit how we think about Kir channel assembly and develop new experimental techniques that incorporate the temporal aspect of channel

assembly to delineate which contacts form early on during channel assembly (i.e. assembly domains), which contacts are present in the mature channel (i.e. interaction domains), and when incompatibility of two subunits for heteromerization is detected (heteromerization domains). In this regard, cross-linking studies have had some success in "freezing" K_V channels in different states of assembly (Deutsch, 2003).

1.4 Kir channel trafficking

The best understood functions of Kir channels occur at the plasma membrane. Although the idea that Kir channels may play intracellular functions surfaces again and again in discussions, there is little data available to demonstrate activity of Kir channels in intracellular membranes (probably due to technical limitations), or implicate K^+ currents conducted by intracellular Kir channels in a physiological response of a cell. It has also been proposed that Kir channel activity in intracellular membranes would be toxic, and that intracellular Kir channels are kept in a closed confirmation due to the low PIP_2 concentration of intracellular membranes (Hilgemann et al., 2001). Kir channel trafficking is therefore understood as the process by which the channels reach the plasma membrane and are removed from it. The former occurs through the secretory pathway, the latter through the endocytic pathway.

To our current knowledge, Kir channel folding and assembly have to be completed before the channels can leave the ER and begin their journey to the plasma membrane. However, it is less well understood how recognition of fully

assembled channels is accomplished. General models of ER quality control mechanisms propose retention of proteins with (i) exposed hydrophobic features, (ii) free cysteine residues, that form disulfide bonds with ER chaperones, (iii) a tendency to aggregate, or (iv) trimmed N-linked oligosaccharides (Ellgaard et al., 1999). In addition, secondary quality control mechanisms that are specific for certain proteins or protein families help with their assembly, escort them to ER exit sites, or guide them through the secretory pathway (Ellgaard and Helenius, 2003). The search for amino acid motifs in Kir channels that interact with secondary ER quality control mechanisms has been quite fruitful. However, our understanding of the machinery that recognizes these motifs is still in its infancy.

Kir6.2 and SUR1, which form the pancreatic K_{ATP} channel, contain an ER retention/retrieval signal composed of the amino acids arginine-lysine-arginine (RKR) (Zerangue et al., 2001). It has been proposed that the RKR sequence is exposed in monomeric subunits and partially assembled K_{ATP} channels, thereby keeping the channels in the ER. In fully assembled channels, the RKR sequences would be hidden from the ER retention/retrieval machinery, thereby allowing the channels to traffic to the cell surface. The finding that COPI components interacted with the RKR motif suggested that RKR is an ER retrieval signal (Yuan et al., 2003). However, it is possible that an additional, unidentified ER retention mechanism prevents partially assembled K_{ATP} complexes from leaving the ER in the first place (Michelsen et al., 2005). Additional complexity is added by the finding that 14-3-3 protein interacted with the RKR motifs and promoted cell surface expression, possibly by masking the partially exposed

RKR motif of SUR1 (Yuan et al., 2003), (Heusser et al., 2006). Also, binding of 14-3-3 protein to an artificial C-terminal motif (SWTY) was able to override ER retention due an internal RKR motif (Coblitz et al., 2005; Shikano et al., 2005). Although an overall picture in which 14-3-3 protein binding to Kir channels promotes cell surface expression is beginning to emerge, the details of these interactions, such as their phosphorylation dependence, and the subcellular compartment where these interactions take place (ER, COPII or COPI vesicles, cis-Golgi) remain to be delineated.

The role of phosphorylation in trafficking has been studied with regard to Kir1.1. A serine residue (S44) in the N-terminus was phosphorylated by serum-glucocorticoid-regulated kinase (SGK), thereby promoting cell surface expression of Kir1.1 (Yoo et al., 2003). The mechanism for phosphorylation-dependent surface expression has been proposed to involve masking of a C-terminal RXR ER retention signal (O'Connell et al., 2005; Yoo et al., 2005). However, it is not known from what the ER retention signal is masked, or whether close proximity of the phospho-serine and RXR motif in the assembled channel provides a binding site for 14-3-3 protein, which in turn would favor ER export and forward trafficking.

Kir2.1, which forms functional homotetrameric channels at the cell surface, contains an ER export signal with the sequence FCYENE (Ma et al., 2001) (Stockklausner et al., 2001). Mutations in the FCYENE motif changed the localization of Kir2.1 from predominantly at the cell surface to the ER. Transfer of the sequence FCYENE to some ER localized proteins enhanced their surface

expression, however, FCYENE was unable to override ER retention/retrieval due to an RKR sequence (Ma et al., 2001). The protein(s) that interact with FCYENE to promote ER export is/are not known. The existence of an ER export signal raises the question of how the machinery that promotes ER export upon recognizing FCYENE interacts with quality control mechanisms that ensure proper folding and assembly before the channel leaves the ER.

The G-protein activated inwardly rectifying K^+ (GIRK) channel Kir3.1 does not form functional channels when expressed alone, however, assembly with Kir3.2 allows the heteromeric channels to traffic to the cell surface where they conduct large currents (Kennedy et al., 1996; Stevens et al., 1997). Ma et al. (Ma et al., 2002) dissected the trafficking signals in Kir3 channels and found that Kir3.2 and Kir3.4 can leave the ER as homotetrameric channels and can promote ER exit of Kir3.1 in heterotetrameric channels because they contain ER export signals (DQDVESPV and ELETEEEE in Kir3.2A and NQDMEIGV in Kir3.4). Mirshahi and Logothetis (Mirshahi and Logothetis, 2004) employed chimeras of Kir3.1 and Kir3.4 to identify regions in Kir3.1 that are responsible for its retention in the ER. The authors propose that the N-terminus may contain an ER retention signal, which is overridden by assembly of Kir3.1 with Kir3.2 or 3.4 through an interaction at the proximal C-terminus.

Golgi export has also been found to be selective and regulated by recognition of certain sequence motifs. Deletion of the N-terminus (amino acid 1-76) of Kir2.1 led to accumulation of the truncated channel in the Golgi (Stockklausner and Klocker, 2003). The sequence responsible for efficient Golgi

export was narrowed down to several positively charged residues within the N-terminus. However, it is not clear how these sequence motifs, which resemble XXRR, RXRR, or KKXX ER retrieval signals, affect Golgi export (Stockklausner and Klocker, 2003). Golgi export of Kir2 channels is further influenced by the motif YIPL, which resembles the adaptin binding consensus sequence YXXΦ (X = any amino acid, Φ = bulky, hydrophobic residue) (Hofherr et al., 2005). Differential Golgi export of Kir2.1 and Kir2.4 was suggested to be regulated by sequences surrounding the YIPL motif (Hofherr et al., 2005).

Kir channel abundance at the cell surface is not only regulated by the number of new channels delivered to the plasma membrane, but also by endocytosis followed by recycling or degradation. Acidic clusters in Kir3.2A (ELETEEEE), Kir3.4 (EAEKEAEAEHDEEEEPNG), and Kir2.1 (EEEEDSE) promoted cell surface expression of the channels (Ma et al., 2002). The acidic clusters interacted with the ADP-ribosylation factor 6 (Arf6)-specific guanosine exchange factor (GEF) EFA6 and Kir channels or reporter proteins harboring acidic clusters were internalized via a non-clathrin-dependent pathway and recycled to the plasma membrane via an Arf6-dependent pathway (Gong et al., 2007). Internalization via a clathrin-dependent pathway was observed for K_{ATP} channels following stimulation of tissue culture cells, cardiomyocytes, or hippocampal neurons with the PKC activator phorbol 12-myristate 13-acetate (PMA) (Hu et al., 2003). The C-terminus of Kir6.2 harbors a dileucine motif, which is required for PMA induced internalization. Dileucine motifs interact with the clathrin adaptor protein AP2 (Bonifacino and Traub, 2003). Interestingly, the

four PKC consensus phosphorylation sites in Kir6.2 are not required for PMA-induced internalization (Hu et al., 2003). Surface expression of Kir1.1 was regulated by monoubiquitination at lysine 22 (Liu et al., 2001). Following monoubiquitination, Kir1.1 is likely to follow the pathway observed for other plasma membrane proteins, namely endocytosis and targeting to lysosomes (Bonifacino and Traub, 2003). It will be interesting to delineate this pathway in more detail as it specifically applies to Kir channels. For example, monoubiquitination of other proteins is preceded by phosphorylation. It is not known whether phosphorylation of Kir1.1 establishes a binding site for ubiquitin ligases, and if so, what signaling cascades trigger the phosphorylation event.

Timing of Kir channel biosynthesis and trafficking

Given the many steps involved in generating functional Kir channels, one may wonder how long the process takes. Crane and Aguilar-Bryan (Crane and Aguilar-Bryan, 2004) used pulse-chase analyses of radioactively labeled K_{ATP} channels to estimate the half-times for different steps of K_{ATP} biosynthesis. Their results suggest that the formation of Kir6.2 tetramers (in the absence of SUR1) occurred with a half-time of ~1.2 h, that assembled K_{ATP} octamers transit the Golgi with a half-time of ~2.2 h, and that surface K_{ATP} channels turn over with a half-life of ~7.3 h.

Sun et al. (Sun et al., 2004) measured the time course of current recovery (assayed by rubidium efflux) after inactivation of Kir2.1 at the cell surface with reducing agents. Half-maximal recovery occurred after 1 hour, and after 5 hours,

rubidium efflux returned to 90% of the control level. Recovery of channel function was dependent on the temperature and was blocked by brefeldin A, an inhibitor of vesicular trafficking along the secretory pathway, suggesting that newly synthesized channels were indeed inserted into the membrane on a time-scale of hours.

1.5 Kir channel function at the plasma membrane

The activity of Kir channels at the plasma membrane is regulated by many factors, including intracellular pH, redox state, ions such as Na^+ and Mg^{2+}, ATP, ADP, reactive oxygen species, G-proteins, scaffolding proteins, kinases, phosphatases, and lipids (Ruppersberg, 2000; Bichet et al., 2003; Tang et al., 2004). These intracellular modulators influence the likelihood that a channel undergoes a gating transition, i.e., that a conformational change occurs which opens or closes the conduction pathway to the flux of ions. Extensive structure-function studies have characterized the effects of intracellular modulators and mapped residues in the channels where modulators bind or that are involved in transmitting the effects of modulators to the channel gate. Appendix 4 summarizes some of this information in the form of an alignment of several Kir channels; residues that have been studied for their effects on channel function are annotated with a brief description of their role and a reference to the primary literature.

Interactions between Kir channels and scaffolding proteins provide an instructive example of the direct effects protein-protein interactions can have on

Kir channel function. Many Kir channels contain PDZ-binding motifs (S/T X I/V/L/M, X = any amino acid) at the very C-terminus. The PDZ ligands interact with PDZ domain-containing (first identified in **P**SD-95, **d**iscs-large, and **z**ona occludens-1) scaffolding proteins such as PSD-95 (postsynaptic density-95) and SAP97 (synapse-associated protein 97) (Cohen et al., 1996; Inanobe et al., 1999; Tanemoto et al., 2002). The affinity of scaffolding proteins for PDZ-ligands is modulated by phosphorylation of the serine or threonine residue in the ligand: Activation of protein kinase A phosphorylated Kir2.2 and Kir2.3 and prevented their association with PSD-95 or SAP97 (Cohen et al., 1996; Leonoudakis et al., 2001). Cohen et al. (Cohen et al., 1996) speculated that tethering of the Kir2.3 C-terminus to a scaffolding protein would prevent blocking of the ion conduction pathway by the channel's C-terminus (analogously to the ball-and-chain model proposed for voltage-gated K^+ channels). However, co-expression of PSD-95 with Kir2.3 in HEK-293 cells suppressed currents by reducing the single channel conductance (Nehring et al., 2000). An activating effect of scaffolding proteins was observed for Kir3 channels. Although homotetrameric Kir3.2c channels expressed in oocytes reached the plasma membrane, they could not be activated by G-protein signaling. Co-expression of SAP97 restored activation of the channels by $G\beta\gamma$-subunits (Hibino et al., 2000). Scaffolding proteins may also affect Kir channel activity at the plasma membrane by altering channel trafficking or localization. In the case of Kir1.1 channels, interaction with the PDZ-domain containing proteins Na^+/H^+ exchange regulatory factors 1 and 2 (NHERF-1 and 2) increased trafficking of the channel to the cell surface and led to coupling

between Kir1.1 and CFTR (cystic fibrosis transmembrane regulator) thereby altering channel properties (Yoo et al., 2004). Leonoudakis et al. (Leonoudakis et al., 2004b; Leonoudakis et al., 2004a) identified a large complex of PDZ-domain containing proteins that associate with Kir2.2 channels and proposed that the interactions may play a role in polarized cell surface targeting of Kir2.2 in neurons.

The idea that Kir channels exist in complexes with other proteins is appealing in other contexts as well. Kir3 channels are activated upon binding of $G\beta\gamma$-subunits that are released from heterotrimeric G-proteins following ligand binding to G-protein coupled receptors (GPCRs). The specificity of activation by pertussis-toxin sensitive GPCRs may be explained by a physical complex consisting of Kir channels, G-proteins, GPCRs, and possibly regulatory proteins (Sadja et al., 2003). The interaction of Kir2.1 with A Kinase Anchoring Protein (AKAP79) may position the channel in close proximity to kinases and phosphatases (Dart and Leyland, 2001). Several kinases, including PKC, PKA, and src kinases have been shown to activate or inhibit Kir channels (Ruppersberg, 2000).

In light of the results of the yeast screen described in Chapter 2, the effects of lipids on channel gating are of particular interest. Three types of interactions between Kir channels and lipids have been observed. (i) Interactions with lipid molecules used in cellular signaling, such as phosphatidylinositol 4,5-bisphoshpate (PIP_2) and arachidonic acid, (ii) general or specific interactions with

phospholipids, one of the major lipid species in eukaryotic lipid bilayers, and (iii) partitioning of Kir channels into lipid rafts rich in sphingolipids and sterols.

A universal requirement for Kir channel function is the presence of PIP_2 (Hilgemann et al., 2001). Structure-function studies have identified several residues that form a binding pocket for PIP_2 and/or constitute the connection between the binding pocket and the channel gate(s) (Logothetis et al., 2007). Although loss of PIP_2 from the membrane was shown to underlie rundown of currents during recordings from excised patches (Huang et al., 1998), it is experimentally difficult to assess whether changes in cellular PIP_2 levels influence Kir channel activity *in vivo* (Hilgemann et al., 2001). Given the increases and decreases in levels of PIP_2 and related lipid species in response to cellular signaling events, the hypothesis that Kir channel activity is fine-tuned by the abundance of these factors is appealing. Other lipid molecules that function in cellular signaling modulate Kir channel activity as well. Kir2, Kir3, and Kir6 channels are activated by arachidonic acid or its metabolites (Lohberger et al., 2000; Liu et al., 2001; Lu et al., 2001b). Kir1 channels, on the contrary, are inhibited by arachidonic acid (Macica et al., 1998).

Molecular dynamics simulations predict that residues in the extracellular loops, at the extracellular ends of the transmembrane helices, in the slide helix M0, and on the surface of the intracellular domain facing the membrane interact with lipid headgroups (Haider et al., 2007). Although most of the contacts between Kir channel residues and lipids are likely of a general nature in that the channel is embedded in the lipids, specific interactions between ion channels and

tightly bound lipid headgroups have been observed for the bacterial K^+ channel KcsA (Valiyaveetil et al., 2002). A crystal structure of KcsA contained an electron density that could represent a lipid molecule tightly bound to the extracellular side of the channel, and biochemical data suggested that the lipid is phosphatidylglycerol. Although the negatively charged phosphatidylglycerol was not necessary for the formation of KcsA tetramers, it was required for the formation of functional channels (Valiyaveetil et al., 2002).

The lipid bilayers that form the plasma membranes of eukaryotic cells have three main components: glycerophospholipids, sphingolipids, and sterols (Dickson et al., 2006). The relative abundance of these components determines the behavior of the lipid bilayer. For example, increasing amounts of cholesterol, a sterol, lead to the formation of a liquid ordered phase, which may coexist with a liquid disordered phase at certain ratios of sphingolipids to phospholipids to sterols (Hancock, 2006). Although partitioning of different lipid species into microdomains occurs in model membranes *in vitro*, the physiological role, size, and exact nature of lipid microdomains or rafts in cells *in vivo* are still debated (Simons and Vaz, 2004; Hancock, 2006; Jacobson et al., 2007). A provisional definition of rafts states: “Membrane rafts are small (10-200 nm), heterogeneous, highly dynamic, sterol- and sphingolipid-enriched domains that compartmentalize cellular processes. Small rafts can sometimes be stabilized to form larger platforms through protein-protein and protein-lipid interactions.” (Pike, 2006; Jacobson et al., 2007). Several ion channels partition into lipid rafts as assayed by detergent insolubility (Martens et al., 2004). Raft association based on

biochemical assays has been documented for Kir3 and Kir2 channels (Delling et al., 2002; Romanenko et al., 2002). Although pharmacological disruption of lipid rafts with lovastatin did not alter Kir3 channel function, an indirect interaction between Kir3 channels and neural cell adhesion molecule 140 (NCAM140) in lipid rafts led to intracellular retention of the channels in the presence of NCAM140 (Delling et al., 2002). Whole cell Kir2.1 and Kir2.3 currents were reduced when cholesterol levels increased. Since the current reduction occurred without a concomitant change in the single channel properties or channel number at the cell surface, cholesterol may trigger an inactive or silent conformation of Kir2 (Romanenko et al., 2004). The decrease in Kir2 currents following cholesterol enrichment correlated with a redistribution of the channels from cholesterol-poor membrane fractions to cholesterol-rich fractions, suggesting that Kir2 channels exist in two different conformations depending on their lipid environment (Tikku et al., 2007). The existence of silent Kir2.1 channels at the cell surface was also observed using Functional Recovery After Chemobleaching (FRAC) (Sun et al., 2004).

1.6 Summary and motivation for thesis project

Our understanding of Kir channel ontogenesis is very detailed in some areas and rather patchy in others. A common theme among many studies of aspects of Kir channel biosynthesis, trafficking, or function at the plasma membrane is their focus on identification of amino acid motifs and structural features in the channel that are important for its function. When I started the project described in this

thesis, we wanted to approach the question of Kir channel ontogenesis from a different angle by asking “Which cellular proteins are required to get a Kir channel to the plasma membrane and have it function appropriately?” Thanks to extensive structure-function studies that had been conducted on Kir channels using computational modeling, biophysical, biochemical, and cell biological techniques, we were able to design a screen that identified exciting leads into the network of cellular proteins involved in Kir channel functional expression at the plasma membrane. The model system we decided to employ was the yeast *Saccharmocyes cerevisiae*.

2 Yeast as a model system to study K^+ channels

2.1 Potassium transport in yeast

Yeast, *Saccharomyces cerevisiae*, can grow in aqueous solutions containing as little as 8 μM K^+ (Rodriguez-Navarro and Ramos, 1984), yet maintain intracellular K^+ concentrations of 130-170 mM (Ogino et al., 1983). K^+ uptake into yeast cells is accomplished by two K^+ transporters: the high affinity Trk1p, and low affinity Trk2p (TRK = TRansport of K^+) (Gaber et al., 1988; Ko et al., 1990). Yeast strains lacking *TRK1* and *TRK2* (*trk1*Δ *trk2*Δ yeast) require 50 to 100 mM K^+ in the media for growth. Growth of *trk1*Δ *trk2*Δ yeast on low K^+ media can be rescued by expression of certain K^+ channels (Nakamura and Gaber, 1998). Although the yeast membrane potential has not been measured electrophysiologically, it is thought to be more hyperpolarized than the K^+

equilibrium potential, therefore allowing passive K^+ uptake via exogenous K^+ channels that are open at hyperpolarized membrane potentials. In fact, it has been proposed that active K^+ uptake is unnecessary in yeast, and that the yeast K^+ transporters may operate as K^+-K^+ symporters under normal growth conditions (pH 6-8). Only at low pH, when the membrane potential is depolarized, would the K^+ transporters operate as K^+-H^+ symporters mediating active K^+ uptake (Rodriguez-Navarro, 2000).

2.2 Sodium transport in yeast

Yeast cells are sensitive to high cytosolic Na^+ concentrations, because certain enzymes such as Hal2p, which hydrolyzes 3'-phosphoadenosine-5'-phosphate (PAP) to adenosine monophosphate, are inhibited by Na^+ (Murguia et al., 1995; Albert et al., 2000). To maintain low cytosolic Na^+ concentrations, yeast extrude Na^+ via plasma membrane Na^+-ATPases encoded by ENA1-5 and the Na^+, K^+/H^+ exchanger encoded by NHA1. In addition, yeast sequester Na^+ into the prevacuolar compartment via the Na^+-H^+-exchanger Nhx1p (Serrano and Rodriguez-Navarro, 2001).

Yeast can tolerate NaCl concentrations in the range of 1 M. For example, Warringer et al. (Warringer et al., 2003) used 0.85 M NaCl for phenotypic profiling of deletion strains in comparison to control BY4742 yeast. When transferred to a high salt environment, yeast cells initially shrink and stop growing (Mager and Siderius, 2002). The loss of turgor pressure and decrease in cell volume induce the high-osmolarity glycerol (HOG) pathway, which regulates

transcription of many genes, including ENA1, that help yeast adapt to high salt osmotic stress. Following the adaptation phase, the cells swell and resume growth.

As discussed below, the Na^+ detoxification systems of yeast, extrusion into the media, and sequestration into the vacuole, can be overwhelmed by expression of mutated, Na^+-permeable inwardly rectifying K^+ channels.

2.3 Structure-function studies using trk1Δ trk2Δ yeast

*Trk1*Δ *trk2*Δ yeast have been used to clone cDNAs of several K^+ channels (Anderson et al., 1992; Sentenac et al., 1992) and to study structure-function relationships of K^+ channels (Nakamura and Gaber, 1998). Tang et al. (Tang et al., 1995) showed that expression of guinea pig Kir2.1 rescued growth of yeast lacking *TRK1* and *TRK2* on low K^+ media. Subsequent studies employed screens in *trk1*Δ *trk2*Δ yeast to characterize the transmembrane structure of Kir2.1 (Minor et al., 1999), to identify constitutively active mutants of the G-protein activated inwardly rectifying K^+ channel Kir3.2 (Sadja et al., 2001; Yi et al., 2001), or to gain insight into the interactions of the K^+ channel blocker Ba^{2+} with Kir2.1 (Chatelain et al., 2005).

The yeast expression system also proved amenable to the study of K^+ channel selectivity. For example, Uozumi et al. (Uozumi et al., 1995) tested the effects of replacing threonine 256 in the plant hyperpolarization-activated K^+ channel KAT1 with other amino acids, and Nakamura et al. (Nakamura et al., 1997) screened a library of KAT1 channels with mutations in the tyrosine and

glycine residues of the K^+ channel signature sequence GYG to identify structural requirements for selectivity. In addition to identifying amino acid substitutions that yielded channels permeable to K^+ and therefore able to rescue growth of *trk1*Δ *trk2*Δ yeast on low K^+ media, growth assays on media containing ammonium or Na^+ were used to test which ionic species passed through the mutated channel pores.

Some KAT1 channels carrying mutations in GYG failed to rescue *trk1*Δ *trk2*Δ yeast on low K^+ media supplemented with moderate amounts of Na^+ (Nakamura et al., 1997). The lack of rescue could have been due to two factors: First, the channels may have been impermeable to ions, including K^+, in the presence of Na^+ due to blockage of the channel pore, altered channel gating, or inactivation of the channel. Second, the channels may have been permeable to Na^+ (as well as K^+), which would lead to growth inhibition due to intracellular Na^+ accumulation. To distinguish these two possibilities, Nakamura et al. (Nakamura et al., 1997) expressed the GYG mutated KAT1 channels in $TRK1^+$ $TRK2^+$ yeast, which do not rely on the K^+ channel for K^+ uptake, and tested yeast growth on high (700 mM) Na^+ media. The reasoning was that if a mutated channel were non-conducting, growth of $TRK1^+$ $TRK2^+$ yeast on high Na^+ media would be unaffected. However, if the mutated channel were Na^+-permeable, Na^+ would enter the cells through the mutated channel pore leading to intracellular Na^+ toxicity and growth inhibition. Indeed, whereas $TRK1^+$ $TRK2^+$ yeast transformed with an empty plasmid or K^+ selective KAT1 channel grew well on high Na^+ media, some of the GYG mutated channels inhibited growth of $TRK1^+$ $TRK2^+$

yeast on high Na^+ media, suggesting that the channels were permeable to Na^+. Other GYG mutated channels did not alter growth of $TRK1^+$ $TRK2^+$ yeast on high Na^+ media, suggesting that they did not conduct ions in the presence of Na^+.

In a screen to identify constitutively open Kir3.2 channels, Yi et al. noticed that channels with certain amino acid substitutions at position S177 (e.g. S177W) did not rescue growth of *trk1*Δ *trk2*Δ yeast, however, when expressed in *Xenopus* oocytes, conducted large K^+ currents in the absence of G-protein signaling. The yeast phenotype was explained by the finding that the channels also conducted large Na^+ currents in oocytes. The conclusion was confirmed by testing growth of *trk1*Δ *trk2*Δ yeast transformed with constitutively active, mutated Kir3.2 channels that were either K^+-selective (Kir3.2S177T) or permeable to K^+ and Na^+ (Kir3.2S177W) on media containing 100 mM K^+ and 1 M Na^+ (Bichet et al., 2004). The high K^+ concentration was used to support growth of *trk1*Δ *trk2*Δ yeast by non-specific K^+ uptake, independently of the Kir channel. The high Na^+ concentration did not slow growth of *trk1*Δ *trk2*Δ yeast expressing the K^+ selective Kir3.2S177T channel, however, it did impair growth when the yeast expressed Kir3.2S177W.

3 Design of yeast screen to identify proteins involved in Kir channel functional expression

Although we know many details about features within Kir channels that are important to obtain a functional channel at the plasma membrane, less is known

about the cell's machinery that is required to transcribe, translate, fold, assemble, traffic, and regulate the channels. We therefore used the yeast *Saccharomyces cerivisae* as a model system to identify proteins that are required for functional expression of a Kir channel at the plasma membrane. The overall approach was to design a growth assay that would allow us to distinguish whether or not yeast expressed a functional Kir channel. The assay would then be applied in a high throughput manner to yeast deletion strains, each lacking one non-essential gene. Since we were interested in identifying basic cellular machinery involved in Kir channel functional expression, yeast provided a powerful, but simple screening platform.

We entertained two ideas for the growth assay. The first was to test for growth rescue on low K^+ media of *trk1*Δ *trk2*Δ yeast expressing the constitutively active, K^+ selective Kir3.2V188G channel (Yi et al., 2001) (Figure 1-4). This assay worked well during initial tests, and we attempted twice to implement it in screens of the entire yeast deletion library. However, difficulties with the selection of four selectable markers, and the overall slow growth of *trk1*Δ *trk2*Δ yeast during the screens, prevented us from interpreting the results (for more details on this screen see Appendix 2).

The second growth assay was based on growth inhibition on high Na^+ media of yeast expressing a Na^+-permeable mutated K^+ channel (Figure 1-5). In pilot experiments, we tested growth of $TRK1^+$ $TRK2^+$ yeast (BY4742 background) carrying a genomic insertion of one of three Na^+ permeable Kir3.2 channels, Kir3.2S177G (Yi et al., 2001), Kir3.2S177W (Yi et al., 2001) or Kir3.2G156S, the

mutation found in weaver mice (Kofuji et al., 1996; Slesinger et al., 1996), on high Na^+ media. Kir3.2S177W slowed yeast growth on rich yeast media containing 500 mM Na^+ (Figure 1-6). The other two mutated channels, Kir3.2S177G and Kir3.2G156S, did not slow yeast growth, likely indicating that the Na^+ currents carried by these channels were not as large as Na^+ currents carried by Kir3.2S177W.

Following identification of a suitable mutated Na^+ permeable Kir channel, we introduced the channel into yeast deletion strains using the method developed for Synthetic Genetic Array analysis (Tong et al., 2001; Schuldiner et al., 2006) and tested the growth of the resulting strains on high Na^+ media. In two attempts, Kir3.2S177W was introduced into the entire set of ~5,000 yeast strains carrying deletions in non-essential genes. The large number of plates (16 per step) involved in these screens allowed us to generate each strain only in duplicate, which in turn prevented us from doing statistical analyses of the results. With the additional complication that the growth inhibition was not pronounced at the high cell densities obtained by pinning the yeast arrays, we were unable to identify reliable candidate strains that may have had reduced functional expression of Kir3.2S177W. However, we identified 67 deletion strains that showed enhanced Na^+ sensitivity. Interestingly, 29 of the strains carried deletions in genes involved in vacuolar trafficking or vacuole morphogenesis. These findings are described in Appendix 1.

In order to generate and test more replicates of each deletion strain expressing Kir3.2S177W, we narrowed down the number of strains. Schuldiner

et al. (Schuldiner et al., 2005) had characterized genetic interactions in a set of 376 yeast strains, each carrying a deletion in an early secretory pathway-localized gene. Given their localization and known functions (for many of them) these genes were interesting candidates to test for their involvement in Kir channel functional expression. In addition to reducing the number of strains tested, we also decided to use Kir3.2S177W carrying a C-terminal GFP tag for the new screen. The fluorescent tag would facilitate follow-up experiments looking at the localization of the channel, and, if the growth assay had failed again, would have allowed for visual screening of the strains to detect mislocalization of the channel. An unintended consequence of using the GFP-tagged channel was that it enhanced the inhibition of yeast growth on high Na^+ media (Figure 1-7).

The results of the yeast screen using 376 deletion strains lacking proteins localized to the early secretory pathway are described in Chapter 2, which has been published as a research article in the Proceedings of the National Academy of Sciences.

Figure 1-1

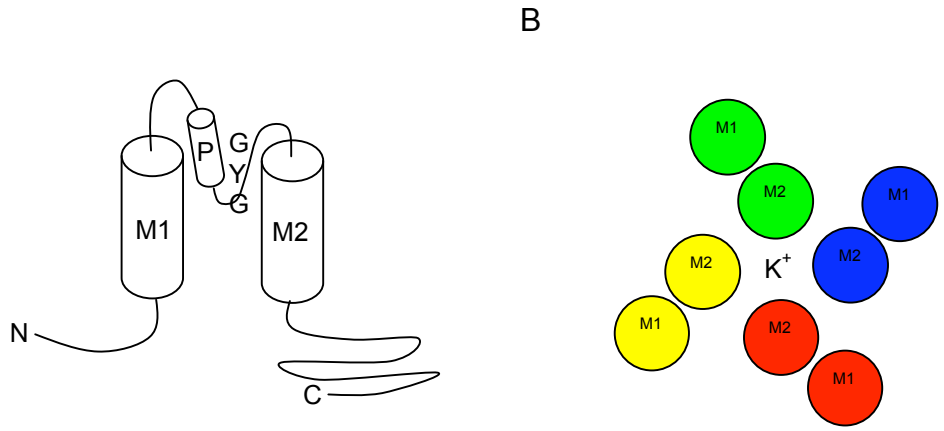

Schematic representation of Kir channel structure. (A) Topology of a single subunit depicting the intracellular N and C termini, the two transmembrane helices M1 and M2, the pore helix P, and the K^+ channel signature sequence glycine-tyrosine-glycine (GYG). (B) Diagram of the arrangement of subunits in an assembled tetrameric Kir channel. K^+ marks the pore, which is lined by the backbone of the amino acids GYG.

Figure 1-2

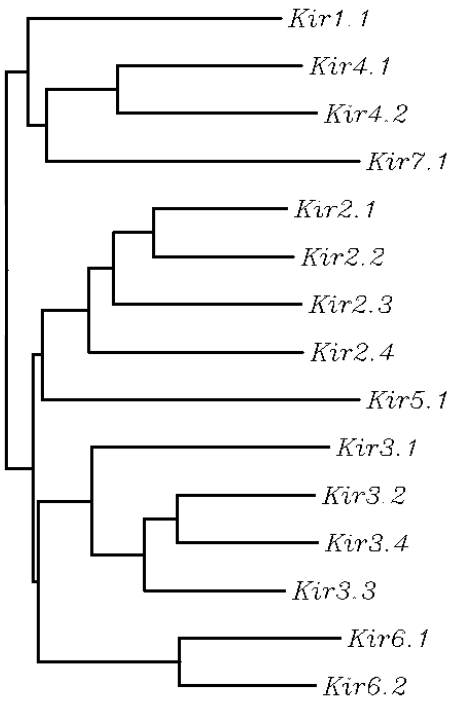

Family of Kir channels. Dendrogram with branch length generated using Clustal W 1.83 (http://align.genome.jp/) based on human Kir channel sequences.

Table 1-1: Kir channel functions

Kir channel	Function	References*
Kir1.1	K^+ homeostasis in the kidney	(Giebisch, 1998)
Kir2.1	Maintenance of resting membrane potential; modulation of action potential waveform in forebrain, heart, skeletal muscle; vasodilation	(Zaritsky et al., 2000; Lopatin and Nichols, 2001)
Kir2.2	Maintenance of resting membrane potential; modulation of action potential waveform in heart	(Lopatin and Nichols, 2001)
Kir2.3	Expressed in specific brain regions, heart and skeletal muscle; possibly glial Kir channel	(Makhina et al., 1994; Perier et al., 1994)
Kir2.4	Proposed to regulate neuronal function in brainstem	(Topert et al., 1998)
Kir3.1 + 3.4	Slowing of heart rate in response to vagal stimulation (cardiac K_{ACh} current)	(Krapivinsky et al., 1995; Wickman et al., 1998)
Kir3.2	Postsynaptic inhibition in substantia nigra	(Inanobe et al., 1999)
Kir3.1 + 3.2	Postsynaptic inhibition in hippocampus	(Luscher et al., 1997)
Kir3.3	Possible negative regulator of Kir3 channel expression	(Ma et al., 2002)
Kir4.1 (+ 5.1)	Regulation of K^+ homeostasis by glia and in kidney	(Butt and Kalsi, 2006)
Kir4.2 (+5.1)	Expressed in many epithelial tissues, also in pancreas and brain	(Gosset et al., 1997; Pessia et al., 2001)
Kir5.1	Potential regulator of excitatory synaptic transmission	(Tanemoto et al., 2002)
Kir6.1 + SUR2B	K_{ATP} in vascular smooth muscle; vasodilation	(Aguilar-Bryan and Bryan, 1999; Miki et al., 2002)
Kir6.2+SUR1	K_{ATP} in pancreas and brain; regulation of insulin secretion by pancreatic β-cells; neuroprotection	(Ashcroft, 2000; Ballanyi, 2004)
Kir6.2+SUR2A	K_{ATP} in heart; cardioprotection; ischemic preconditiong	(Gross and Peart, 2003)
Kir7.1	Maintenance of resting membrane potential in brain; K^+ recycling in specialized epithelia	(Krapivinsky et al., 1998; Nakamura et al., 1999)

Figure 1-3

A

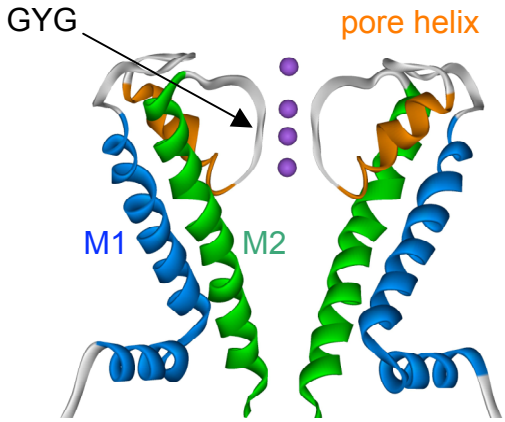

B

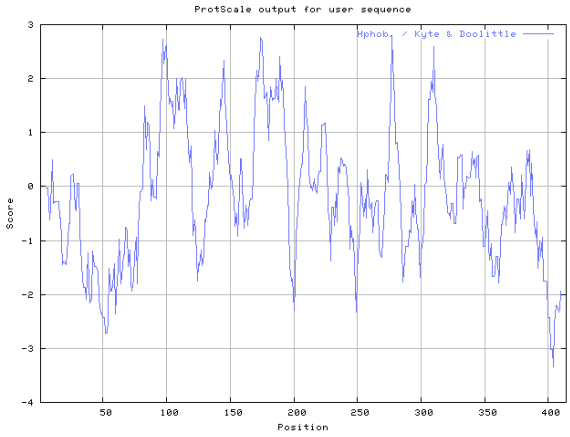

Folding of Kir channel pore loop. (A) Ribbon diagram of the transmembrane structure of KirBac, a bacterial Kir channel, based on the X-ray crystal structure published by Kuo et al. (Kuo et al., 2003) (generated based on PDB coordinates using VMD, http://www.ks.uiuc.edu/ Research /vmd/). Two subunits are shown. M1 is depicted in blue, the pore helix, which forms the “descending” part of the pore loop, is shown in orange, M2 is shown in blue. Four purple K^+ ions are depicted in the selectivity filter, which is lined by the GYG K^+ channel signature sequence, the “ascending” part of the pore loop. (B) Kyte-Doolittle hydrophobicity plot of Kir3.2. The approximate location of M1 is position 91-113, the pore loop is between positions 141-165, and M2 between positions 166-196. Generated using ProtScale at http://us.expasy.org/tools/protscale.html

Figure 1-4

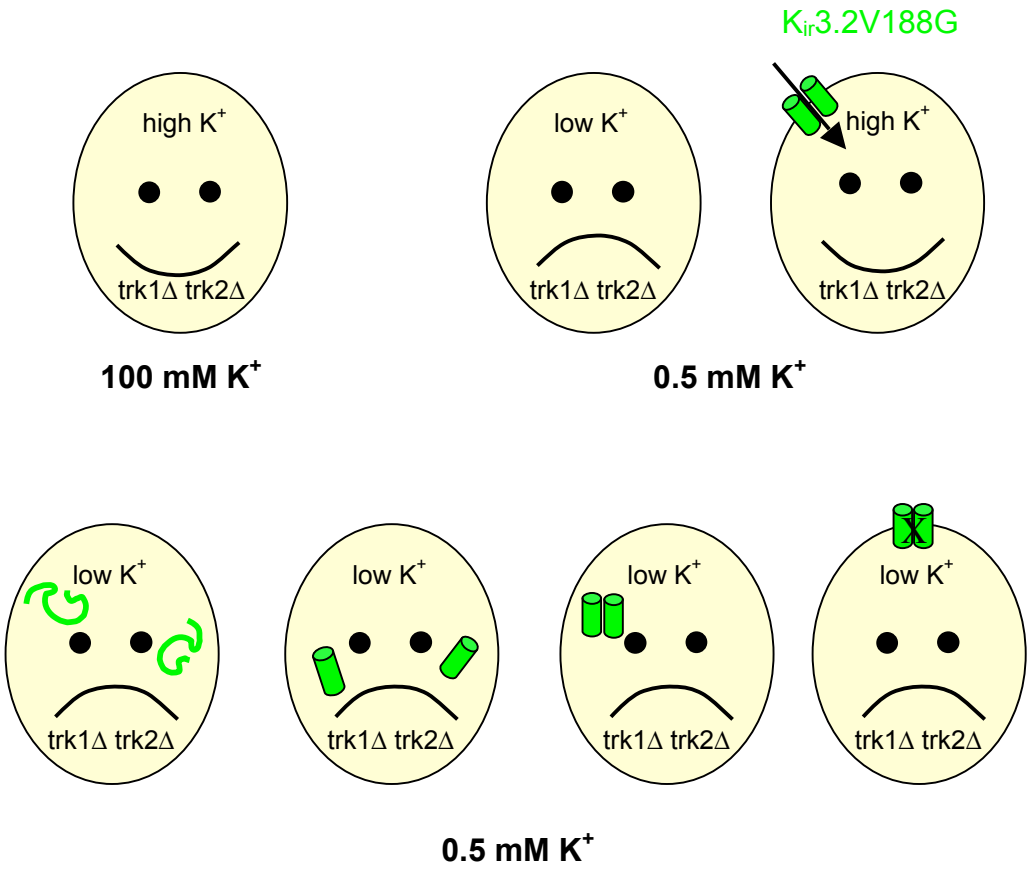

Schematic representation of K^+ screen. Yeast lacking the K^+ transporters Trk1p and Trk2p grow well on media supplemented with 100 mM K^+, but are starved for K^+ and therefore grow slowly on media containing only 0.5 mM K^+. Growth of *trk1*Δ *trk2*Δ yeast on low K^+ media is rescued by expression of Kir3.2V188G, a K^+ selective, constitutively open channel. No rescue would occur if folding, assembly, trafficking, or function of the channel were disrupted due to deletion of a yeast gene.

Figure 1-5

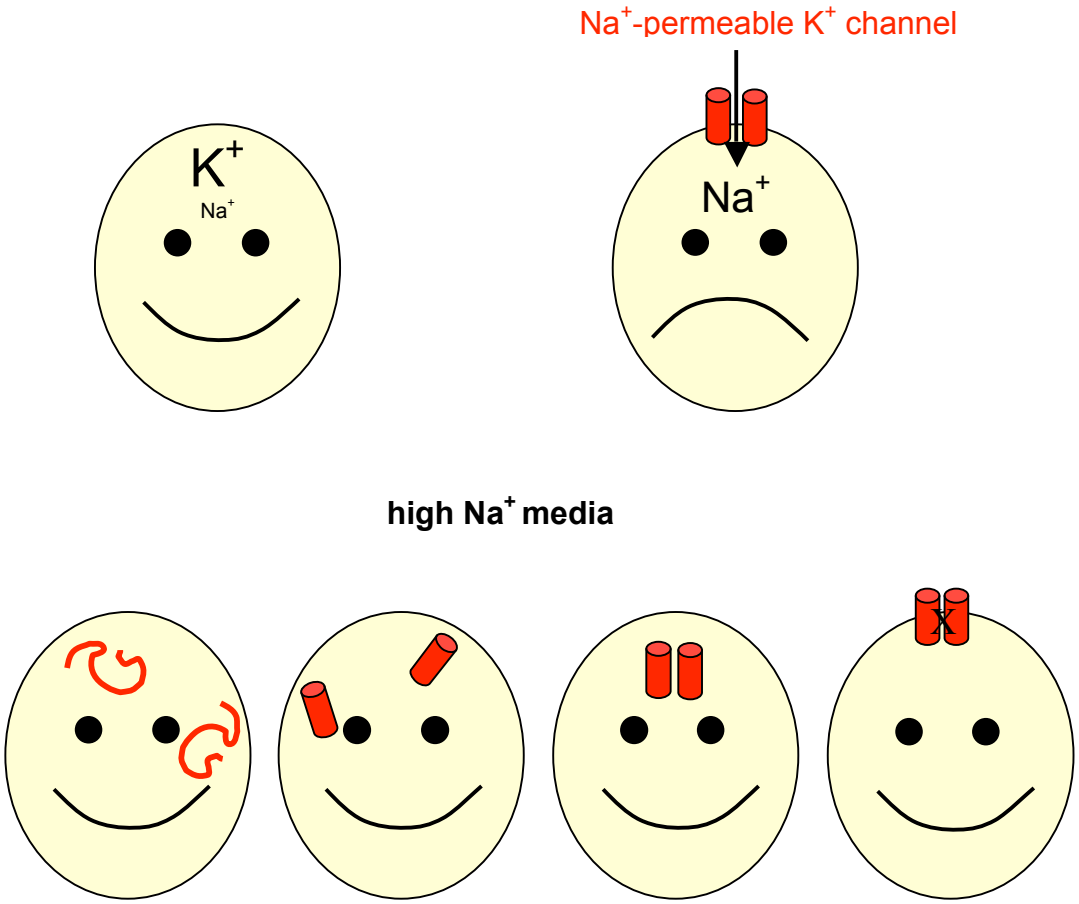

Schematic representation of Na^+ screen. Control yeast, not expressing a Na^+-permeable K^+ channel, grow well on high Na+ media. Expression of a Na^+-permeable K^+ channel slows yeast growth on high Na^+ media. Slow growth is expected to be reversed if folding, assembly, trafficking, or function of the channel were disrupted due to deletion of a yeast gene.

Figure 1-6

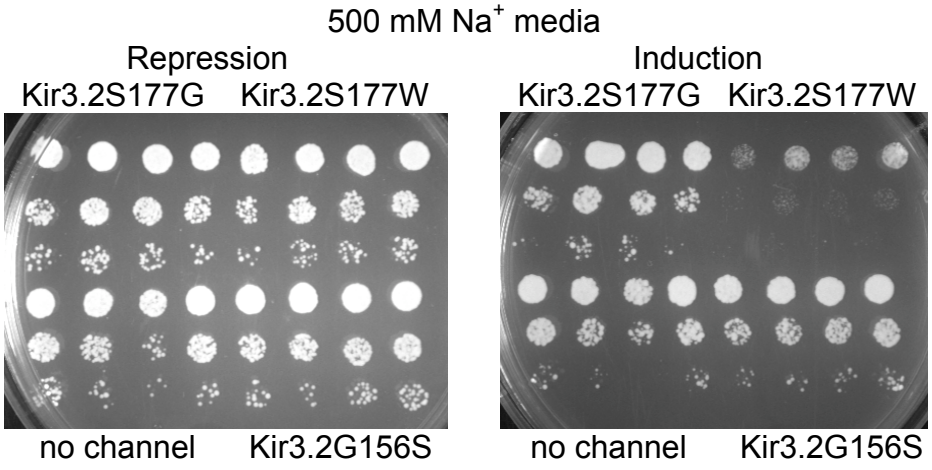

Growth inhibition by Kir3.2S177W on high Na^+ media. Induction of Kir3.2S177W expression slowed growth of yeast (BY4742 background) on high Na^+ media. Control yeast not expressing a channel or expressing Kir3.2S177G or Kir3.2G156S grew well on high Na^+ media. Three ten fold serial dilutions of yeast carrying a genomic insertion of the channels under a galactose inducible/ dextrose repressible promoter (GAL1pr) were plated on 500 mM Na^+ media under repressing conditions (YPAD, left panel) or inducing conditions (YPAGR, right panel). Each yeast strain is shown in quadruplicate.

Figure 1-7

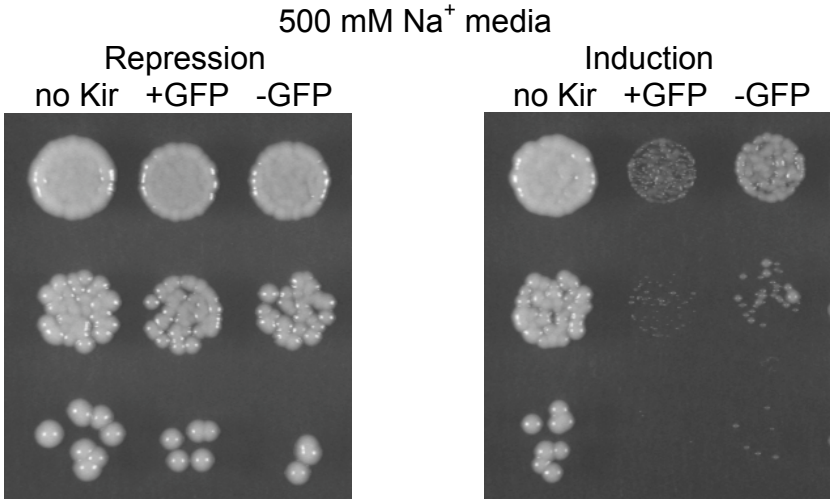

Comparison of Kir3.2S177W and Kir3.2S177W-GFP. Induction of Kir3.2S177W-GFP expression slowed growth of yeast (BY4742 background) on high Na^+ media more than induction of Kir3.2S177W without a C-terminal GFP tag. Control yeast not expressing a channel grew well on high Na^+ media. Three ten-fold serial dilutions of yeast carrying a genomic insertion of the channels under a galactose inducible/ dextrose repressible promoter (GAL1pr) were plated on 500 mM Na^+ media under repressing conditions (YPAD, left panel) or inducing conditions (YPAGR, right panel).

Chapter 2: Identification of yeast proteins necessary for cell surface function of a potassium channel

Friederike A. Haass[1,2], Martin Jonikas[3,4], Peter Walter[4], Jonathan S. Weissman[3], Yuh Nung Jan[2,4], Lily Y. Jan[2,4], Maya Schuldiner[3]

Author affiliation: [1]Neuroscience graduate program, [2]Howard Hughes Medical Institute and Department of Physiology, [3]HHMI and Department of Cellular and Molecular Pharmacology, [4]HHMI and Department of Biochemistry and Biophysics; University of California San Francisco, San Francisco, CA 94158

Corresponding author: Maya Schuldiner, Department of Cellular and Molecular Pharmacology, Howard Hughes Medical Institute, University of California San Francisco, 1700 4th Street, Byers Hall, San Francisco, CA 94158-2330, USA. Tel.: +1 415 502 8089; Fax: +1 415 514 4140;

Email: mschuldiner@cmp.ucsf.edu

Author contributions: FAH designed and performed research, analyzed data, wrote the paper; MJ and PW provided data and analysis on UPR; JSW contributed new reagents and analytic tools; Y-NJ and LYJ designed research, wrote the paper; MS designed research, analyzed data, wrote the paper.

Abbreviations: Kir channel - inwardly rectifying K^+ channel, Kir3.2 - the G-protein activated inwardly rectifying K^+ channel GIRK2, Kir* - Kir3.2S177W, ER - endoplasmic reticulum, GPI-AP - glycosylphosphatidylinositol anchored proteins, YPAGR - rich, galactose media, YPAD - rich, dextrose media

Abstract

Inwardly rectifying potassium (Kir) channels form gates in the cell membrane that regulate the flow of K^+ ions into and out of the cell, thereby influencing the membrane potential and electrical signaling of many cell types including neurons and cardiomyocytes. Kir channel function depends on other cellular proteins that aid in folding of channel subunits, assembly into tetrameric complexes, trafficking of quality controlled channels to the plasma membrane, and regulation of channel activity at the cell surface. We used the yeast *Saccharomyces cerevisiae* as a model system to identify proteins necessary for the functional expression of a mammalian Kir channel at the cell surface. A screen of 376 yeast strains each lacking one non-essential protein localized to the early secretory pathway identified seven deletion strains in which functional expression of the Kir channel at the plasma membrane was impaired. Six deletions were of genes with known functions in trafficking and lipid biosynthesis (*sur4*Δ, *csg2*Δ, *erv14*Δ, *emp24*Δ, *erv25*Δ, *bst1*Δ) and one deletion was of an uncharacterized gene (*yil039w*Δ). We provide genetic and functional evidence that Yil039wp, a conserved, phosphoesterase domain-containing protein, which we named **T**rafficking of **E**mp24p/Erv25p-dependent cargo **D**isrupted 1 (Ted1p), acts together with Emp24p/Erv25p in cargo exit from the ER. The seven yeast proteins identified in our screen likely impact Kir channel functional expression at the level of vesicle budding from the ER and/or the local lipid environment at the plasma membrane.

Introduction

Inwardly rectifying potassium (Kir) channels serve important physiological functions by regulating the membrane potential of many cell types including neurons, cardiomyocytes, and hormone secreting cells. Disruption of Kir channel function has been linked to human diseases such as periodic paralysis and neonatal diabetes (Neusch et al., 2003).

Kir channel activity at the plasma membrane is influenced by the abundance of channels and by their functional properties. The number of channels at the cell surface is regulated at the level of channel transcription, biosynthesis, trafficking, and turnover (Deutsch, 2002). The functional properties of Kir channels are influenced by the membrane potential, local lipid environment, small molecules, and interacting proteins (Ruppersberg, 2000; Logothetis et al., 2007). Structure-function studies have identified amino acid motifs and structural features of Kir channels involved in folding, assembly, and trafficking as well as in gating and selectivity (Tinker and Jan, 1999; Ma and Jan, 2002; Bichet et al., 2003). However, less is known about the cellular machinery that interacts with these motifs and allows Kir channels to reach the cell surface and function appropriately. We took advantage of the knowledge gained from structure-function studies of Kir channels and the genetic tools available in the yeast *Saccharomyces cerevisiae* to design a yeast screen aimed at identifying cellular proteins that play a role in Kir channel functional expression.

We chose to study Kir3.2, a mammalian G-protein activated inwardly rectifying K^+ channel, that can form homotetrameric channels and mediates

inhibitory post-synaptic potentials in midbrain dopamine neurons (Mark and Herlitze, 2000). The mutation S177W (referred to as Kir*) renders Kir3.2 constitutively open in the absence of G-protein signaling, permeable to Na^+ as well as K^+, and does not disrupt functional expression of the channel at the cell surface of yeast or *Xenopus* oocytes (Yi et al., 2001; Bichet et al., 2004). Expression of mutated K^+ channels that are permeable to Na^+ overwhelms the Na^+ detoxification systems of yeast (Nakamura and Gaber, 1998). Functional expression of Kir* can therefore be assayed based on growth inhibition, reflected by small yeast colony size, on media containing high Na^+ concentrations. We reasoned that growth inhibition conferred by Kir* could be overcome if channel biogenesis, trafficking, or function were disrupted.

The *Saccharomyces* Genome Deletion Project has generated a library of yeast strains each lacking one non-essential gene (Giaever et al., 2002). Additional transgenes can be introduced into the deletion strains using methods developed for Synthetic Genetic Array analysis (Tong et al., 2001; Schuldiner et al., 2006). We used these tools to introduce an inducible Kir* transgene into 376 yeast deletion strains each lacking an early secretory pathway-localized protein (Schuldiner et al., 2005) and tested the resulting strains for growth inhibition on high Na^+ media conferred by Kir*. We identified seven yeast deletion strains with reduced growth inhibition on high Na^+ media, indicating that the strains are missing a gene involved in Kir* functional expression.

Results

Kir* slows yeast growth on high Na^+ media.

Kir3.2S177W tagged with GFP at the C-terminus (referred to as Kir*) was integrated into the genome of yeast (BY4742 background) under the control of a galactose inducible/ dextrose repressible promoter. Whereas yeast not carrying Kir* doubled every 3 hours in YPAGR media containing 500 mM Na^+, expression of Kir* slowed the doubling time to 7 hours (Fig. 2-1 A). The inhibition of yeast growth by Kir* was also observed on solid media containing 500 mM Na^+ (Fig. 2-1 A). Integration of the channel into the yeast genome did not affect yeast growth when channel expression was repressed by dextrose (Fig. 2-1 B) or under low sodium conditions (Fig. 2-1 C). Growth on high Na^+ media of yeast expressing Kir* was rescued in the vicinity of a filter disk containing the Kir channel blocker barium (Kubo et al., 2005) (Fig. 2-6), supporting the conclusion that growth inhibition conferred by Kir* was due to Na^+ influx through the channel.

Yeast screen

Using the mating and random spore selection scheme developed for Synthetic Genetic Array (SGA) analysis (Tong et al., 2001; Schuldiner et al., 2006), we introduced the genomically integrated copy of Kir* into 376 strains from the MATa (BY4741) yeast deletion library (Giaever et al., 2002), each carrying a deletion of an early secretory pathway-localized protein (Schuldiner et al., 2005) (see Table 2-2 for a list of the deletions, Table 2-3 for the selection scheme). Growth of the deletion strains carrying Kir* was tested on high Na^+

media containing galactose to induce Kir* expression and, to account for strain specific growth differences, normalized to growth on high Na^+ media containing dextrose where Kir* expression was repressed. Most deletion strains behaved like control (BY4741) yeast and showed growth inhibition on high Na^+ media when Kir* was expressed. However, several strains grew into large colonies even though Kir* expression was induced. Follow-up tests of the Na^+-tolerant strains in liquid culture identified seven yeast deletion strains (*sur4*Δ, *csg2*Δ, *erv14*Δ, *emp24*Δ, *erv25*Δ, *bst1*Δ, *yil039w*Δ) that grew well under high Na^+, Kir*-inducing conditions.

Deletion strains resistant to growth inhibition by Kir*

The candidates fell into two categories (Table 2-1). First, enzymes involved in sphingolipid biosynthesis: Sur4p, which catalyzes the formation of very long chain fatty acids (Rossler et al., 2003), and Csg2p, a regulatory subunit of the complex that attaches mannose to inositol phosphorylceramide (Uemura et al., 2007). Second, proteins involved in cargo selection and vesicle budding during ER-Golgi trafficking: Erv14p, a protein required for packaging of specific cargo into COPII vesicles (Powers and Barlowe, 1998; Nakanishi et al., 2007); Emp24p and Erv25p, p24 proteins that form a complex involved in COPII vesicle budding and trafficking of GPI-anchored and soluble proteins (Kaiser, 2000); Bst1p, an enzyme that removes the acyl chain from GPI anchors, thereby allowing GPI-anchored proteins to leave the ER (Tanaka et al., 2004; Fujita et al.,

2006); Yil039wp, a conserved, metallophosphoesterase domain-containing protein, with previously unknown function.

To ensure correct identification of the deletions and to rule out differences in the genetic background, mutations in the transgene or influences of mating type, the seven candidate deletion strains were remade using PCR-mediated gene disruption in the BY4742 background and the phenotypes confirmed using growth assays in liquid culture and on agar plates. When Kir* expression was induced by galactose the seven deletion strains grew faster than the control strain in media containing high Na^+ (500 mM YPAGR) (Fig. 2-1 A). The ability of the deletion strains to grow faster in high Na^+ media was not due to general Na^+ tolerance, because when Kir* expression was repressed by dextrose, the deletion strains grew at a similar rate or, in the case of *sur4*Δ and *yil039w*Δ, more slowly than the control strain in media containing high Na^+ (500 mM YPAD) (Fig. 2-1 B). The deletions did not enhance the ability of the yeast to metabolize galactose, as shown by comparable or slower growth in galactose-containing media under conditions of low Na^+ (YPAGR, ~30 mM Na^+) (Fig. 2-1 C). Finally, Na^+ tolerance under Kir* inducing conditions was not explained by osmotolerance, because the deletion strains grew at similar rates or more slowly than control yeast in hyperosmotic media containing 1 M sorbitol (data not shown).

Although the deletion strains expressing Kir* grew faster than the control strain expressing Kir* in 500 mM Na^+ YPAGR (Fig. 2-1 A), they did not grow as fast as a control strain without genomic insertion of Kir*, likely because the deletions did

not entirely abolish Kir* function at the plasma membrane. This would be expected for deletions affecting trafficking or quality control, which often employ backup pathways (Springer et al., 2000; Olkkonen and Ikonen, 2006). In addition, the Na^+ sensitivity (Fig. 2-1 B) and slow growth in galactose media (Fig. 2-1 C) of some of the strains (*sur4*Δ, *erv14*Δ, *bst1*Δ, *yil039W*Δ) may have contributed to the incomplete rescue, because for these strains, even complete loss of the Kir* function would not have resulted in the same growth as control yeast not carrying Kir*.

Based on the result that reduced growth inhibition of the deletion strains is dependent on Kir* expression in the presence of high Na^+, we concluded that Kir* functional expression at the plasma membrane was disrupted in these strains. However, it was also possible that the membrane potential of the deletion strains was depolarized.

Hygromycin B sensitivity of deletion strains

Na^+ influx through Kir* is driven by the hyperpolarized membrane potential of yeast. Therefore, growth inhibition by high Na^+ would be reduced if the deletion strains had more depolarized membrane potentials than control yeast. The small size of yeast precludes electrophysiological measurements of their membrane potential, however, relative membrane potentials can be assayed based on uptake of lipophilic cations or sensitivity to the antibiotic hygromycin B (Perlin et al., 1988; Vallejo and Serrano, 1989; Rodriguez-Navarro, 2000). We therefore tested whether the seven deletion strains were hygromycin resistant,

indicative of depolarization, compared to control yeast. To ensure that our assay would detect depolarization of the membrane potential, we tested the yeast strain *pma1-105*, which carries a mutation in the proton ATPase Pma1p and has previously been shown to be depolarized (McCusker et al., 1987; Perlin et al., 1988). Growth of the *pma1-105* strain was inhibited less by hygromycin B than growth of the corresponding control DBY745 strain (Fig. 2-2 A). Comparing the deletion strains identified in our screen to the corresponding control BY4742 strain (Fig. 2-2 B), the *sur4*Δ and *erv14*Δ strains were slightly less inhibited by hygromycin, indicating that they may be more depolarized. Hygromycin resistance has been reported for *sur4*-mutant strains in the BWG1-7A genetic background (Garcia-Arranz et al., 1994). However, the differences in relative growth rates in our experiment were not statistically significant (Dunnett's test comparing BY4742 to each deletion strain, $p>0.05$). Because hygromycin B sensitivity cannot be calibrated in terms of absolute changes in membrane potential, we cannot rule out that the tendency towards hygromycin resistance in *sur4*Δ and *erv14*Δ strains accounted, at least in part, for the reduced growth inhibition by Na^+ influx through Kir*. The *csg2*Δ strain showed a tendency (but Dunnett's test $p>0.05$) towards increased hygromycin sensitivity and the *emp24*Δ, *erv25*Δ, *bst1*Δ, and *yil039w*Δ strains had comparable hygromycin sensitivity to the control strain, suggesting that depolarization did not account for the ability of these deletion strains to grow under high Na^+ conditions while expressing Kir*.

Impaired complementation of *trk1*D *trk2*D yeast by Kir3.2V188G

To corroborate that the seven deletions impaired functional expression of Kir* at the cell surface we employed an independent assay. Yeast lacking the K^+ transporters Trk1p and Trk2p are starved for K^+ and therefore grow slowly on Low Salt media supplemented with low concentrations (0.5 mM) of K^+ (Ko et al., 1990). Growth is rescued by expression of Kir3.2V188G, a constitutively active, K^+ selective Kir3.2 channel (Yi et al., 2001). If the deletions identified in our screen disrupted Kir channel trafficking or function, we predicted that rescue of *trk1*Δ *trk2*Δ yeast by Kir3.2V188G would be impaired in the deletion background. Indeed, Kir3.2V188G rescued growth on 0.5 mM K^+ media poorly or not at all when *trk1*Δ *trk2*Δ yeast carried a deletion of *SUR4*, *CSG2*, *EMP24*, *ERV25*, *BST1* or *YIL039W* (Fig. 2-3). These yeast strains grew well on Low Salt media supplemented with 100 mM K^+, where they did not depend on functional expression of Kir3.2V188G. The *erv14*Δ *trk1*Δ *trk2*Δ strain expressing Kir3.2V188G could not be tested in this assay, because the strain grew slowly on Low Salt plates even when supplemented with 100 mM K^+.

Kir* expression levels and localization in the deletion strains

The Na^+ tolerant phenotype, impaired rescue of *trk1*Δ *trk2*Δ yeast and the known functions of Sur4p, Csg2p, Erv14p, Emp24p, Erv25p, and Bst1p, suggested that the deletions might have affected Kir channel maturation or trafficking. We therefore performed Western blot analysis on each of the strains to test whether the deletions altered total protein levels of Kir*. Similar amounts

of Kir* were present in samples from yeast expressing Kir* in the control or deletion background (Fig. 2-4 A).

Given comparable expression levels of Kir* in the deletion strains, we examined whether the deletions altered the subcellular localization of the channel. Yeast were grown in galactose containing media to induce Kir* expression, fixed and mounted for imaging of the GFP-tagged Kir*. Optical sections through the middle of yeast cells showed two rings of GFP fluorescence and sections through the periphery of the cells showed tubular distribution of the GFP-tagged channel (Fig. 2-4 B). The pattern of Kir*-GFP fluorescence was typical of ER-localized proteins (Huh et al., 2003) even in the control strain. This was consistent with studies showing heavy ER localization of Kir3.2 in mammalian cells (Ma et al., 2002). Given the predominant ER localization of Kir* even in the control background, alterations in ER retention in the deletion strains could not be readily detected.

Deletion of *YIL039W* slows Gas1p trafficking

Six of the seven mutants identified by our screen had well-characterized functions impacting trafficking and lipid biosynthesis, which could explain their effects on Kir* channel functional expression (see Discussion). However, it was unclear how the uncharacterized, but conserved Yil039wp influenced Kir* activity. A previously published quantitative genetic interaction map suggested that Yil039wp acts together with Emp24p and Erv25p in mediating trafficking of cargo out of the ER. In this epistasis mini array profile (E-MAP), colony sizes for all

double mutant combinations were used to assess genetic interactions between ~400 strains each carrying a deletion in an early secretory pathway gene. When strains were clustered based on the similarity in their patterns of genetic interactions, the *emp24*Δ and *erv25*Δ strains alongside *erp1*Δ were most similar to each other out of all 400 strains. This similarity was expected, because Emp24p, Erv25p, and Erp1p act together in a physical complex (Belden and Barlowe, 1996; Marzioch et al., 1999). The next most similar, and therefore most functionally related gene was *YIL039W*. Moreover, the double mutants of *yil039w*Δ and *emp24*Δ or *erv25*Δ displayed buffering genetic interactions (Fig. 2-5 A adapted from (Schuldiner et al., 2005)), i.e. in the absence of Emp24p/Erv25p there was little additional fitness cost to losing Yil039wp. Buffering genetic interactions were also observed using a fluorescent reporter of Unfolded Protein Response-induction. Both *yil039w*Δ and *erv25*Δ yeast (*emp24*Δ was not assayed for technical reasons) showed UPR activation. Deletion of *YIL039W* and *ERV25* together did not exacerbate the phenotype to the extent expected for functionally unrelated genes (e.g. *ALG3*, *OST3*, and *SPC2*, Fig. 2-5 B). These relationships indicate that Yil039wp functions in a concerted manner with Emp24p/Erv25p.

To directly test whether Yil039wp, Emp24p, and Erv25p share a common function, we investigated whether ER exit of the GPI-anchored protein Gas1p, which is delayed in *emp24*Δ and *erv25*Δ strains (Belden and Barlowe, 1996; Elrod-Erickson and Kaiser, 1996), was affected in the yil*039w*Δ strain. Western blot analysis of whole cell extracts showed that Gas1p accumulated in its 100 kDa core-glycosylated ER form to a similar extent in yeast lacking EMP24,

ERV25, or *YIL039W* (Fig. 2-5 C). We therefore named *YIL039W* **T**rafficking of **E**mp24p/Erv25p-dependent cargo **D**isrupted 1 (*TED1*).

Discussion

Yeast has been used extensively as a model system to study K^+ channel structure-function relationships due to its sensitivity to even small currents and easy manipulation, which allows for screening of thousands of mutated channels (Nakamura and Gaber, 1998). We chose to study yeast as a model system due to its powerful genetic tools. Since cellular trafficking is a highly conserved process, we reasoned that secretory pathway conditions that influence a mammalian Kir channel in yeast would inform us of similar requirements in less genetically amenable mammalian systems. Taking advantage of the yeast deletion library (Giaever et al., 2002) and SGA methodology (Tong et al., 2001; Schuldiner et al., 2006), we found that deletion of *SUR4*, *CSG2*, *ERV14*, *EMP24*, *ERV25*, *BST1*, or *YIL039W*/*TED1* impaired Kir channel functional expression: First, the deletions partially restored yeast growth on high Na^+ media in the presence of the mutated, Na^+ permeable K^+ channel Kir3.2S177W (Kir*). Second, a K^+ selective Kir channel (Kir3.2V188G) was unable to rescue growth on low K^+ media of *trk1*Δ *trk2*Δ yeast also carrying one of the deletions.

A common theme among five of the proteins identified by our screen (Erv14p, Emp24p, Erv25p, Bst1p, Yil039wp/Ted1p) is that they affect maturation and trafficking of GPI anchored proteins. This was unexpected because Kir

channels are transmembrane proteins not known to be modified by a GPI anchor. It is possible that the machinery required for ER exit of GPI anchored proteins has additional functions in trafficking of transmembrane proteins. In fact, deletion of Erv14p leads to ER retention of the transmembrane proteins Axl2p and Sma1p (Powers and Barlowe, 1998; Nakanishi et al., 2007). Alternatively, GPI-anchored proteins may indirectly affect Kir channel trafficking. Slowed ER exit of GPI-anchored proteins in *gwt1-10* yeast has been shown to disrupt the formation of lipid domains in the ER and thereby to indirectly affect sorting and budding of transmembrane proteins (Okamoto et al., 2006). We speculate that the interplay between different classes of proteins during the formation of lipid microdomains (Hancock, 2006) may affect trafficking of Kir channels.

Deletion of the other two candidates identified by our screen, *SUR4* or *CSG2*, alters the lipid composition of yeast cells by reducing synthesis of C_{24} and C_{26} fatty acids (Oh et al., 1997; Rossler et al., 2003) or of sphingolipids with mannose modification of their headgroups (Uemura et al., 2003), respectively. The lipid composition of membranes may influence Kir channel functional expression in two ways. First, lipid rafts rich in sphingolipids or their precursor, ceramide, play a role in trafficking at the level of ER exit (Horvath et al., 1994; Dupre and Haguenauer-Tsapis, 2003; Toulmay and Schneiter, 2007) and at the level of protein sorting at the Golgi (Simons and Ikonen, 1997). Second, the local lipid environment at the plasma membrane may influence channel activity. For example, enrichment of membranes with cholesterol induced an inactive channel conformation in Kir2.1 (Romanenko et al., 2004) and a specific interaction

between the bacterial K^+ channel KcsA and phosphatidylglycerol is required for channel function (Valiyaveetil et al., 2002). C_{24} and C_{26} fatty acids are also found in remodeled GPI anchors (Pittet and Conzelmann, 2007), opening the possibility that deletion of SUR4 affects Kir channel trafficking through indirect effects on GPI-anchored proteins as discussed above.

Our screen identified a phenotype for the previously uncharacterized gene *YIL039W*, which encodes a metallophosphoesterase domain-containing protein conserved in eukaryotes, including humans (MPPE1). Genetic interaction data based on yeast growth (Schuldiner et al., 2005) and UPR activation, as well as biochemical data showing ER retention of Gas1p in *emp24*Δ, *erv25*Δ (Belden and Barlowe, 1996; Elrod-Erickson and Kaiser, 1996), and *yil039w*Δ yeast provide evidence that Yil039wp acts together with Emp24p and Erv25p in cargo exit from the ER. We therefore named *YIL039W* **T**rafficking of **E**mp24p/Erv25p-dependent cargo **D**isrupted 1 (*TED1*). It is interesting to note that the *bst1*Δ strain, in which Gas1p maturation was also delayed (as previously reported (Vashist et al., 2001)), displayed an aggravating genetic interaction with *ted1*Δ, but buffering interactions with *emp24*Δ and *erv25*Δ. We therefore predict that Bst1p and Ted1p function in parallel pathways to regulate Emp24p/Erv25p function. Since Yil039wp/Ted1p contains a predicted phosphoesterase domain, it will be of interest to identify the protein and/or lipid targets that are dephosphorylated by Ted1p. One candidate substrate is the amphiphysin homologue Rvs167p, which is phosphorylated by Pho85-Pcl1 (Dephoure et al., 2005) and was shown in a

large-scale pull down study to physically interact with Ted1p (Krogan and others, 2006)*.

Since Kir3.2 is not native to yeast, our screen was intended to identify global requirements for Kir channel functional expression and probably precluded the identification of specific chaperoning interactions, which would require co-evolution. The seven proteins identified by our screen and their cellular roles are conserved up to mammals, highlighting the appropriate nature of yeast as a model system to uncover basic cellular machinery involved in Kir channel functional expression. The results provide important leads that will allow us to probe deeper into the mechanisms that regulate trafficking and activity of Kir channels in mammalian systems.

Footnote: * Intriguingly, *SUR4* was identified as a suppressor of *rvs161* and *rvs167* (Desfarges et al., 1993).

Materials and Methods

Yeast Strains and Media

Yeast strains were picked from the deletion library (Giaever et al., 2002) or constructed by PCR-mediated gene disruption in the BY4742 background (Brachmann et al., 1998). Table 2-4 lists strains, primers and plasmids. Yeast media recipes were based on (Nakamura and Gaber, 1998; Schuldiner et al., 2006) or are provided as Supplemental Methods.

Yeast Screen

376 yeast strains from the MATa deletion library (Table 2-2) (Giaever et al., 2002; Schuldiner et al., 2005) were mated to yeast expressing Kir3.2S177W-GFP using SGA methodology (Tong et al., 2001; Schuldiner et al., 2006). The selection scheme is shown in Table 2-3. Growth of the double mutant strains was tested on synthetic media containing 750 mM Na^+ and dextrose or galactose. Plates were photographed using a ChemiImager Ready (Alpha Innotech Corp.) and colony sizes, S_{gal} and S_{dex}, measured using software developed by (Collins et al., 2006). Initial Na^+-tolerant candidates had to meet the criterion that four out of six replicates or the average of the six colony size differences $|S_{gal}*100/S_{dex} – 100|$ were smaller than the average $|S_{gal}*100/S_{dex} – 100|$ for all strains tested minus one standard deviation.

Yeast Assays

Doubling times and growth rates were determined at 30°C by diluting over night cultures to $2 * 10^6$ cells/ml and measuring the optical density (OD_{660}) at 0 h and 4 or 8 h later. For growth tests on plates, over night liquid cultures were adjusted to equal ODs and 10-fold serial dilutions plated. Photographs were taken three days after plating. The experiments were repeated at least two times. Yeast protein samples were prepared by the post-alkaline lysis method (Kushnirov, 2000). Western blots were probed with rabbit anti-GIRK2 (Alomone), mouse anti-PGK (Molecular Probes), or rabbit anti-Gas1p (Walter lab)

antibodies. Fixed yeast cells were imaged using widefield epifluorescence on a Nikon TE2000 microscope. Images presented are single planes from the middle and top of deconvolved stacks. For the UPR assay, fluorescence signals from 4xUPRE-GFP normalized to TEF2pr-RFP were measured using Flow Cytometry. For detailed procedures see Supplemental Methods.

Statistics

One-way ANOVA followed by Dunnett's test and unpaired t-test were performed with GraphPad Prism 4.0.

Acknowledgements

We thank B. Schwappach for the pYES2 plasmid; C. Boone and A. Tong for yeast strains; J. Haber for the *pma1-105* and control strains; S. Collins for the colony measuring software and help with data analysis; R. Shaw for help with image acquisition and use of the microscope; and members of the Jan and Weissman labs for stimulating discussions. This work was supported by NIMH MERIT Award R37MH065334. MS was supported by the International Human Frontier Science Program Organization and a NIH K99/R00 award, MJ by the National Science Foundation. PW, JW, Y-NJ, and LYJ are HHMI investigators.

Figure 2-1

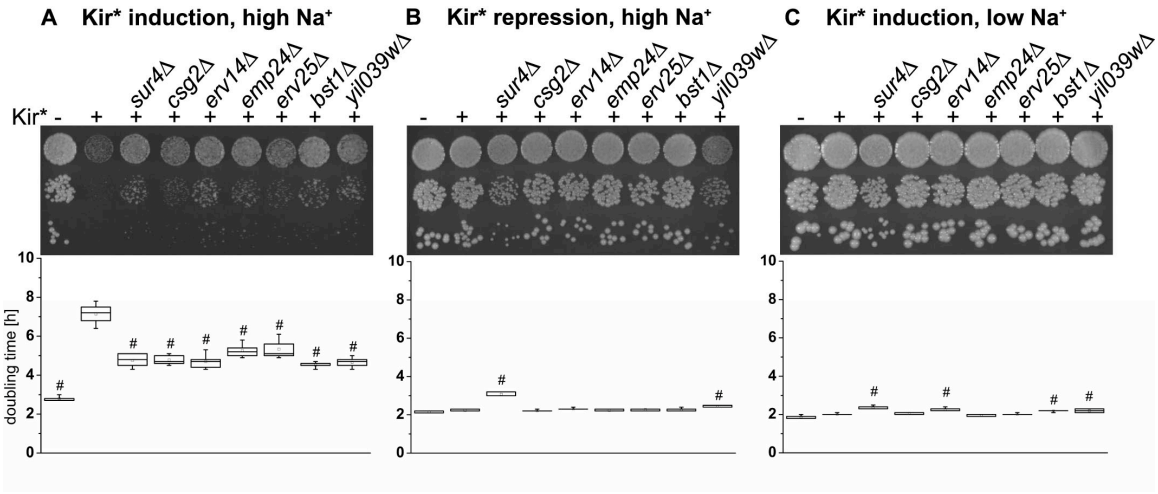

Deletion of seven early secretory pathway-localized proteins reduced Na^+ toxicity conferred by Kir*. Growth of yeast strains carrying Kir* alone or in combination with the deletions was assayed by 10 fold serial dilutions on agar plates (top) or by doubling time measurements in liquid culture (bottom). (A) Expression of Kir* in control yeast slowed growth in 500 mM Na^+ YPAGR. Growth inhibition by Kir* was partially reversed in yeast strains carrying deletions of seven early secretory pathway-localized proteins. (B) The deletions did not enhance growth in high Na^+ media when Kir* was repressed (500 mM Na^+ YPAD) or (C) in low Na^+ media when Kir* was induced (YPAGR). Whiskers - min. and max., box - 25th to 75th percentile and median, open square - mean, n = 5. # - statistically significant difference compared to yeast expressing Kir* in the control background ($p<0.01$, Dunnett's test).

Table 2-1: Functions of proteins deleted in strains identified by Kir* screen.

name	ORF	localization	function	deletion phenotype
SUR4	YLR372W	ER	Elongase for very long chain fatty acids	Reduced VLCFA levels. Lipid raft association and targeting of H^+ ATPase disrupted. (Garcia-Arranz et al., 1994; Oh et al., 1997; Rossler et al., 2003; Toulmay and Schneiter, 2007)
CSG2	YBR036C	ER	Regulatory subunit of mannosyl-tranferases Csg1p and Csh1p	Reduced mannosylinositol phosphorylceramide levels. (Uemura et al., 2003; Uemura et al., 2007)
ERV14	YGL054C	ER	COPII vesicle packaging chaperone	ER retention of TM proteins Axl2p and Sma2p. Delay in ER exit of GPI-AP. (Powers and Barlowe, 1998; Nakanishi et al., 2007)
EMP24	YGL200C	COPII vesicles	Cargo receptor in p24 protein family	Delay in ER exit of GPI-AP and soluble cargo. Secretion of ER proteins. Suppression of *sec13*Δ. (Belden and Barlowe, 1996; Elrod-Erickson and Kaiser, 1996; Marzioch et al., 1999; Kaiser, 2000; Springer et al., 2000)
ERV25	YML012W	COPII vesicles	Cargo receptor in p24 protein family	
BST1	YFL025C	ER	GPI inositol deacylase	Delay in ER exit of GPI-AP. Secretion of ER proteins. Suppression *sec13*Δ. (Elrod-Erickson and Kaiser, 1996; Vashist et al., 2001; Tanaka et al., 2004; Fujita et al., 2006)
TED1	YIL039W	ER	Uncharacterized	Uncharacterized

Figure 2-2

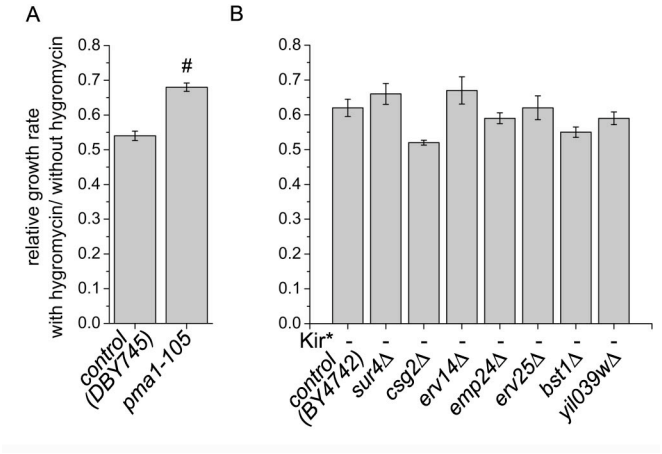

Hygromycin B sensitivity of deletion strains. Growth rates measured in 500 mM Na^+ YPAGR liquid media with 500 mg/L hygromycin B were normalized to growth rates in 500 mM Na^+ YPAGR. (A) The assay detected hygromycin resistance of *pma1-105* yeast compared to control DBY745 yeast ($p<0.01$, t-test). (B) The seven deletion strains showed no significant difference in hygromycin sensitivity compared to control BY4742 yeast ($p>0.05$, Dunnett's test), although the *csg2*Δ strain showed a tendency toward increased hygromycin sensitivity and the *sur4*Δ and *erv14*Δ strains towards hygromycin resistance. Error bars are standard errors, n=3.

Figure 2-3

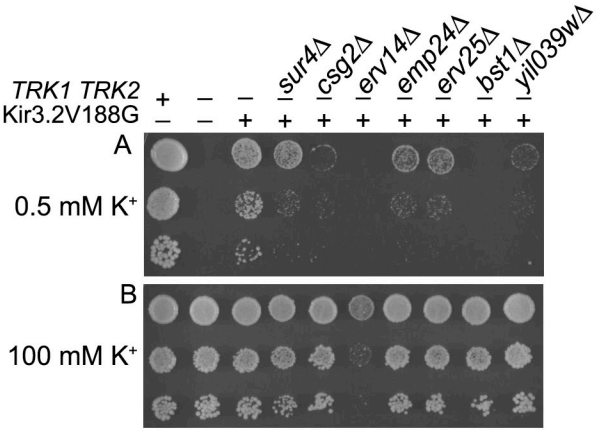

The seven deletions impaired rescue of *trk1*Δ *trk2*Δ yeast by Kir3.2V188G. Ten fold serial dilutions were spotted onto Low Salt plates containing 0.5 mM KCl or 100 mM KCl. (A) *trk1*Δ *trk2*Δ yeast did not grow on 0.5 mM K^+ media. Growth was rescued by expression of Kir3.2V188G. In triple mutant yeast lacking Trk1p, Trk2p, and one of seven early secretory pathway-localized proteins, Kir3.2V188G only partially restored growth on 0.5 mM K^+ media. (B) The triple mutant yeast strains, except *erv14*Δ, grew well on 100 mM K^+ media, where Kir3.2V188G is dispensable for growth.

Figure 2-4

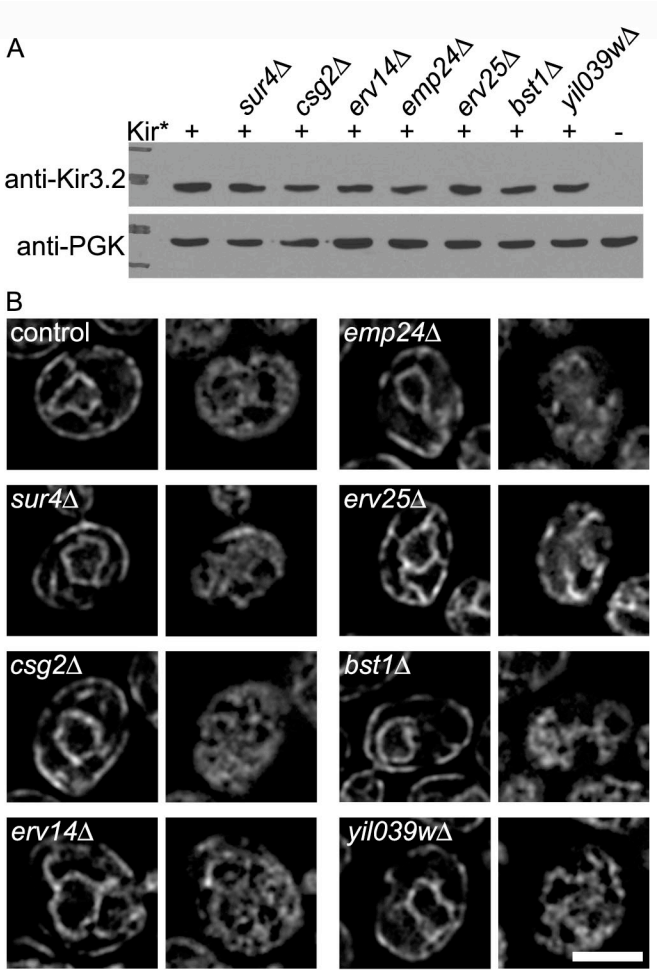

Total protein levels and distribution of Kir*-GFP. (A) Western blot of yeast expressing Kir* in the control or deletion background was probed with anti-Kir3.2 antibody. A band of similar intensity was detected in all strains carrying Kir*. Phosphoglycerate kinase (PGK) served as a loading control. Molecular weight markers are 100 and 75 for anti-Kir3.2, 50 and 37 kDa for anti-PGK. (B) Deconvolved optical z sections through the middle (left) or periphery (right) of yeast expressing Kir* tagged with eGFP at the C-terminus. In all strains, Kir* localized to the perinuclear and peripheral ER. Scale bar = 2.5 μm.

Figure 2-5

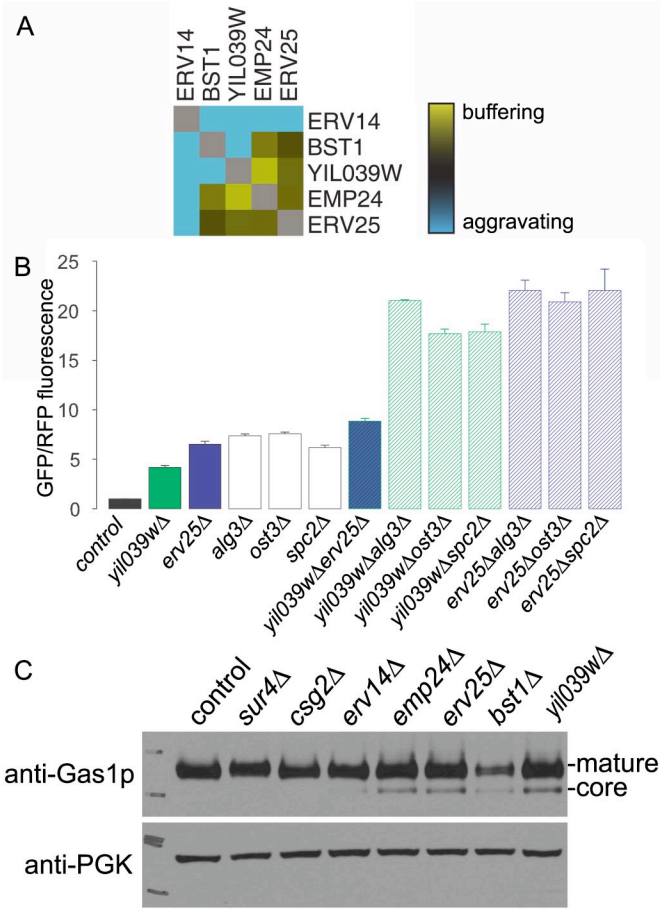

Ted1p, encoded by *YIL039W*, is involved in trafficking of the GPI-anchored protein Gas1p. (A) *YIL039W*, *EMP24*, and *ERV25* were predicted to act in a concerted manner based on their buffering genetic interactions as determined by (Schuldiner et al., 2005). (B) UPR induction assayed by expression of GFP from a UPR inducible promoter. Combining deletion of *YIL039W* and *ERV25* did not enhance UPR activation to the extent expected for unrelated genes (e.g. *ALG3*, *OST3*, *SPC2*), suggesting that Yil039wp and Erv25p share a common function. (C) Western blot of whole cell extracts probed with an antibody to Gas1p. Deletion of *YIL039W*/*TED1* led to accumulation of Gas1p in its 100 kDa core

glycosylated ER form as previously observed for *emp24*Δ and *erv25*Δ strains (Belden and Barlowe, 1996; Elrod-Erickson and Kaiser, 1996).

Figure 2-6

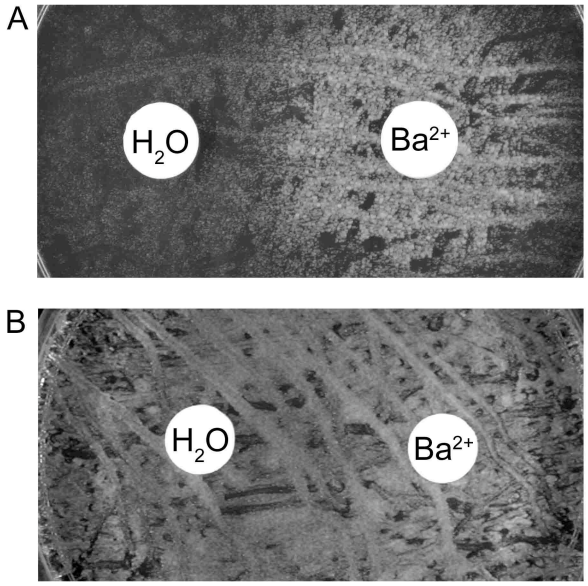

Barium prevents growth inhibition conferred by Kir*. Filter disks containing either water or 100 mM $BaCl_2$ were placed on 500 mM NaCl YPAGR plates with lawns of wildtype yeast carrying (A) or not carrying (B) a genomic insertion of Kir* under a galactose inducible/dextrose repressible promoter. Growth of the Kir* expressing yeast strain was restored in a halo around the disk with barium, but not the disk with water, indicating that growth inhibition was due to Na^+ influx through Kir*. Yeast not carrying Kir* grew on the entire plate.

Table 2-2: Yeast deletion strains used in screen

locus	name	function	locus	name	function	locus	name	function
YCR011C	ADP1	ambiguous	YOL013C	HRD1	ERAD and uibiquitin degradation	YMR214W	SCJ1	Protein maturation, protein maturation
YDR100W	TVP15	ambiguous	YDL091C	UBX3	ERAD and uibiquitin degradation	YMR152W	YIM1	Protein maturation, protein maturation
YAL026C	DRS2	ambiguous	YBR273C	UBX7	ERAD and uibiquitin degradation	YNL238W	KEX2	Protein maturation, protein maturation
YDR084C	TVP23	ambiguous	YIL030C	SSM4	ERAD and uibiquitin degradation	YMR274C	RCE1	Protein maturation, protein maturation
YEL005C	VAB2	ambiguous	YDR057W	YOS9	ERAD and uibiquitin degradation	YDR519W	FPR2	Protein maturation, protein maturation
YGL084C	GUP1	ambiguous	YER151C	UBP3	ERAD and uibiquitin degradation	YLR246W	ERF2	Protein maturation, protein maturation
YDR411C	DFM1	ambiguous	YOR036W	PEP12	Golgi-endosome-vacuole traffic	YOL110W	SHR5	Protein maturation, protein maturation
YER004W	FMP52	ambiguous	YJL029C	VPS53	Golgi-endosome-vacuole traffic	YJL073W	JEM1	Protein maturation, protein maturation
YGL020C	MDM39	ambiguous	YDR137W	RGP1	Intra Golgi traffic	YJR117W	STE24	Protein maturation, protein maturation
YEL064C	AVT2	ambiguous	YGL005C	COG7	Intra Golgi traffic	YKL119C	VPH2	Protein maturation, vATPase complex assembly
YDR233C	RTN1	ambiguous	YHL031C	GOS1	Intra Golgi traffic	YHR060W	VMA22	Protein maturation, vATPase complex assembly
YDR349C	YPS7	ambiguous	YKL212W	SAC1	Intra Golgi traffic	YGR105W	VMA21	Protein maturation, vATPase complex assembly
YEL031W	SPF1	ambiguous	YOR216C	RUD3	Intra Golgi traffic	YGL012W	ERG4	Steroid/sterol biosynthesis
YER083C	RMD7	ambiguous	YOR070C	GYP1	Intra Golgi traffic	YGR177C	ATF2	Steroid/sterol biosynthesis
YDR320C	SWA2	ambiguous	YOL018C	TLG2	Intra Golgi traffic	YLR056W	ERG3	Steroid/sterol biosynthesis
YIL090W	ICE2	ambiguous	YPL051W	ARL3	Intra Golgi traffic	YMR015C	ERG5	Steroid/sterol biosynthesis
YIL043C	CBR1	ambiguous	YBR164C	ARL1	Intra Golgi traffic	YML008C	ERG6	Steroid/sterol biosynthesis
YIL027C	KRE27	ambiguous	YBL102W	SFT2	Intra Golgi traffic	YMR202W	ERG2	Steroid/sterol biosynthesis

YHR039C	MSC7	ambiguous	YNL041C	COG6	Intra Golgi traffic	YLR242C	ARV1	Steroid/sterol biosynthesis
YHR136C	SPL2	ambiguous	YDL137W	ARF2	Intra Golgi traffic	YNL280C	ERG24	Steroid/sterol biosynthesis
YLR023C	IZH3	ambiguous	YJR031C	GEA1	Intra Golgi traffic	YDL019C	OSH2	Steroid/sterol biosynthesis
YJL178C	ATG27	ambiguous	YNL051W	COG5	Intra Golgi traffic	YNR019W	ARE2	Steroid/sterol biosynthesis
YKL094W	YJU3	ambiguous	YML071C	COG8	Intra Golgi traffic	YNR008W	LRO1	Steroid/sterol biosynthesis
YJL192C	SOP4	ambiguous	YLR039C	RIC1	Intra Golgi traffic	YML075C	HMG1	Steroid/sterol biosynthesis
YKL179C	COY1	ambiguous	YDL192W	ARF1	Intra Golgi traffic	YCR048W	ARE1	Steroid/sterol biosynthesis
YKL065C	YET1	ambiguous	YEL022W	GEA2	Intra Golgi traffic	YLR450W	HMG2	Steroid/sterol biosynthesis
YLR350W	ORM2	ambiguous	YBL011W	SCT1	Lipid biosynthesis	YGR086C	PIL1	TOR/PKC signalling
YMR029C	FAR8	ambiguous	YBR183W	YPC1	Lipid biosynthesis	YJR066W	TOR1	TOR/PKC signalling
YLR250W	SSP120	ambiguous	YDR294C	DPL1	Lipid biosynthesis	YIL105C	SLM1	TOR/PKC signalling
YNL156C	NSG2	ambiguous	YDR297W	SUR2	Lipid biosynthesis	YER019C-A	SBH2	translocation
YOR092W	ECM3	ambiguous	YGR202C	PCT1	Lipid biosynthesis	YKL073W	LHS1	translocation
YOR198C	BFR1	ambiguous	YGR170W	PSD2	Lipid biosynthesis	YLR292C	SEC72	translocation
YOR165W	SEY1	ambiguous	YGR157W	CHO2	Lipid biosynthesis	YOL031C	SIL1	translocation
YOR042W	CUE5	ambiguous	YHL003C	LAG1	Lipid biosynthesis	YBR171W	SEC66	translocation
YMR251W-A	HOR7	ambiguous	YKL020C	SPT23	Lipid biosynthesis	YML055W	SPC2	translocation
YPR028W	YOP1	ambiguous	YKL140W	TGL1	Lipid biosynthesis	YBR283C	SSH1	translocation
YPL246C	RBD2	ambiguous	YKL008C	LAC1	Lipid biosynthesis	YJR010C-A	SPC1	translocation
YPL170W	DAP1	ambiguous	YJL134W	LCB3	Lipid biosynthesis	YER087C-B	SBH1	translocation
YOR311C	HSD1	ambiguous	YLL043W	FPS1	Lipid biosynthesis	YLL052C	AQY2	transport
YOR307C	SLY41	ambiguous	YJL196C	ELO1	Lipid biosynthesis	YLL028W	TPO1	transport
YOR284W	HUA2	ambiguous	YLR372W	SUR4	Lipid biosynthesis	YMR054W	STV1	transport
YPR149W	NCE102	ambiguous	YOR245C	DGA1	Lipid biosynthesis	YCL025C	AGP1	transport, amino acid transport
YBR162W-A	YSY6	ambiguous	YNL323W	LEM3	Lipid biosynthesis	YLR220W	CCC1	transport, Ca transport
YFR041C	ERJ5	ambiguous	YOR049C	RSB1	Lipid biosynthesis	YGL167C	PMR1	transport, Ca transport
YML048W	GSF2	ambiguous	YOR171C	LCB4	Lipid biosynthesis	YDR270W	CCC2	transport, heavy metal transport
YDL100C	ARR4	ambiguous	YMR272C	SCS7	Lipid biosynthesis	YOR079C	ATX2	transport, heavy metal transport
YDR492W	IZH1	ambiguous	YOR377W	ATF1	Lipid biosynthesis	YDR205W	MSC2	transport, heavy metal transport
YGL161C	YIP5	ambiguous	YOL065C	INP54	Lipid biosynthesis	YJR040W	GEF1	transport, heavy metal transport
YNR039C	ZRG17	ambiguous	YPL087W	YDC1	Lipid biosynthesis	YLR130C	ZRT2	transport, heavy metal transport
YCR044C	PER1	ambiguous	YDL052C	SLC1	Lipid biosynthesis	YBR132C	AGP2	transport
YBR177C	EHT1	ambiguous	YJR073C	OPI3	Lipid biosynthesis	YJL198W	PHO90	transport, phosphate transport

YBR290W	BSD2	ambiguous	YDR503C	LPP1	Lipid biosynthesis	YBR106W	PHO88	transport, phosphate transport
YBR264C	YPT10	ambiguous	YML059C	NTE1	Lipid biosynthesis	YNR013C	PHO91	transport, phosphate transport
YNL008C	ASI3	ambiguous	YGL126W	SCS3	Lipid biosynthesis	YJL212C	OPT1	transport, sulfur transport
YML038C	YMD8	ambiguous	YIL124W	AYR1	Lipid biosynthesis	YPL274W	SAM3	transport, sulfur transport
YGR089W	NNF2	ambiguous	YKR067W	GPT2	Lipid biosynthesis	YHR079C	IRE1	unfolded protein response
YJR118C	ILM1	ambiguous	YIR033W	MGA2	Lipid biosynthesis	YDR056C	YDR056C	unknown
YGR038W	ORM1	ambiguous	YNL130C	CPT1	Lipid biosynthesis	YCL056C	YCL056C	unknown
YJR134C	SGM1	ambiguous	YKR053C	YSR3	Lipid biosynthesis	YCL045C	YCL045C	unknown
YER120W	SCS2	ambiguous	YCR034W	FEN1	Lipid biosynthesis	YEL001C	YEL001C	unknown
YMR052W	FAR3	ambiguous	YBR159W	YBR159W	Lipid biosynthesis	YDR307W	YDR307W	unknown
YBR287W	ZSP1	ambiguous	YHR123W	EPT1	Lipid biosynthesis	YEL043W	YEL043W	unknown
YMR119W	ASI1	ambiguous	YOR317W	FAA1	Lipid biosynthesis	YGL010W	YGL010W	unknown
YNL125C	ESBP6	ambiguous	YMR313C	TGL3	Lipid biosynthesis	YDR221W	YDR221W	unknown
YJL078C	PRY3	ambiguous	YBR036C	CSG2	Lipid biosynthesis	YDR222W	YDR222W	unknown
YDL072C	YET3	ambiguous	YPR135W	CTF4	miscellaneous, chromatin adhesion	YDR357C	YDR357C	unknown
YDR525W	API2	ambiguous	YJL168C	SET2	miscellaneous, histone methyltransferase	YDR344C	YDR344C	unknown
YOL101C	IZH4	ambiguous	YHR135C	YCK1	miscellaneous, kinase	YER071C	YER071C	unknown
YML101C	CUE4	ambiguous	YBL082C	RHK1	N-linked glycosylation	YIL039W	YIL039W	unknown
YOL137W	BSC6	ambiguous	YAL058W	CNE1	N-linked glycosylation	YGL231C	YGL231C	unknown
YMR065W	KAR5	ambiguous	YGR036C	CAX4	N-linked glycosylation	YLL014W	YLL014W	unknown
YHR181W	SVP26	ambiguous	YGL226C-A	OST5	N-linked glycosylation	YLR064W	YLR064W	unknown
YMR123W	PKR1	ambiguous	YML019W	OST6	N-linked glycosylation	YLR042C	YLR042C	unknown
YNR075W	COS10	ambiguous	YOR002W	ALG6	N-linked glycosylation	YJL171C	YJL171C	unknown
YHR004C	NEM1	ambiguous	YOR067C	ALG8	N-linked glycosylation	YLL055W	YLL055W	unknown
YDL222C	FMP45	ambiguous	YNL219C	ALG9	N-linked glycosylation	YKL063C	YKL063C	unknown
YJL079C	PRY1	ambiguous	YPL227C	ALG5	N-linked glycosylation	YLL023C	YLL023C	unknown
YKR088C	TVP38	ambiguous	YGR227W	DIE2	N-linked glycosylation	YMR010W	YMR010W	unknown
YDL204W	RTN2	ambiguous	YNR030W	ECM39	N-linked glycosylation	YLR194C	YLR194C	unknown
YDR032C	PST2	ambiguous	YJR131W	MNS1	N-linked glycosylation	YMR163C	YMR163C	unknown
YAR044W	OSH1	ambiguous	YOR085W	OST3	N-linked glycosylation	YMR031C	YMR031C	unknown
YEL015W	EDC3	ambiguous	YDL232W	OST4	N-linked glycosylation	YOR214C	YOR214C	unknown

YIL040W	APQ12	ambiguous	YCR017C	CWH43	O-linked glycosylation, GPI, cell wall biosynthesis	YNL194C	YNL194C	unknown
YNL085W	MKT1	ambiguous	YEL004W	YEA4	O-linked glycosylation, GPI, cell wall biosynthesis	YNL190W	YNL190W	unknown
YER044C	ERG28	ambiguous	YMR215W	GAS3	O-linked glycosylation, GPI, cell wall biosynthesis	YOR175C	YOR175C	unknown
YEL003W	GIM4	cytoskeleton assembly	YLR120C	YPS1	O-linked glycosylation, GPI, cell wall biosynthesis	YOR044W	YOR044W	unknown
YNL153C	GIM3	cytoskeleton assembly	YNL327W	EGT2	O-linked glycosylation, GPI, cell wall biosynthesis	YMR253C	YMR253C	unknown
YMR299C	DYN3	cytoskeleton assembly	YMR307W	GAS1	O-linked glycosylation, GPI, cell wall biosynthesis	YPR003C	YPR003C	unknown
YDR424C	DYN2	cytoskeleton assembly	YOL030W	GAS5	O-linked glycosylation, GPI, cell wall biosynthesis	YOL047C	YOL047C	unknown
YDR108W	GSG1	ER/Golgi traffic	YBR067C	TIP1	O-linked glycosylation, GPI, cell wall biosynthesis	YPL207W	YPL207W	unknown
YAL007C	ERP2	ER/Golgi traffic	YLR390W-A	CCW14	O-linked glycosylation, GPI, cell wall biosynthesis	YPL206C	YPL206C	unknown
YAL042W	ERV46	ER/Golgi traffic	YER005W	YND1	O-linked glycosylation, GPI, Golgi glycosylation	YOR285W	YOR285W	unknown
YGL200C	EMP24	ER/Golgi traffic	YEL042W	GDA1	O-linked glycosylation, GPI, Golgi glycosylation	YOR291W	YOR291W	unknown
YGL054C	ERV14	ER/Golgi traffic	YDR483W	KRE2	O-linked glycosylation, GPI, Golgi glycosylation	YPR148C	YPR148C	unknown
YHR110W	ERP5	ER/Golgi traffic	YBR229C	ROT2	O-linked glycosylation, GPI, GPI anchor biosynthesis	YBR052C	YBR052C	unknown
YIL076W	SEC28	ER/Golgi traffic	YFL025C	BST1	O-linked glycosylation, GPI, GPI anchor biosynthesis	YPR114W	YPR114W	unknown
YIL044C	AGE2	ER/Golgi traffic	YJL062W	LAS21	O-linked glycosylation, GPI, GPI anchor biosynthesis	YPR063C	YPR063C	unknown
YLR080W	EMP46	ER/Golgi traffic	YAL023C	PMT2	O-linked glycosylation, GPI, O-linked glycosylation	YPR071W	YPR071W	unknown
YML012W	ERV25	ER/Golgi traffic	YGL027C	CWH41	O-linked glycosylation, GPI, O-linked glycosylation	YDL121C	YDL121C	unknown

YLR268W	SEC22	ER/Golgi traffic	YGR199W	PMT6	O-linked glycosylation, GPI, O-linked glycosylation	YJR088C	YJR088C	unknown
YOR115C	TRS33	ER/Golgi traffic	YHR142W	CHS7	O-linked glycosylation, GPI, O-linked glycosylation	YDL099W	YDL099W	unknown
YMR292W	GOT1	ER/Golgi traffic	YOR321W	PMT3	O-linked glycosylation, GPI, O-linked glycosylation	YGR263C	YGR263C	unknown
YOR016C	ERP4	ER/Golgi traffic	YDL093W	PMT5	O-linked glycosylation, GPI, O-linked glycosylation	YGR266W	YGR266W	unknown
YCL001W	RER1	ER/Golgi traffic	YDL095W	PMT1	O-linked glycosylation, GPI, O-linked glycosylation	YNL146W	YNL146W	unknown
YDL018C	ERP3	ER/Golgi traffic	YBL017C	PEP1	Post-Golgi traffic	YCR043C	YCR043C	unknown
YDR524C	AGE1	ER/Golgi traffic	YEL013W	VAC8	Post-Golgi traffic	YNR021W	YNR021W	unknown
YFL048C	EMP47	ER/Golgi traffic	YMR183C	SSO2	Post-Golgi traffic	YCR061W	YCR061W	unknown
YNL044W	YIP3	ER/Golgi traffic	YNL297C	MON2	Post-Golgi traffic	YNL046W	YNL046W	unknown
YNL049C	SFB2	ER/Golgi traffic	YOR089C	VPS21	Post-Golgi traffic	YGR106C	YGR106C	unknown
YML067C	ERV41	ER/Golgi traffic	YPL195W	APL5	Post-Golgi traffic	YER113C	YER113C	unknown
YER122C	GLO3	ER/Golgi traffic	YPR173C	VPS4	Post-Golgi traffic	YJR015W	YJR015W	unknown
YAR002C-A	ERP1	ER/Golgi traffic	YDR484W	VPS52	Post-Golgi traffic	YNL095C	YNL095C	unknown
YCR067C	SED4	ER/Golgi traffic	YGR261C	APL6	Post-Golgi traffic	YPL137C	YPL137C	unknown
YGR284C	ERV29	ER/Golgi traffic	YJL024C	APS3	Post-Golgi traffic	YGR130C	YGR130C	unknown
YNR051C	BRE5	ER/Golgi traffic	YJL004C	SYS1	Post-Golgi traffic	YBR255W	YBR255W	unknown
YJL117W	PHO86	ER/Golgi traffic	YBR288C	APM3	Post-Golgi traffic	YDR476C	YDR476C	unknown
YDL226C	GCS1	ER/Golgi traffic	YDL231C	BRE4	Post-Golgi traffic	YOL107W	YOL107W	unknown
YGL223C	COG1	ER/Golgi traffic	YIL005W	EPS1	Protein maturation, disulfide bond formation	YHR045W	YHR045W	unknown
YBR201W	DER1	ERAD and uibiquitin degradation	YHR176W	FMO1	Protein maturation, disulfide bond formation	YLR050C	YLR050C	unknown
YHR204W	MNL1	ERAD and uibiquitin degradation	YOR288C	MPD1	Protein maturation, disulfide bond formation	YJL123C	YJL123C	unknown
YMR022W	QRI8	ERAD and uibiquitin degradation	YDR518W	EUG1	Protein maturation, disulfide bond formation	YBR096W	YBR096W	unknown
YLR207W	HRD3	ERAD and uibiquitin degradation	YIR038C	GTT1	Protein maturation, disulfide bond formation	YER053C-A	YER053C-A	unknown
YML013W	SEL1	ERAD and uibiquitin degradation	YOL088C	MPD2	Protein maturation, disulfide bond	YNL300W	TOS6	unknown

					formation			
YMR161W	HLJ1	ERAD and uibiquitin degradation	YGL203C	KEX1	Protein maturation, protein maturation	YIL016W	SNL1	unknown
YMR264W	CUE1	ERAD and uibiquitin degradation	YDR304C	CPR5	Protein maturation, protein maturation	YML128C	MSC1	unknown
			YDR410C	STE14	Protein maturation, protein maturation	undefin	NO GENE	

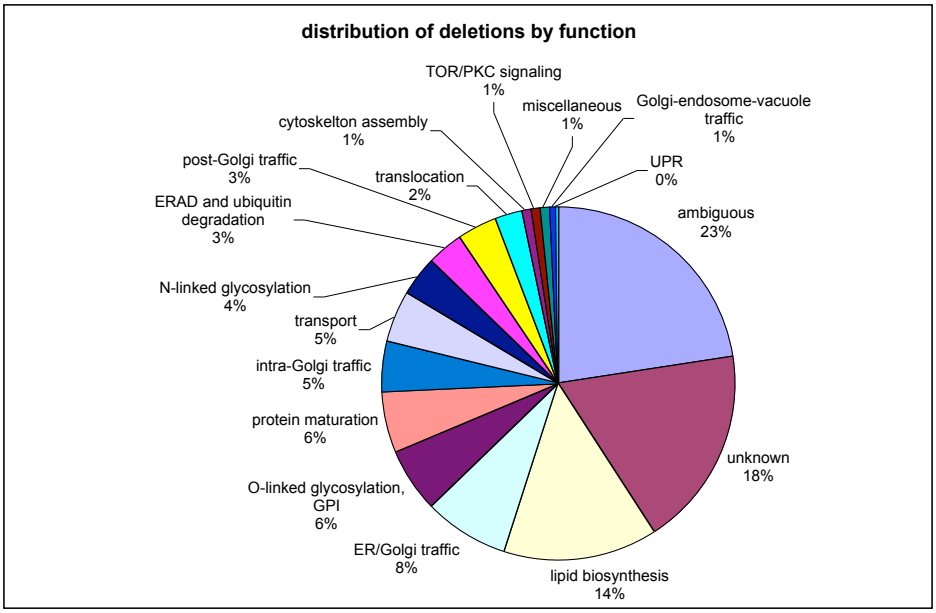

Table 2-3: Yeast screen selection scheme

MATalpha: ura3Δ::URA3/GAL1pr-Kir3.2S177W-GFP can1Δ::STE2pr-spHIS5 lyp1Δ::STE3pr-LEU2 LYS2+ his3Δ1 leu2Δ0 cyh2

MATa: YYYΔ::Kan^r CAN1 LYP1 LYS2+ his3Δ1 leu2Δ0 ura3Δ0 met15Δ0

Step	Media	Time	Temp.	Gentotype
1.a MATalpha 1.b MATa	SD(MSG)-URA YPAD+G418	2 days	30ºC	
2. Mating	YPAD	1 day	RT	
3. Diploid selection	SD(MSG)-URA+G418	2 days	30ºC	
4. Sporulation	sporulation media	5 days	22ºC	
5. Haploid selection 1	SD(MSG) –HIS–ARG–LYS +CAN +S-AEC	2 days	30ºC	can1Δ::STE2pr-HIS3, lyp1Δ
6. Haploid selection 2	SD(MSG) –HIS–ARG–LYS +CAN +S-AEC	1 day	30ºC	can1Δ::STE2pr-HIS3, lyp1Δ
7. Double mutant selection 1	SD(MSG) –HIS–ARG–LYS–URA +CAN +S-AEC +G418	2 days	30ºC	can1Δ::STE2pr-HIS3, lyp1Δ, YYYΔ::Kan^r, ura3Δ::URA3/ GAL1pr-S177W-GFP
8. Double mutant selection 2	SD(MSG) –HIS–ARG–LYS–URA +CAN +S-AEC +G418	2 days	30ºC	can1Δ::STE2pr-HIS3, lyp1Δ, YYYΔ::Kan^r, ura3Δ::URA3/ GAL1pr-S177W-GFP
9. Tests	750 Na SD(MSG) –HIS–ARG–LYS–URA +CAN +S-AEC +G418 750 Na SGR(MSG) –HIS–ARG–LYS–URA +CAN +S-AEC +G418	2 days	30ºC	can1Δ::STE2pr-HIS3, lyp1Δ, YYYΔ::Kan^r, ura3Δ::URA3/ GAL1pr-S177W-GFP

Table 2-4: Yeast strains used in this study and primers used to generate these strains

name genotype plasmid
forward primer for genome insertion
reverse primer for genome insertion
forward primer for check PCR
reverse primer for check PCR

YMS613 MATalpha can1D::STE2pr-spHIS5 lyp1D::STE3pr-LEU2 LYS2+ his3D1 leu2D0 ura3D cyh2 #

YMS614 YMS613 + sur4D::Kanr pFA6a KAN MX6
ATTCGGCTTTTTTCCGTTTGTTTACGAAACATAAACAGTCGGTCGACGGATCCCCGGGTT
TTTTCTTTTTCATTCGCTGTCAAAAATTCTCGCTTCCTATTCGATGAATTCGAGCTCGTT
TGGTTTTTGACAGCTCTTCACTCG
GTATTCTGGGCCTCCATGTCG
YMS615 YMS613 + csg2D::Kanr pFA6a KAN MX6
GCTGGTGAGTTAGCACGATAACAAACAAAGATACAGCGTCGGTCGACGGATCCCCGGGTT
TGTTACATCATCATCAGTCATATAAAGTATGTTGTCCGTATCGATGAATTCGAGCTCGTT
GAGGCATGGTACTCCTTCTTATTC
GTATTCTGGGCCTCCATGTCG
YMS616 YMS613 + erv14D::Kanr pFA6a KAN MX6
CAATTAAAGTAAAGTAAAAAAATTAAGAATAAAAAGAAAAGGTCGACGGATCCCCGGGTT
TGGCCCTTCAGTCTTCTTTGGATTTCAATGTCTTGTTGGATCGATGAATTCGAGCTCGTT
TTAATACGAAGGAGAGACCTGG
GTATTCTGGGCCTCCATGTCG
YMS617 YMS613 + emp24D::Kanr pFA6a KAN MX6
TTAATAGTATCCCTCCGCACAAAAATACACACGCATAAGGGGTCGACGGATCCCCGGGTT
GCAAAAGTAAATAGATATGAACTACATTTTCCTGCTTTACTCGATGAATTCGAGCTCGTT
GACGCGAGGAAAGTCAGAAAAG
GTATTCTGGGCCTCCATGTCG
YMS618 YMS613 + erv25D::Kanr pFA6a KAN MX6
TATAACTCAGTTGATCTCATAAGTGAAAAGCAAAAAAAGGGGTCGACGGATCCCCGGGTT
AGCTGATACACAAATGCATGGTGTGGTCCTCTTCCTTTGCTCGATGAATTCGAGCTCGTT
CGCGTACAAAGAGTTTCTGG
GTATTCTGGGCCTCCATGTCG
YMS619 YMS613 + bst1D::Kanr pFA6a KAN MX6
TATCTTAGGCTTACCATCATACAAAAATCTTCATTTCGTTGGTCGACGGATCCCCGGGTT
GCAATATATACAGTTAATCTTTTTTTACTGGGTTGTAGTTTCGATGAATTCGAGCTCGTT
GGCGCGAATTTTGAAAAAGG
GTATTCTGGGCCTCCATGTCG
YMS620 YMS613 + YIL039WD::Kanr pFA6a KAN MX6
CTGAAAACAACAGCAGCAGCATTGTACCAAGAATCCCAAGGGTCGACGGATCCCCGGGTT
ATCTCTATACAGGAGTTTTATCTTCTTTACTCTTTTTTGTTCGATGAATTCGAGCTCGTT
GCTAGATTCCTCCCCTAGTCAC
GTATTCTGGGCCTCCATGTCG
YMS621 MATalpha can1D::STE2pr-spHIS5 lyp1D::STE3pr-LEU2 LYS2+ his3D1 leu2D0 ura3D::URA3/GAL1pr-no insert cyh2 empty pYES2-2micron origin ###
AGTTTTGACCATCAAAGAAGGTTAATGTGGCTGTGGTTTCgggtaataactgatataatt
AGCTTTTTCTTTCCAATTTTTTTTTTTTTCGTCATTATAGAgcaaattaaagccttcgagc
CGACGTTGAAATTGAGGCTACTGCGCCA
GCGGCCAGCAAAACTAAAAAACTGTATT
YMS622 MATalpha can1D::STE2pr-spHIS5 lyp1D::STE3pr-LEU2 LYS2+ his3D1 leu2D0 ura3D::URA3/GAL1pr-Kir3.2S177W-GFP cyh2 Kir3.2S177W-GFP in pYES2-2micron origin ##
AGTTTTGACCATCAAAGAAGGTTAATGTGGCTGTGGTTTCgggtaataactgatataatt
AGCTTTTTCTTTCCAATTTTTTTTTTTTTCGTCATTATAGAgcaaattaaagccttcgagc
CGACGTTGAAATTGAGGCTACTGCGCCA

GCGGCCAGCAAAACTAAAAAACTGTATT

YMS623 YMS622 + sur4D::Kanr pFA6a KAN MX6
ATTCGGCTTTTTTCCGTTTGTTTACGAAACATAAACAGTCGGTCGACGGATCCCCGGGTT
TTTTCTTTTTCATTCGCTGTCAAAAATTCTCGCTTCCTATTCGATGAATTCGAGCTCGTT
TGGTTTTTGACAGCTCTTCACTCG
GTATTCTGGGCCTCCATGTCG

YMS624 YMS622 + csg2D::Kanr pFA6a KAN MX6
GCTGGTGAGTTAGCACGATAACAAACAAAGATACAGCGTCGGTCGACGGATCCCCGGGTT
TGTTACATCATCATCAGTCATATAAAGTATGTTGTCCGTATCGATGAATTCGAGCTCGTT
GAGGCATGGTACTCCTTCTTATTC
GTATTCTGGGCCTCCATGTCG

YMS625 YMS622 + erv14D::Kanr pFA6a KAN MX6
CAATTAAAGTAAAGTAAAAAAATTAAGAATAAAAAGAAAAGGTCGACGGATCCCCGGGTT
TGGCCCTTCAGTCTTCTTTGGATTTCAATGTCTTGTTGGATCGATGAATTCGAGCTCGTT
TTAATACGAAGGAGAGACCTGG
GTATTCTGGGCCTCCATGTCG

YMS626 YMS622 + emp24D::Kanr pFA6a KAN MX6
TTAATAGTATCCCTCCGCACAAAAATACACACGCATAAGGGGTCGACGGATCCCCGGGTT
GCAAAAGTAAATAGATATGAACTACATTTTCCTGCTTTACTCGATGAATTCGAGCTCGTT
GACGCGAGGAAAGTCAGAAAAG
GTATTCTGGGCCTCCATGTCG

YMS627 YMS622 + erv25D::Kanr pFA6a KAN MX6
TATAACTCAGTTGATCTCATAAGTGAAAAGCAAAAAAAGGGGTCGACGGATCCCCGGGTT
AGCTGATACACAAATGCATGGTGTGGTCCTCTTCCTTTGCTCGATGAATTCGAGCTCGTT
CGCGTACAAAGAGTTTCTGG
GTATTCTGGGCCTCCATGTCG

YMS628 YMS622 + bst1D::Kanr pFA6a KAN MX6
TATCTTAGGCTTACCATCATACAAAAATCTTCATTTCGTTGGTCGACGGATCCCCGGGTT
GCAATATATACAGTTAATCTTTTTTTACTGGGTTGTAGTTTCGATGAATTCGAGCTCGTT
GGCGCGAATTTTGAAAAAGG
GTATTCTGGGCCTCCATGTCG

YMS629 YMS622 + YIL039WD::Kanr pFA6a KAN MX6
CTGAAAACAACAGCAGCAGCATTGTACCAAGAATCCCAAGGGTCGACGGATCCCCGGGTT
ATCTCTATACAGGAGTTTTATCTTCTTTACTCTTTTTTGTTCGATGAATTCGAGCTCGTT
GCTAGATTCCTCCCCTAGTCAC
GTATTCTGGGCCTCCATGTCG

YMS630 MATalpha trk1D::URA3/MET25pr-empty trk2D::Natr can1D::STE2pr-spHIS5 lyp1D::STE3pr-LEU2 LYS2+ his3D1 leu2D0 ura3D0 cyh2 empty pYESMET25-2micron origin ### and pFA6a NAT
trk1D:CATTTTACTTAAAGTTATTACCTTTTTTTTGATAACTAACAgggtaataactgatataatt
trk2D:TGTACTATTCACCGACGATAAGAGGCTGTAAGAACCACTCGGTCGACGGATCCCCGGGTT
trk1D:TTGAGTACGAAAACCTATTTCTAAAGAATGAGTATATATGgcaaattaaagccttcgagc
trk2D:ACGTTGGCTCTTATGTAGGTAAAGAGGGGTAAACTTGATTTCGATGAATTCGAGCTCGTT
trk1D:CCTTTCGCCCATTGTTTTTA
trk2D:GTTTCCCGTTTCTCTCTTTCAC
trk1D:GCGGCCAGCAAAACTAAAAAACTGTATT
trk2D:GTATTCTGGGCCTCCATGTCG

YMS631 MATalpha trk1D::URA3/MET25pr-Kir3.2V188G-GFP trk2D::Natr can1D::STE2pr-spHIS5 lyp1D::STE3pr-LEU2 LYS2+ his3D1 leu2D0 ura3D0 cyh2 Kir3.2V188G-GFP in pYESMET25-2micron origin ## and pFA6a NAT
trk1D:CATTTTACTTAAAGTTATTACCTTTTTTTTGATAACTAACAgggtaataactgatataatt
trk2D:TGTACTATTCACCGACGATAAGAGGCTGTAAGAACCACTCGGTCGACGGATCCCCGGGTT
trk1D:TTGAGTACGAAAACCTATTTCTAAAGAATGAGTATATATGgcaaattaaagccttcgagc
trk2D:ACGTTGGCTCTTATGTAGGTAAAGAGGGGTAAACTTGATTTCGATGAATTCGAGCTCGTT
trk1D:CCTTTCGCCCATTGTTTTTA
trk2D:GTTTCCCGTTTCTCTCTTTCAC
trk1D:GCGGCCAGCAAAACTAAAAAACTGTATT
trk2D:GTATTCTGGGCCTCCATGTCG

YMS632 YMS631 + sur4D::Kanr pFA6a KAN MX6
ATTCGGCTTTTTTCCGTTTGTTTACGAAACATAAACAGTCGGTCGACGGATCCCCGGGTT
TTTTCTTTTTCATTCGCTGTCAAAAATTCTCGCTTCCTATTCGATGAATTCGAGCTCGTT
TGGTTTTTGACAGCTCTTCACTCG
GTATTCTGGGCCTCCATGTCG
YMS633 YMS631 + csg2D::Kanr pFA6a KAN MX6
GCTGGTGAGTTAGCACGATAACAAACAAAGATACAGCGTCGGTCGACGGATCCCCGGGTT
TGTTACATCATCATCAGTCATATAAAGTATGTTGTCCGTATCGATGAATTCGAGCTCGTT
GAGGCATGGTACTCCTTCTTATTC
GTATTCTGGGCCTCCATGTCG
YMS634 YMS631 + erv14D::Kanr pFA6a KAN MX6
CAATTAAAGTAAAGTAAAAAAATTAAGAATAAAAAGAAAAGGTCGACGGATCCCCGGGTT
TGGCCCTTCAGTCTTCTTTGGATTTCAATGTCTTGTTGGATCGATGAATTCGAGCTCGTT
TTAATACGAAGGAGAGACCTGG
GTATTCTGGGCCTCCATGTCG
YMS635 YMS631 + emp34D::Kanr pFA6a KAN MX6
TTAATAGTATCCCTCCGCACAAAAATACACACGCATAAGGGGTCGACGGATCCCCGGGTT
GCAAAAGTAAATAGATATGAACTACATTTTCCTGCTTTACTCGATGAATTCGAGCTCGTT
GACGCGAGGAAAGTCAGAAAAG
GTATTCTGGGCCTCCATGTCG
YMS636 YMS631 + erv25D::Kanr pFA6a KAN MX6
TATAACTCAGTTGATCTCATAAGTGAAAAGCAAAAAAAGGGGTCGACGGATCCCCGGGTT
AGCTGATACACAAATGCATGGTGTGGTCCTCTTCCTTTGCTCGATGAATTCGAGCTCGTT
CGCGTACAAAGAGTTTCTGG
GTATTCTGGGCCTCCATGTCG
YMS637 YMS631 + bst1D::Kanr pFA6a KAN MX6
TATCTTAGGCTTACCATCATACAAAAATCTTCATTTCGTTGGTCGACGGATCCCCGGGTT
GCAATATATACAGTTAATCTTTTTTTACTGGGTTGTAGTTTCGATGAATTCGAGCTCGTT
GGCGCGAATTTTGAAAAAGG
GTATTCTGGGCCTCCATGTCG
YMS638 YMS631 + YIL039WD::Kanr pFA6a KAN MX6
CTGAAAACAACAGCAGCAGCATTGTACCAAGAATCCCAAGGGTCGACGGATCCCCGGGTT
ATCTCTATACAGGAGTTTTATCTTCTTTACTCTTTTTTGTTCGATGAATTCGAGCTCGTT
GCTAGATTCCTCCCCTAGTCAC
GTATTCTGGGCCTCCATGTCG
deletion library MATa: YYYΔ::Kanr CAN1 LYP1 LYS2+ his3Δ1 leu2Δ0 ura3Δ0 met15Δ0 pFA6a KAN MX6
see Saccharomyces Genome Deletion Project
(http://www-sequence.stanford.edu/group/yeast_deletion_project/deletions3.html)

YMS660 MATalpha ade1-100 leu2-3 leu2-112 ura3-52 ####

YMS661 MATalpha ade1-100 leu2-3 leu2-112 ura3-52 MAL2 transformed with pma1-105::URA3 fragment ####

kindly provided by Charles Boone and Amy Tong, reference: Tong et al. 2001, Science Vol. 294 pp2364-2368"
Mouse Kir3.2S177W and Kir3.2V188G (Yi et al, 2001, Neuron, Vol. 29, pp. 657-667; Bichet et al. 2004, PNAS Vol. 101, No. 13, pp. 4441-4446) were cloned into pYES2 (Invitrogen) and pYESMET25 (Minor et al. 1999, Cell, Vol. 96, pp. 879-891), respectively. The 2µ origin was removed using NdeI and NgoMIV followed by blunt end ligation. Channels were tagged with eGFP (Clontech) at the C-terminus. "
pYES2-2µ origin and pYESMET25-2µ origin without inserts were used as PCR templates.
kind gift of James E. Haber, strain YMS660 = A612 in Haber lab collection, YMS661 = SN19, reference: Perlin et al. 1988, JBC Vol. 263, No. 34, pp. 18118-18122"

Supplemental methods

Yeast Strains

Yeast strains were either picked from the yeast deletion library (Giaever et al., 2002) or re-constructed by PCR-mediated gene disruption in a BY4742 (Brachmann et al., 1998) derived background (MATalpha *can1*Δ::STE2pr-*spHIS5* *lyp1*Δ::STE3pr-*LEU2* *LYS2*$^{+}$ *MET*$^{+}$ *his3*Δ1 *leu2*Δ0 *ura3*Δ *cyh2*, a kind gift from Amy Tong and Charles Boone). Table 2-4 lists strains, primers and plasmids. Mouse Kir3.2S177W and Kir3.2V188G (Yi et al., 2001; Bichet et al., 2004) were cloned into pYES2 (Invitrogen) and pYESMET25 (Minor et al., 1999), respectively. Channels were tagged with eGFP (Clontech) at the C-terminus. For integration into the yeast genome, the 2μ origin was removed from pYES2 and pYESMET25 using NdeI and NgoMIV followed by blunt end ligation. Integration of gene disruption cassettes was confirmed by colony PCR.

Yeast Media

Synthetic media (SD or SGR) was prepared from 1.7 g yeast nitrogen base without amino acids and without ammonium sulfate (Difco), 2 g amino acid drop out powder containing all amino acids except those used for selection (Treco and Lundblad, 1993) (amino acids from Sigma), 1 g monosodium glutamic acid (Sigma), and either 20 g dextrose (Riedel-de Haen) or 20 g galactose (Sigma) and 20 g raffinose (Acros) in 1 liter water. Rich media (YPAD or YPAGR) was prepared from 10 g yeast extract (Difco), 20 g peptone (Difco), 120 mg adenine (Sigma) and either 20 g dextrose or 20 g galactose and 20 g raffinose in

1 liter water. Yeast plates contained 2% agar (Difco). For high Na^+ tests, 500 mM NaCl (Fisher) was added to the media. Geneticin (Invitrogen) was used at 200 mg/L, ClonNat (Werner Biotechnology) at 100 mg/L, hygromycin (Invitrogen) at 500 mg/L. Low Salt plates were prepared from 15 g Seakem LE agarose (BMA), 2.1 g free arginine base (Sigma), 1 ml 1 M $MgSO_4$, 100 ml 1 M $CaCl_2$, 1.5 g dropout powder, 20 g dextrose, 2 ml 500x trace minerals (Q Biogene), 1 ml 1000x vitamins (Nakamura and Gaber, 1998) in 1 liter water and adjusted to pH 6.0 with phosphoric acid. KCl was added to 100 mM or 0.5 mM.

Yeast Screen

A subset of the yeast deletion library (Giaever et al., 2002) consisting of 376 yeast strains (Table 2-2) each carrying a deletion in an early secretory pathway-localized protein (Schuldiner et al., 2005) was mated to yeast expressing Kir3.2S177W-GFP using a modified version of the method for Synthetic Genetic Array analysis (Schuldiner et al., 2006). The selection scheme is shown in Table 2-3. After sporulation, strains were plated in triplicate. Growth of the double mutant strains was tested on synthetic media containing 750 mM NaCl and dextrose or galactose, to repress or induce channel expression, respectively. Growth tests were performed in duplicate (diagonally pinned) for each of the triplicates. Plates were photographed using a ChemiImager Ready (Alpha Innotech Corp.) and colony sizes, S_{gal} and S_{dex}, measured using software developed by Collins et al. (Collins et al., 2006). Colony sizes were analyzed by calculating the difference in size of each colony on galactose versus dextrose

(S_{gal}*100/S_{dex} – 100). Initial Na^+-tolerant candidates had to meet the criterion that four out of six replicates or the average of the six colony size differences |S_{gal}*100/S_{dex} – 100| were smaller than the average |S_{gal}*100/S_{dex} – 100| for all strains tested minus one standard deviation.

Yeast Media for screen

Yeast media was prepared according to (Schuldiner et al., 2006). For tests on high Na^+, the following media was prepared analogously to the procedures for single mutant and double mutant selection plates described in (Schuldiner et al., 2006):

Na test: 750 mM Na SD(MSG)-HIS-ARG-LYS-URA+CAN+S-AEC+G418+citrate

agar [g]	20
water [ml]	700

YNB -aa -(NH4)SO4 [g]	1.7
aa -HIS-ARG-LYS-URA [g]	2
MSG [g]	1
40% dextrose [ml]	50
water [ml]	250
100 mg/ml canavanine [ml]	0.5
100 mg/ml S-AEC [ml]	0.5
50 mg/ml geneticin [ml]	4
Na_3 citrate [g]	5.9
NaCl [g]	40.3

pH 7 with 1 M Tris

Na test: 750 mM Na SGR(MSG)-HIS-ARG-LYS-URA+CAN+S-AEC+G418+citrate

agar [g]	20
water [ml]	700

YNB -aa -(NH4)SO4 [g]	1.7
aa -HIS-ARG-LYS-URA [g]	2
MSG [g]	1
20% galactose [ml]	100
20% raffinose [ml]	100
water [ml]	100
100 mg/ml canavanine [ml]	0.5
100 mg/ml S-AEC [ml]	0.5
50 mg/ml geneticin [ml]	4
Na_3 citrate [g]	5.9
NaCl [g]	40.3

pH 7 with 1 M Tris

Barium test

Control yeast (BY4742 background) with or without a genomic insertion of Kir* were plated in a lawn on 500 mM NaCl YPAGR media. Filter disks (Whatman, 1 cm diameter) soaked in 100 µl water or 100 µl 100 mM $BaCl_2$ were placed on the lawns as described in (Chatelain et al., 2005). Photographs were taken two or three days after plating.

Growth assays

Doubling times and growth rates were determined at 30°C by diluting over night cultures to about 2 * 10^6 cells/ml into 2 ml media, allowing the cells to adjust for one hour before measuring the 0 hour (t0) optical density (OD) at 660 nm in a spectrophotometer (Ultrospec 21000 Pro, Amersham). The second time point (t1) was measured 4 h (for YPAGR) or 8 h (for 500mM NaCl YPAGR, 500 mM NaCl YPAD, 500 mM NaCl YPAGR with 500 mg/L hygromycin) later. Optical densities were converted to cell numbers (N) based on the polynomial

$$N\ [cells/ml] = 0.0219 + 1.3223 * OD - 0.601 * OD^2 + 1.1309 * OD^3$$

fitted to the table published by (Amberg et al., 2005). Doubling times were calculated based on (Amberg et al., 2005):

$$t_{double} = (t1-t0) * \ln 2 / \ln(N_{t1}/N_{t0})$$

Relative growth rates with versus without hygromycin were calculated as:

relative growth rate with hygromycin/no hygromycin

$= t_{double}$ without hygromycin / t_{double} with hygromycin

(growth rate = $\ln 2 / t_{double}$).

For dilutions on rich media, over night cultures grown in YPAD or YPAGR were diluted to 2 * 10^5, 2 * 10^4, and 2 * 10^3 cells/ml in water and 2.5 ml drops spotted onto agar plates. For dilutions on Low Salt plates, over night cultures grown in 100 mM KCl SD-MET media were diluted to 10^6, 10^5, and 10^4 cells/ml in 25% glycerol and 10 ml drops spotted onto agar plates. 25% glycerol was used to overcome the high surface tension of water on Low Salt plates, which caused the cells to clump at the center of the drops as the water evaporated. Photographs were taken three days after plating.

Western sample preparation

Yeast protein samples were prepared by the post-alkaline lysis method (Kushnirov, 2000). Briefly, 2 * 10^7 cells from an over night culture were pelleted at 1,000 g for 1 minute and resuspended in 100 ml water. 100 ml 0.2 M NaOH was added and the cells incubated for 4 minutes at RT, followed by pelleting for 1 min at 1,000 g and resuspension in 200 ml sample buffer (60 mM TrisHCl pH6.8, 2% SDS, 10% glycerol, 0.0025% bromophenol blue, 4% b-mercaptoethanol), and heating to 95°C for 3 minutes. Proteins were separated on 10% Bis-tris gels in MOPS running buffer (Invitrogen) with antioxidant (Invitrogen) in the upper chamber or on 10% Tris-glycine gels (BioRad) in Tris-glycine buffer and transferred in Tris-glycine-methanol buffer to PVDF membrane (Millipore). Membranes were blocked with 3% milk and probed with rabbit anti-GIRK2 1:1000 (Alomone), mouse anti-PGK 1:1000 (Molecular Probes), or rabbit anti-Gas1p 1:2500 (Walter lab) antibodies. Binding of HRP conjugated secondary

antibodies 1:10,000 (Jackson Immuno) was detected using Pico ECL substrate (Pierce) and captured on film (Denville).

Imaging

Yeast strains were grown for 12 h in SGR media supplemented with adenine, fixed by addition of 8% methanol-free formaldehyde (Polysciences) in 2x PBS for 1 h at RT, washed once with PBS, and mounted in DAPI containing Prolong Gold antifade (Molecular Probes). Imaging was performed with a widefield epifluorescence Exfo X-Cite 120 source connected to a Nikon TE2000 inverted microscope using a CFI Plan Apochromat TIRF 100x objective (NA 1.49) and Photometrics CoolSnap HQ2 camera. Optical z stacks (100 nm thickness, 47 planes, 300 ms exposure per plane) were acquired using Nikon Elements AR 2.30 imaging software. Stacks were deconvolved with 3D blind deconvolution algorithms using MediaCybernetics AutoDeblur X1.4.1. Images presented are single planes from the middle and top of deconvolved stacks. A single image of DAPI fluorescence at the center of the cells was acquired (not shown).

Unfolded protein response assay

The YMS612 strain contains a genomically integrated reporter construct consisting of four repeats of the Unfolded Protein Response Element (UPRE) upstream of GFP immediately followed by mCherry RFP driven from a TEF2 promoter. The mCherry served as a normalization reference to compensate for

changes in cell fluorescence due to cell growth rates and abnormal size distributions that were unrelated to UPR induction. Single mutants expressing the reporter were made by mating YMS612 with strains taken from the MATa KAN^r yeast deletion library (Giaever et al., 2002). Diploids were made using a NAT^r cassette.

Strains were inoculated in 25 µl YEPD and allowed to saturate overnight in a 384 well plate at 30°C without shaking. They were observed to reach OD_{600}=8-9. Cultures were back-diluted to OD=0.08-0.09, incubated for 4.5-5.5 h until they reached OD=0.3-0.6 and injected into a Becton Dickinson LSRII flow cytometer using a high throughput sampler (Newman et al., 2006). The normalized GFP/RFP fluorescence ratio for each sample was obtained by taking the median of the GFP to RFP ratios of all events in a sample. The reported values represent means of the GFP/RFP fluorescence ratio of at least two measurements. Error bars represent standard error of the mean.

Chapter 3: Conclusions and future directions

The life of Kir channel proteins begins with the translation of channel mRNAs at the ribosome. The nascent channel subunits are threaded into the membrane of the endoplasmic reticulum where they fold and assemble with other subunits into tetrameric channels. The channels then travel through the secretory pathway to the plasma membrane, where the mature channels fulfill their physiological roles. The life of Kir channels ends when endocytosed channels are targeted for degradation in lysosomes instead of recycled back to the plasma membrane. Throughout their lifetimes, Kir channels interact with many cellular proteins. For my thesis project, I was interested in identifying proteins that are necessary for the formation of functional Kir channels. Given that many of the interwoven steps of Kir channel biosynthesis, trafficking and function at the plasma membrane involve basic cell biological functions, we chose the yeast *Saccharomyces cerevisiae* as a simple screening platform to identify cellular proteins and processes required for Kir channel function at the plasma membrane.

Yeast had previously been used to study structure-function relationships of Kir channels. We took advantage of the knowledge gained from these studies to develop a high-throughput assay in which expression of a mutated, Na^+ permeable Kir channel resulted in yeast growth inhibition. We then used two genetic tools available in yeast to identify yeast proteins required for functional expression of the Kir channel. First, a consortium of labs has generated a library of yeast strains each lacking a single non-essential gene (Giaever et al., 2002). Second, the mating and random spore selection scheme developed for Synthetic

Genetic Array analysis can be used to introduce transgenes into the entire yeast deletion library with relatively little effort (Tong et al., 2001; Schuldiner et al., 2006). Although we initially introduced a mammalian Kir channel into the entire deletion library, narrowing the set of deletion strains tested to 376 strains lacking proteins localized to the early secretory pathway allowed us to generate each strain in triplicate, and to thereby gain confidence in the resulting growth phenotypes. Following identification of seven candidates by our screen, we recreated the deletion strains by PCR-mediated gene disruption, to confirm the correct identification of the deletions and rule out differences in the genetic background, differences in the transgene, or effects of mating type. The resulting yeast strains produced reliable phenotypes with regard to growth in different media, distribution of the GFP-tagged channel, and expression levels of the channel. The clonal nature of the strains and the ability to store the strains at –80 degrees Celsius for extended periods of time increased the reproducibility of the results and reduced the variability in the experimental system.

The strategy of using yeast as a model system to study mammalian Kir channels has limitations. Since yeast do not express endogenous Kir channels (only a distantly related two-pore K^+ channel encoded by *TOK1*), we could not expect to identify proteins that specifically interact with mammalian Kir channels. However, the basic components of ER translocation, ER quality control, and the secretory pathway are well conserved in eukaryotes. Therefore, our goal was to identify basic cellular machinery involved in Kir channel biosynthesis, trafficking, and function. The identification by our screen of seven proteins that fulfill

conserved cellular functions and have homologs in other eukaryotes including mammals validated our approach.

Since some of the deletion strains tested in our screen grew more slowly than control yeast, we normalized growth of yeast expressing the Kir channel to growth of yeast not expressing the channel. To make this comparison, we used the galactose inducible/ dextrose repressible Gal1 promoter to drive expression of the Kir channel. Induction of Kir channel expression on media containing 2% galactose led to high expression levels based on Western blot analysis of total protein levels and imaging of the GFP-tagged channel. It is possible that the predominant ER localization of the channel is, at least in part, due to the high expression levels, which may have led to less efficient ER export by the limited availability of endogenous trafficking machinery. Other artifacts due to over-expression are possible as well. For example, there may have been increased ER-associated degradation or overall increased channel turnover. Future studies using lower galactose concentrations to induce Kir channel expression or transgenes with weaker promoters may help to address these concerns. As discussed below, the role of the seven candidates identified by our screen will ultimately have to be studied in a mammalian system, preferably using a Kir channel expressed from its endogenous promoter.

A third caveat of using yeast as a model system is its intractability to electrophysiological assays. Ion channel biology is ultimately concerned with currents conducted by the channels, and electrophysiology has proven to be a sensitive and versatile technique to characterize ion channel function. Without

electrophysiological recordings, it will be difficult to distinguish effects of the gene deletions on Kir channel abundance at the plasma membrane from changes in single channel properties. We attempted to use imaging and biochemical (cell surface biotinylation) techniques to approach this question, but without success. Although no well-informed estimates of the number of heterologously expressed Kir channels at the cell surface of yeast have been made, our hunch is that the number is small. Even though assays of Kir channel expression at the cell surface of yeast may not be possible, two other approaches may be applied to the study of Kir channels in the yeast deletion strains identified by our screen. The first experiment would be based on the idea of using glycosylation as a marker for progression through the secretory pathway. Kir3.2, the channel studied in our screen, can form heterotetramers with Kir3.1, which cannot leave the ER in the absence of Kir3.2 (Kennedy et al., 1996; Stevens et al., 1997). Kir3.1 is glycosylated at position N119 (Pabon et al., 2000). Glycosylation begins with the attachment of several core sugar molecules in the ER, which shifts the size of the Kir3.1 protein on Western blots by a few kDalton. In the Golgi, the sugars are modified by the addition of additional sugar molecules, thereby increasing the size of the Kir3.1 protein on Western blots by 10-20 kDalton. Pulse-chase studies followed by Western blotting of yeast expressing Kir3.1 and Kir3.2 in a control or deletion background could be used to assay whether the deletions identified by our screen delay the appearance of maturely glycosylated Kir3.1. The sensitivity of the assay may be enhanced by immunoprecipitating Kir3.1 followed by detection with a glycosylation-specific antibody, such as anti-

1,6-mannose. The second approach to studying the effects of the seven deletions identified by our screen in the yeast system would be to perform *in vitro* ER budding reactions. Schekman and colleagues have developed a reconstituted system that recapitulates budding of COPII vesicles from the ER (Shimoni and Schekman, 2002). By preparing ER membranes from control or deletion yeast strains and assaying for incorporation of Kir3.2 into COPII vesicles, the requirements for efficient Kir channel trafficking could be explored.

Ultimately, the results obtained by our yeast screen will only be meaningful if they can be translated into experimental insights in mammalian systems. One possible future direction extending the findings from our yeast screen to a mammalian system would be to study the mammalian homologs of the seven candidates we identified and test their role in Kir channel biosynthesis, trafficking, and function. We conducted pilot experiments using RNA interference (RNAi) knockdown of five of the candidate genes (ERV14 = CNIH4, EMP24 = TMED2, ERV25 = TMED10, BST1 = PGAP1, YIL039W = MPPE1) in human embryonic kidney (HEK293) cells. Initial attempts did not show reduced Kir3.2 surface expression following transfection of RNAis targeting CNIH4, TMED2, TMED10, PGAP1, or MPPE1. However, it is too early to conclude that there is no effect, because several aspects of the experiment would need optimization. The timing and efficiency of RNAi transfection may not have been optimal. We also did not pursue controls to establish that the RNAi reduces expression of the targeted RNA and protein (by quantitative reverse transcription-polymerase chain reaction (RT-PCR) or Western blotting). Although cell surface biotinylation of Kir3.2

channels works efficiently, the changes in surface expression may be subtle at steady state. It may be necessary to look at the rate of appearance of new channel proteins at the cell surface, or at the rate of trafficking of channel proteins at various steps along the secretory pathway. We did notice that transfection of RNAis targeting TMED2 and PAGP1 caused cell death in HEK293 cells. The cell death may have been a side effect of the RNAi transfection or indicate an essential function of these genes in human cells. An essential function of p24 proteins in mammals was suggested by the observation that knock-out of p23 (the mouse homolog of TMED10) is embryonic lethal (Denzel et al., 2000).

An alternative future direction to the pursuit of specific genes would be to investigate more generally the role of protein-protein and protein-lipid interactions in the formation of lipid microdomains and their effects on Kir channel biosynthesis, trafficking, and function. Many experimental results point to the importance of lipids in regulation ion channel function. For example, a crystal structure of the bacterial K^+ channel KcsA contained a tightly bound lipid molecule; Kir2.1 channels entered a silent conformation in cholesterol rich lipid domains; and all Kir channels studied to date are inactive in the absence of PIP_2. The results of our screen suggest new ways in which the lipid composition of biological membranes may not only regulate the function of Kir channels, but also affect their trafficking. As new technologies and tools for the study of lipids are being developed and adapted to the study of biological systems (e.g. fluorescence correlation spectroscopy, image correlation spectroscopy, single-

particle tracking, single-molecule fluorescence imaging, thinning out clusters while conserving stoichiometry of labeling) (Jacobson et al., 2007), it will be exciting to characterize the organizational effects exerted on each other by proteins and lipids.

Last but not least, future studies will focus on further characterization of YIL039W/TED1 and its human homolog MPPE1. Ted1p contains a predicted phosphoesterase domain, which may dephosphorylate proteins, lipids, or nucleic acids. Based on the localization of Ted1p to the ER, similar genetic interaction patterns and buffering genetic interactions between TED1 and EMP24 or ERV25, and the accumulation of Gas1p in the ER of *ted1*Δ yeast, we predict that dephosphorylation of the target protein(s) of Ted1p (or possibly lipids, less likely nucleic acids) aids in packaging of Emp24p/Erv25p-dependent cargo molecules into COPII vesicles. A potential target for Ted1p is Rvs167p, which was found in a physical complex with Ted1p and is phosphorylated by Pho85-Pcl1. However, other components of the ER export machinery are phosphorylated as well (e.g. Sec31, (Salama et al., 1997)) and could potentially be dephosphorylated by Ted1p.

During my thesis work, I came across three observations that may be of interest to other scientists, but that I did not pursue. These observations are described in the Appendix. First, analysis of yeast deletion strains showing enhanced Na^+ sensitivity when expressing Kir* revealed that most of these strains carried deletions in proteins required for vacuole function. It may thus be possible to identify new genes involved in vacuolar morphogenesis or function

based on Na^+ sensitivity conferred by Kir*. Two candidates from our screen would be *YHR151C* and *YOR092W* (*ECM3*).

Second, we attempted to implement a second screen based on rescue of *trk1*Δ *trk2*Δ yeast by Kir3.2V188G. The screen did not yield any results, because most triple deletion strains were slow growing. Future studies may address whether loss of TRK1 and/or TRK2 in fact leads to widespread synthetic lethal interactions with other genes. Characterization of the genetic interaction profiles of TRK1 and/or TRK2 may provide new insights into the role of ionic gradients and the membrane potential in cellular functions such as nutrient uptake, cell wall biosynthesis, trafficking, or protein localization at the plasma membrane.

Third, although many labs use Kir channels carrying extracellular tags, such as the hemagglutinin (HA) tag, my results in yeast showed that these channels do no function in the same manner as their untagged counterparts. Given the importance of extracellular tags as a research tool in the study of Kir channels, it will be important to carefully assess the functionality of tagged Kir channels in the experimental system under study.

Appendix

1 Na^+ sensitive yeast

The yeast screen aimed at identifying yeast proteins involved in K^+ channel functional expression was initially performed with the entire set of yeast strains (about 5,000) carrying deletions in non-essential genes. For at least two reasons, this screen did not allow us to identify strains that grew well under high Na^+, Kir3.2S177W-inducing conditions. First, although Kir3.2S177W slowed yeast growth at low densities as tested by dilutions on agar plates, the phenotype was not pronounced at the high densities plated by the yeast robot used for the screen. Later on we discovered that tagging Kir3.2S177W C-terminally with GFP enhanced the slow growth phenotype on high Na^+ media, which, in addition to performing the pinning by hand, may explain why the screen focused on the early secretory pathway localized proteins yielded convincing results. Second, due to the large number of strains in the complete deletion library, the tests were only performed in duplicate. Without the comparison across multiple independent colonies, it was not possible to identify Na^+ tolerant candidates with reasonable confidence.

However, several strains showed enhanced Na^+ sensitivity when expressing Kir3.2S177W. We analyzed the Na^+-sensitive strains because they may have had enhanced Kir3.2S177W expression at the cell surface. The initial Na^+ sensitive strains carried deletions in genes from four functional categories: (i) 2 HOG pathway components, (ii) 12 mitochondrial proteins, (iii) 6 genes required for galactose metabolism, (iv) 33 genes involved in vacuole morphogenesis and

function. A further 6 genes with miscellaneous functions and 7 genes with unknown functions were identified. The strains were retested by plating dilutions on 0 mM NaCl, 375 mM NaCl, 750 mM NaCl, or 1 M sorbitol YPAD or YPAGR. Table A-1 lists the strains that were slow growing on 375 mM or 750 mM NaCl YPAGR (Kir3.2S177W induction), but grew similarly to control strains on all other media. The HOG pathway deletion strains were eliminated because they were slow growing on high salt media even when they did not express Kir3.2S177W. The mitochondrial deletion strains were slow growing in general. The galactose metabolism deletion strains were unable to grow on galactose media. The miscellaneous and several of the unknown gene deletion strains were also eliminated, because they showed growth defects on media other than high Na^+ YPAGR.

Almost all of the remaining strains carried deletions in genes whose products are needed for vacuole function. Although it remains possible that the Na^+ sensitive yeast strains expressed more Kir3.2S177W at the cell surface, it seems more likely that expression of Kir3.2S177W even at low levels enhanced the Na^+ sensitive phenotype seen in vacuolar protein deletion strains due their reduced ability to sequester Na^+ in the vacuole. Warringer et al. (Warringer et al., 2003) observed Na^+ sensitivity in many of the candidates identified by our screen.

A potentially interesting finding is the identification of *YHR151C* and *YOR092W* (*ECM3*). Both ORFs encode proteins of unknown function. Based on genetic and physical interaction data, *YHR151C* and *YOR092W* may play a role in vacuole morphogenesis or function. For example, *YHR151C* showed genetic

interactions with *SWF1* (Tong et al., 2004), which may play a role in vacuole fusion. A yeast two-hybrid screen identified *YOR092W* as an interacting partner of *PPA1*, a component of the vacuolar ATPase (Miller et al., 2005). A role for *YHR151C* and *YOR092W* in vacuole function would be supported by their identification in our screen. However, *YHR151C* and *YOR092W* also show many other interactions.

I remade the deletions *yhr151c*Δ and *yor092w*Δ by PCR-mediated gene disruption and confirmed the Na^+ sensitivity of the deletion strains when they express Kir3.2S177W. I also generated strains in which *YHR151C* or *YOR092W* are GFP tagged at the C-terminus to assay their subcellular localization. Upon cursory imaging, no signal was detected. However, further analysis with a more sensitive microscope and camera should be performed. The relevant strains are Y#153 through Y#162.

Table A-1: Na^+ sensitive yeast					
#	ORF name	name	description		
34	YKR001C	VPS1, GRD1, LAM1, SPO15, VPL1, VPT26	GTPase required for vacuolar protein sorting, functions in actin cytoskeleton organization via its interaction with Sla1p; required for late Golgi-retention of some proteins including Kex2p; involved in regulating peroxisome biogenesis	class F	dynamin related GTPase, retrieval of VPS10
9	YDR080W	VPS41, CVT8, FET2, SVL2, VAM2, VPL20	Vacuolar membrane protein that is a subunit of the homotypic vacuole fusion and vacuole protein sorting (HOPS) complex; essential for membrane docking and fusion at the Golgi-to-endosome and endosome-to-vacuole stages of protein transport	class B	vacuole fusion, tethering
61	YDL077C	VAM6, CVT4, VPL18, VPL22, VPS39	Vacuolar protein that plays a critical role in the tethering steps of vacuolar membrane fusion by facilitating guanine nucleotide exchange on small guanosine triphosphatase Ypt7p	class B	vacuole fusion, tethering
22	YGL212W	VAM7, VPS43	Component of the vacuole SNARE complex involved in vacuolar morphogenesis; SNAP-25 homolog; functions with a syntaxin homolog Vam3p in vacuolar protein trafficking	class B	vacuole fusion, tethering
3	YML001W	YPT7 (AST4, VAM4)	GTPase; GTP-binding protein of the rab family; required for homotypic fusion event in vacuole inheritance, for endosome-endosome fusion, similar to mammalian Rab7		GTPase, nucleotide exchange stimulated by VPS39
5	YOR068C	VAM10	Protein involved in vacuole morphogenesis; acts at an early step of homotypic vacuole fusion that is required for vacuole tethering		vacuole fusion
62	YGL124C	MON1, AUT12	Protein required for fusion of cvt-vesicles and autophagosomes with the vacuole; associates, as a complex with Ccz1p, with a perivacuolar compartment; potential Cdc28p substrate		vacuole fusion
66	YNL296W	N/A	Hypothetical protein, overlaps MON2/YNL297C (=Peripheral membrane protein with a role in endocytosis and vacuole integrity, interacts with Arl1p and localizes to the endosome; member of the Sec7p family of proteins)		vacuole fusion
29	YPR173C	VPS4, CSC1, END13, GRD13, VPL4, VPT10, DID6	AAA-type ATPase required for efficient late endosome to vacuole transport; catalyzes the release of an endosomal membrane-associated class E VPS protein complex; cytoplasmic protein that is also associated with an endosomal compartment	class E	interacts with ESCRT III complex
35	YKR035W-A	DID2, FTI1, CHM1, VPS46	Class E protein of the vacuolar protein-sorting (Vps) pathway, associates reversibly with the late endosome, has human ortholog that may be altered in breast tumors	class E	interacts with ESCRT III complex
37	YKR035C	OPI8 (reserved name)	Dubious open reading frame unlikely to encode a protein, based on available experimental and comparative sequence data; partially overlaps verified gene DID2(FTI1, CHM1, VPS46)/YKR035W-A	overlaps DID2, VPS46	interacts with ESCRT III complex
58	YDR486C	VPS60, MOS10, CHM5	Cytoplasmic and vacuolar membrane protein involved in late endosome to vacuole transport; required for normal filament maturation during pseudohyphal growth; may function in targeting specific cargo proteins for degradation	class E	interacts with ESCRT III complex
7	YDR069C	DOA4, DOS1, MUT4, NPI2, SSV7, UBP4	Ubiquitin hydrolase, required for recycling ubiquitin from proteasome-bound ubiquitinated intermediates, acts at the late endosome/prevacuolar compartment to recover ubiquitin from ubiquitinated membrane proteins en route to the vacuole	class E	interacts with ESCRT III complex

48	YNR006W	VPS27, GRD11, SSV17, VPL23, VPL27, VPT27, DID7	Endosomal protein that forms a complex with Hse1p; required for recycling Golgi proteins, forming lumenal membranes and sorting ubiquitinated proteins destined for degradation; has Ubiquitin Interaction Motifs which bind ubiquitin (Ubi4p)	class E	ESCRT 0
38	YJL053W	PEP8, GRD6, VPS26, VPT4	Vacuolar protein sorting protein that forms part of the multimeric membrane-associated retromer complex along with Vps35p, Vps29p, Vps17p, and Vps5p; essential for endosome-to-Golgi retrograde protein transport	class F	retromer complex, cargo selection subcomplex
16	YHR012W	VPS29	Endosomal protein that is a subunit of the membrane-associated retromer complex essential for endosome-to-Golgi retrograde transport; forms a subcomplex with Vps35p and Vps26p that selects cargo proteins for endosome-to-Golgi retrieval	class A	retromer complex, cargo selection subcomplex
25	YJL154C	VPS35, GRD9, VPT7	Endosomal protein that is a subunit of the membrane-associated retromer complex essential for endosome-to-Golgi retrograde transport; forms a subcomplex with Vps26p and Vps29p that selects cargo proteins for endosome-to-Golgi retrieval	class A	retromer complex, cargo selection subcomplex
20	YOR132W	VPS17, PEP21	Subunit of the membrane-associated retromer complex essential for endosome-to-Golgi retrograde protein transport; peripheral membrane protein that assembles onto the membrane with Vps5p to promote vesicle formation	class B	retromer complex, cargo selection subcomplex
21	YLR360W	VPS38, VPL17	Part of a Vps34p phosphatidylinositol 3-kinase complex that functions in carboxypeptidase Y (CPY) sorting; binds Vps30p and Vps34p to promote production of phosphatidylinositol 3-phosphate (PtdIns3P) which stimulates kinase activity	class A	retromer adaptor
10	YPL120W	VPS30, APG6, VPT30, ATG6	Protein that forms a membrane-associated complex with Apg14p that is essential for autophagy; involved in a retrieval step of the carboxypeptidase Y receptor, Vps10p, to the late Golgi from the endosome; involved in vacuolar protein sorting	class A	retromer adaptor
36	YKR020W	VPS51, WHI6, API3, VPS67	Component of the GARP (Golgi-associated retrograde protein) complex, Vps51p-Vps52p-Vps53p-Vps54p, which is required for the recycling of proteins from endosomes to the late Golgi; links the (VFT/GARP) complex to the SNARE Tlg1p	class B	GARP
57	YDR484W	VPS52, SAC2	Component of the GARP (Golgi-associated retrograde protein) complex, Vps51p-Vps52p-Vps53p-Vps54p, which is required for the recycling of proteins from endosomes to the late Golgi; involved in localization of actin and chitin	class B	GARP
42	YDR027C	VPS54, LUV1, CGP1, TCS3	Component of the GARP (Golgi-associated retrograde protein) complex, Vps51p-Vps52p-Vps53p-Vps54p, which is required for the recycling of proteins from endosomes to the late Golgi; potentially phosphorylated by Cdc28p	class B	GARP
26	YLR262C	YPT6	GTPase, Ras-like GTP binding protein involved in the secretory pathway, required for fusion of endosome-derived vesicles with the late Golgi, maturation of the vacuolar carboxypeptidase Y; has similarity to the human GTPase, Rab6		GTPase binds directly to GARP

45	YDL192W	ARF1	ADP-ribosylation factor, GTPase of the Ras superfamily involved in regulation of coated formation vesicles in intracellular trafficking within the Golgi; functionally interchangeable with Arf2p		GTPases
55	YBR164C	ARL1, DLP2	Soluble GTPase with a role in regulation of membrane traffic; regulates potassium influx; G protein of the Ras superfamily, similar to ADP-ribosylation factor		GTPases
33	YKL212W	SAC1, RSD1	Lipid phosphoinositide phosphatase of the ER and Golgi, involved in protein trafficking and secretion		
1	YAL026C	DRS2 (FUN38, SWA3)	Integral membrane Ca(2+)-ATPase involved in aminophospholipid translocation; required to form a specific class of secretory vesicles that accumulate upon actin cytoskeleton disruption; mutation affects maturation of the 18S rRNA		
8	YDR388W	RVS167	Actin-associated protein, subunit of a complex (Rvs161p-Rvs167p) involved in regulation of actin cytoskeleton, endocytosis, and viability following starvation or osmotic stress; homolog of mammalian amphiphysin		
30	YBL007C	SLA1	Cytoskeletal protein binding protein required for assembly of the cortical actin cytoskeleton; contains 3 SH3 domains		
32	YGR227W	DIE2, ALG10	Dolichyl-phosphoglucose-dependent glucosyltransferase of the ER		
4	YOR092W	ECM3 (YOR3165W)	Non-essential protein of unknown function		
15	YHR151C	N/A	Putative protein of unknown function		

2 K^+ screen

A second yeast screen aimed at identifying proteins involved in functional expression of Kir channels was based on growth rescue of *trk1*Δ *trk2*Δ yeast by expression of the K^+ selective, constitutively open channel Kir3.2V188G (Yi et al., 2001). The selection scheme used to obtain strains expressing Kir3.2V188G in a *trk1*Δ *trk2*Δ background with an additional deletion in a non-essential gene is shown in Table A-2.

In the first round of this screen, tests were performed on Low Salt media supplemented with 0.5 or 100 mM K^+. We expected most strains to grow well on media containing 100 mM K^+, because they would not rely on Kir3.2V188G expression for K^+ uptake. This was not the case. Overall most strains were slow growing even on 100 mM K^+. Due to the poor growth of the test strains on 100 mM K^+ media, the results of the screen could not be interpreted with respect to Kir channel trafficking.

In a second attempt to use the "K^+ screen," tests were performed on low and high pH synthetic media. Yeast strains lacking the K^+ transporters TRK1 and TRK2 are sensitive to low pH, a phenotype that can be rescued by expression of certain K^+ channels (Nakamura and Gaber, 1998), including Kir3.2V188G (Figure A-1). We reasoned that synthetic media may contain a better balance of nutrients, and therefore would support growth of the triple mutant strains.

Testing the deletion strains on synthetic media also failed due to slow growth of the test deletion strains even on high pH media. It is possible that our test conditions were too stringent. Yeast lacking the K^+ transporter Trk1p and

Trk2p appear somewhat unhealthy, an effect that may be exacerbated by the additional deletions. However, it is unclear whether our observations reflect true synthetic lethal interactions on a wide scale or whether our growth and test conditions were not optimal. The fact that six of the deletions discovered by our Na^+ screen supported growth of yeast on 100 mM K^+ in a *trk1*Δ *trk2*Δ background argues for the latter. Future experiments may address which deletions are truly synthetic lethal with *trk1*Δ *trk2*Δ.

An additional factor that may have affected the outcome of the K^+ screen was related to the use of a methionine repressible promoter (MET25pr) to drive Kir3.2V188G expression. The MET25pr allows transcription only in the absence of methionine. Since the deletion library yeast strains are methionine auxotroph (*met15*Δ), selection for methionine prototrophy (conferred by MET15 from the parental MATalpha strain) had to be added to the selection scheme. This led to loss of strains due to linkage, and maybe also due to low representation of $MET15^+$ haploids after random spore selection.

Table A-2 : Selection scheme for K^+ screen

Yeast strains:
MATalpha trk1Δ::URA3/MET25pr-Kir3.2V188G-GFP trk2Δ::NAT^r can1Δ::STE2pr-spHIS5 lyp1Δ::STE3pr-LEU2 LYS2$^+$ his3Δ1 leu2Δ0 MET15$^+$ cyh2

MATa YYYΔ::Kan^r CAN1 LYP1 LYS2$^+$ his3Δ1 leu2Δ0 ura3Δ0 met15Δ0

STEP	MEDIA	GENOTYPE
1. a) DMA b) QMA	YPAD+G418 100K SD(MSG)-URA+NAT pH6	
2. Mating	100K YPAD	
3. Diploid	100K YPAD +G418 +NAT	
4. PRESPO	Presporulation media	
5. SPO	Sporulation media	
6. HS1	100K SD(MSG) –HIS–ARG–LYS +can +S-AEC pH6	can1Δ::STE2pr-HIS3, lyp1Δ
7. HS2	100K SD(MSG) –HIS–ARG–LYS +can +S-AEC pH6	can1Δ::STE2pr-HIS3, lyp1Δ
8. SM	100K SD(MSG) –HIS–ARG–LYS +can +S-AEC +G418 pH6	can1Δ::STE2pr-HIS3, lyp1Δ, YYYΔ::Kan^r
9. DM	100K SD(MSG) –HIS–ARG–LYS–URA +can +S-AEC +G418 pH6	can1Δ::STE2pr-HIS3, lyp1Δ, YYYΔ::Kan^r, trk1Δ::URA3/ MET25pr-V188G-GFP
10. TM	100K SD(MSG) –HIS–ARG–LYS–URA +can +S-AEC +G418 +NAT pH6	can1Δ::STE2pr-HIS3, lyp1Δ, YYYΔ::Kan^r, trk1Δ::URA3/ MET25pr-V188G-GFP, trk2Δ::NAT^r
11. QM	100K SD(MSG) –HIS–ARG–LYS–URA–MET +can +S-AEC +G418 +NAT pH6	can1Δ::STE2pr-HIS3, lyp1Δ, YYYΔ::Kan^r, trk1Δ::URA3/ MET25pr-V188G-GFP, trk2Δ::NAT^r, MET15
12. test pH4	SD(MSG) –HIS–ARG–LYS–URA–MET +can +S-AEC +G418 +NAT pH4	can1Δ::STE2pr-HIS3, lyp1Δ, YYYΔ::Kan^r, trk1Δ::URA3/ MET25pr-V188G-GFP, trk2Δ::NAT^r, MET15
test pH6	SD(MSG) –HIS–ARG–LYS–URA–MET +can +S-AEC +G418 +NAT pH6	can1Δ::STE2pr-HIS3, lyp1Δ, YYYΔ::Kan^r, trk1Δ::URA3/ MET25pr-V188G-GFP, trk2Δ::NAT^r, MET15

Figure A-1

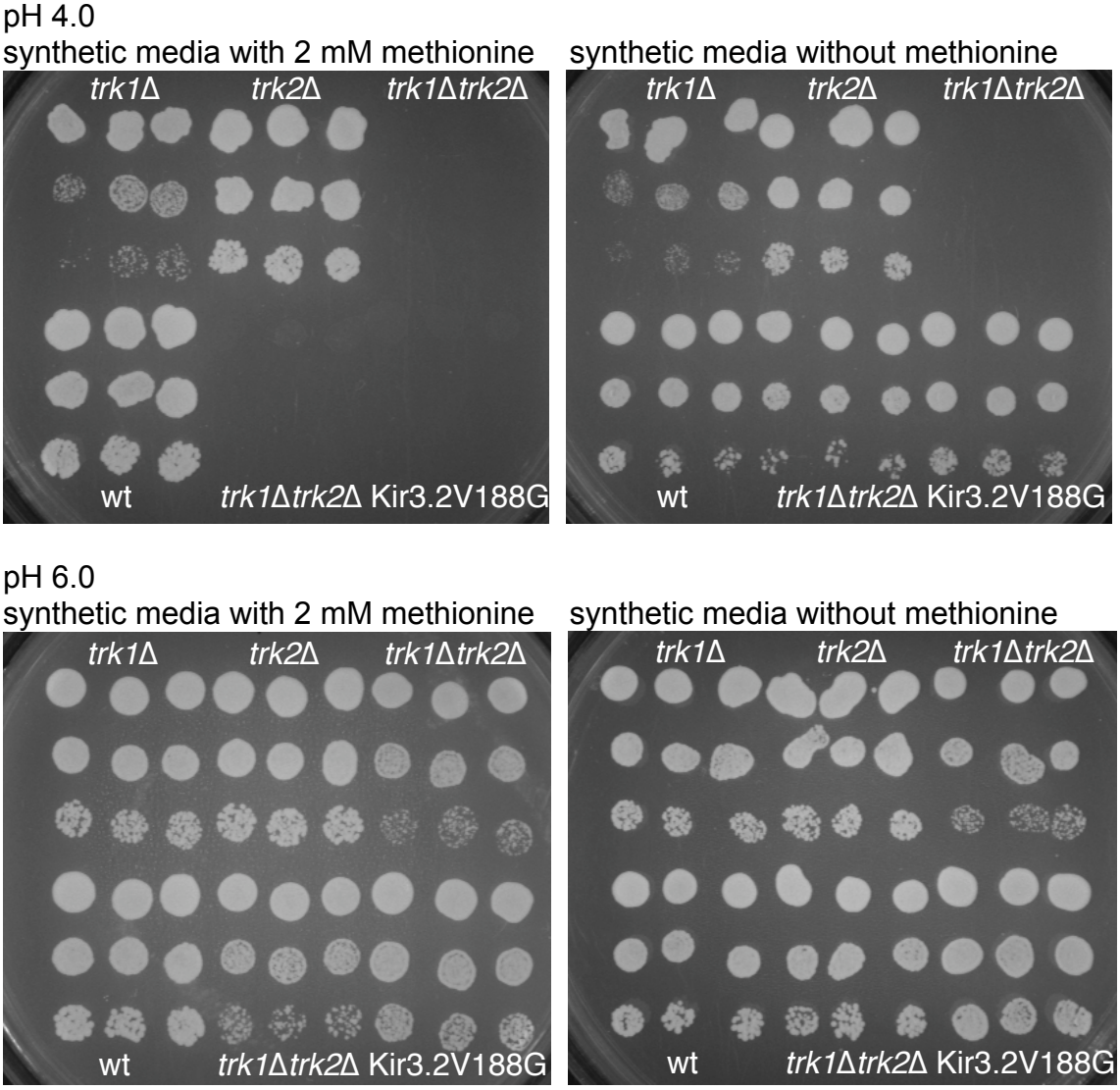

Growth rescue of *trk1*Δ *trk2*Δ yeast on low pH media by expression of Kir3.2V188G-GFP. Ten-fold serial dilutions (25,000; 2,500; 250 cells per spot) were plated on synthetic media adjusted to pH 4.0 with phosphoric acid or pH 6.0 with Tris. Yeast strains lacking the high (*trk1*Δ) or low (*trk2*Δ) affinity K^+ transporters individually can grow on low pH media. However, deletion of both transporters slows yeast growth on low pH media. Growth is restored by

expression of Kir3.2V188G with a C-terminal GFP tag. Kir3.2V188G expression was driven by a methionine repressible promoter (MET25pr). Therefore, rescue only occurs on media without methionine. All the strains grew well on pH 6.0 media.

3 Kir3.2 with extracellular tags

Kir channels have small extracellular loops, which have so far not been used successfully to generate antibodies that detect the channel at the cell surface. Therefore, cell surface localization of Kir channels has commonly been measured using extracellular tags introduced between the first transmembrane segment (M1) and the pore helix (Kennedy et al., 1999; Zerangue et al., 1999; Chen et al., 2002; Ma et al., 2002).

We attempted to assay surface localization of Kir3.2S177W in yeast using immunofluorescence. To this end, we introduced an extracellular HA or aldehyde tag (Carrico et al., 2007) between I126 and E127 of mouse or rat Kir3.2. The channels carrying the extracellular tags proved non-functional in two yeast assays. First, Kir3.2S177W carrying an extracellular HA or aldehyde tag did not impair growth of yeast on high Na^+ media (Figure A-2). The same result was obtained for Kir3.2S177W-GFP with an extracellular HA or aldehyde tag. Second, Kir3.2V188G carrying an extracellular HA tag did not rescue growth of *trk1*Δ *trk2*Δ yeast on low K^+ media (Figure A-3). Kir3.2V188G with a C-terminal GFP rescued growth. Rescue by Kir3.2V188G without any tags was not tested, but it was shown by Yi et al. (Yi et al., 2001) to rescue growth. It remains to be determined whether the extracellular tag interfered with channel folding, assembly, trafficking or gating.

By Western blot, expression levels of Kir3.2S177W-HA were reduced in comparison to Kir3.2S177W or Kir3.2S177W with the aldehyde tag (Figure A-4). Expression levels of the other constructs were comparable. The same result was

observed in two separate instances. At the time the Western analysis was done, samples were separated on Tris glycine gels. Later, I found that the double band seen for Kir3.2 on Tris glycine gels was not present on Bis Tris gels. Curiously, Kir3.2S177WHA-GFP did not run as a doublet on a Tris glycine gel.

Figure A-2

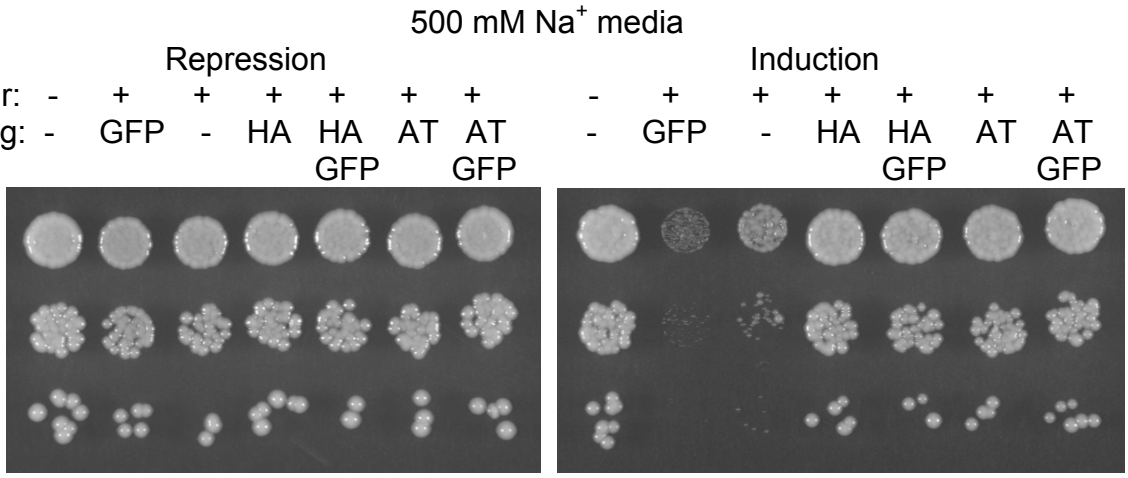

Yeast strains carrying genomic insertions of Kir3.2S177W with different tags under a galactose inducible/dextrose repressible promoter (Gal1pr). Control yeast grew well on 500 mM Na^+ media containing galactose or dextrose. Yeast expressing Kir3.2S177W or Kir3.2S177W-GFP grew slowly on high Na^+, inducing media, indicating that functional channels reached the cell surface and allowed Na^+ to enter the cell. The growth inhibition was not observed for induction of Kir3.2S177W carrying an extracellular hemagglutinin tag (HA) or aldehyde tag (AT) indicating that channel function and/or cell surface localization were disrupted by the extracellular tags.

Figure A-3

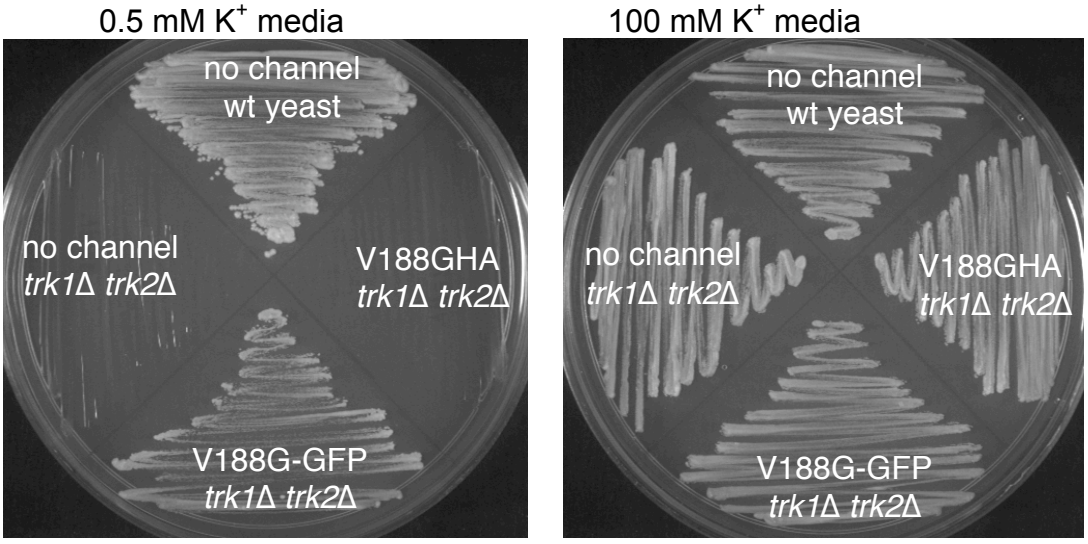

Growth rescue of *trk1*Δ *trk2*Δ yeast on low K^+ media. Growth of *trk1*Δ *trk2*Δ yeast on low (0.5 mM) K^+ media was rescued by expression of Kir3.2V188G with a C-terminal GFP tag (V188G-GFP), but not by Kir3.2V188G carrying an extracellular HA tag (V188GHA). Control $TRK1^+$ $TRK2^+$ yeast not expressing a channel grew well 0.5 mM K^+ media. *trk1*Δ *trk2*Δ yeast did not grow on 0.5 mM K^+ media. All strains grew on 100 mM K^+ media, where *trk1*Δ *trk2*Δ yeast relied on non-specific K^+ uptake for survival.

Figure A-4

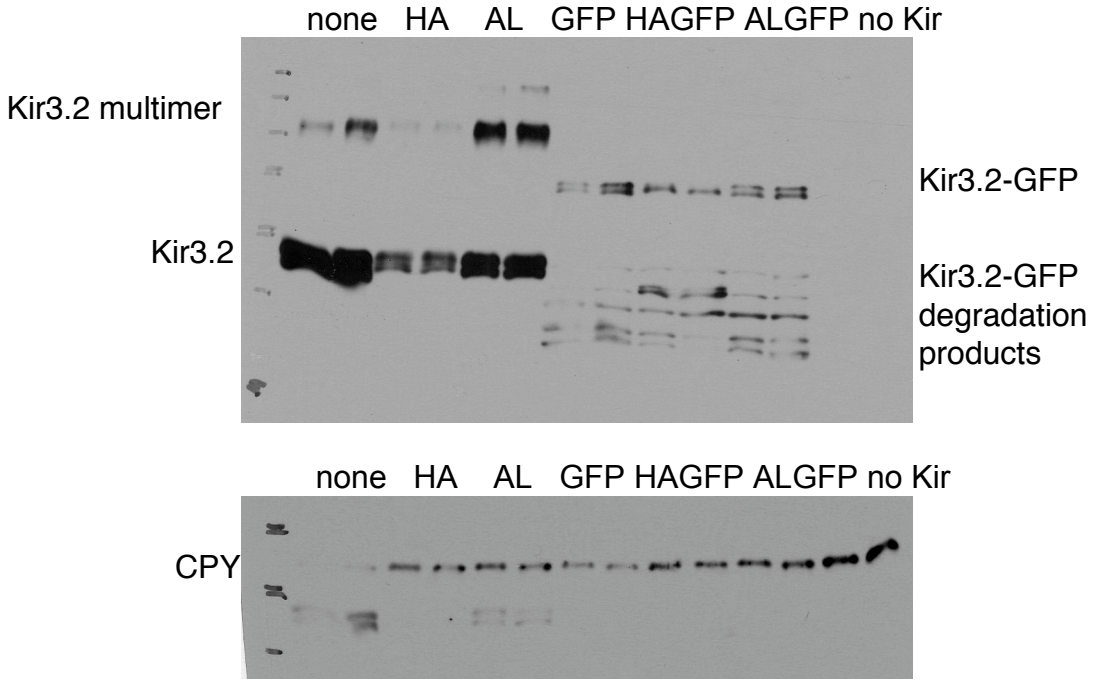

Western blot of whole yeast cell samples probed with antibodies to Kir3.2 (Alomone) and carboxypeptidase Y (CPY) (Maya Schuldiner). Yeast strains are shown twice, the first sample originated from the strain grown at room temperature, the second sample from the strain grown at 30°C. We suspected that folding of the channel may be temperature sensitive, however this hypothesis did not hold. Expression levels of Kir3.2S177W with different tags were comparable, except for a reduction in Kir3.2S177W-HA levels. The degradation products observed for Kir3.2S177W with a GFP tag seem to accumulate during lysis. With a faster protocol and heating to 95°C instead of 75°C, less degradation was observed.

4 Structure-function information on Kir channels

The following alignment (Table A-3) shows amino acids in various Kir channels that have been studied using mutagenesis or chimeric channels and implicated in certain functions such as channel gating, selectivity, or modulation. References are given as first author followed by the year of publication.

Table A-3: Structure-function information on Kir channels

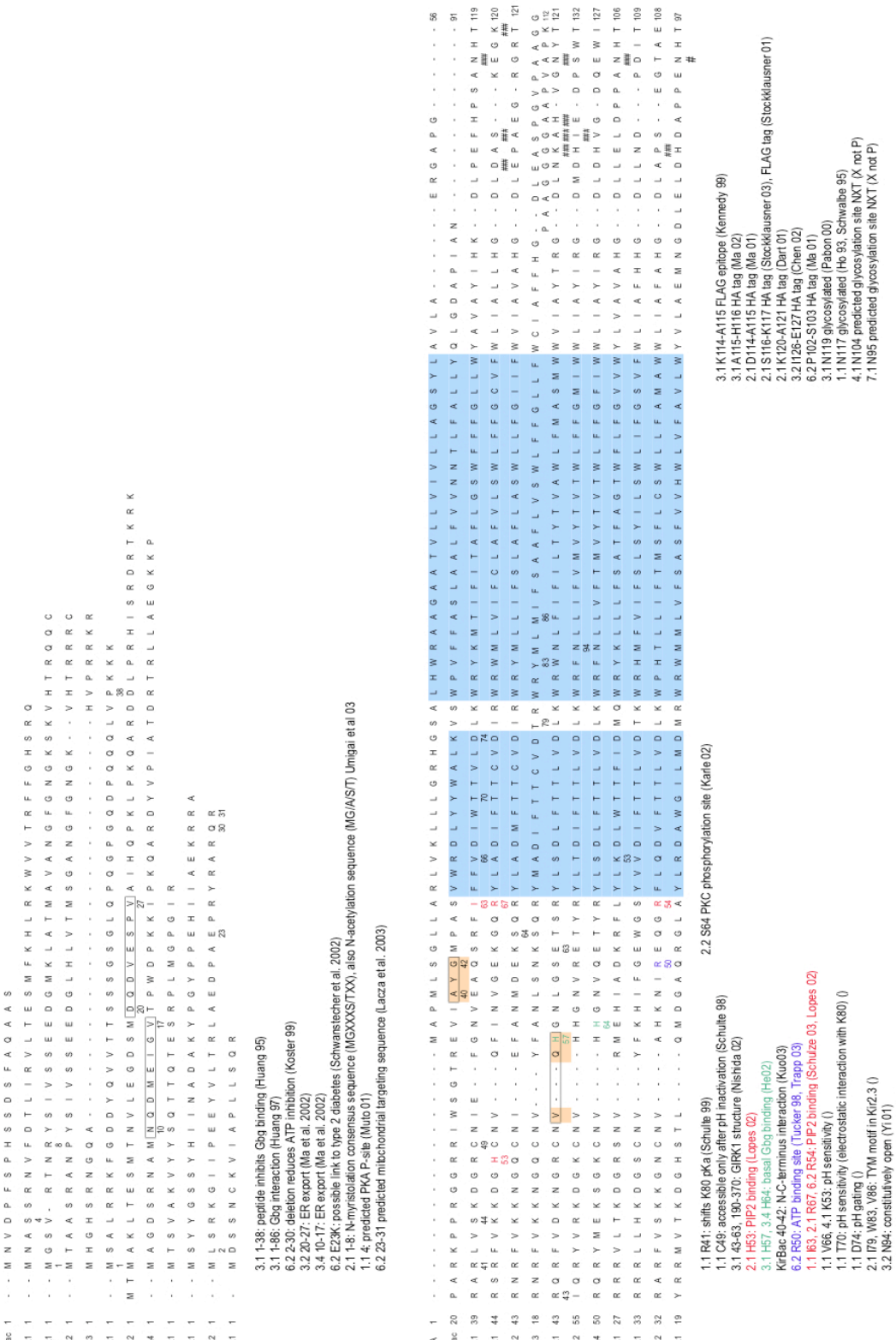

3.1 1-38; peptide inhibits Gbg binding (Huang 95)
3.1 1-86: Gbg interaction (Huang 97)
6.2 2-30: deletion reduces ATP inhibition (Koster 99)
3.2 20-27: ER export (Ma et al. 2002)
3.4 10-17: ER export (Ma et al. 2002)
6.2 E23K: possible link to type 2 diabetes (Schwanstecher et al. 2002)
2.1 1-8: N-myristoilation consensus sequence (MGXXXS/TXX), also N-acetylation sequence (MG/A/S/T) Umigai et al 03
1.1 4: predicted PKA P-site (Muto 01)
6.2 23-31 predicted mitochondrial targeting sequence (Lacza et al. 2003)

1.1 R41: shifts K80 pKa (Schulte 99)
1.1 C49: accessible only after pH inactivation (Schulte 98)
3.1 43-63, 190-370: GIRK1 structure (Nishida 02)
2.1 H53: PIP2 binding (Lopes 02)
3.1 H57, 3.4 H64: basal Gbg binding (He02)
Kir/Bac 40-42: N-C-terminus interaction (Kuo03)
6.2 R50: ATP binding site (Tucker 98, Trapp 03)
1.1 I63, 2.1 R67, 6.2 R54: PIP2 binding (Schulze 03, Lopes 02)
1.1 V66, 4.1 K53: pH sensitivity ()
1.1 T70: pH sensitivity (electrostatic interaction with K80) ()
1.1 D74: pH gating ()
2.1 I79, W83, V86: TYM motif in Kir2.3 ()
3.2 N84: constitutively open (Yi 01)
1.1 S44 PKA phosphorylation site Muto 01

2.2 S64 PKC phosphorylation site (Kahle 02)

3.1 K114-A115 FLAG epitope (Kennedy 98)
3.1 A115-H116 HA tag (Ma 02)
2.1 D114-A115 HA tag (Ma 01)
2.1 S116-K117 HA tag (Stockklausner 03), FLAG tag (Stockklausner 01)
2.1 K120-A121 HA tag (Dart 01)
3.2 I126-E127 HA tag (Chen 02)
6.2 P102-S103 HA tag (Ma 01)
3.1 N119 glycosylated (Pabon 00)
1.1 N117 glycosylated (Ho 93, Schwalbe 95)
4.1 N104 predicted glycosylation site NXT (X not P)
7.1 N95 predicted glycosylation site NXT (X not P)

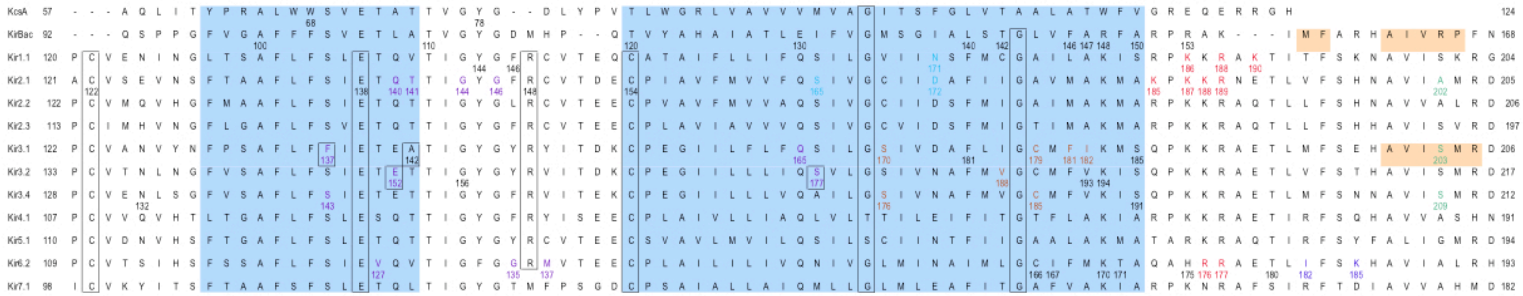

2.1 Q140: gating @SF (Guo and Kubo 98)
3.2 F137 gating @SF, selectivity (Chan 96, Kofuji 96, Slesinger 01)
3.4 S143: gating @SF (Chan 96, Kofuji 96)
3.2 A142: selectivity (Slesinger 01)
3.2 E152: gating @SF, selectivity (Yi 01)
6.2 V127, G135, M137: s. ch. cond. decreased (Proks 01, Capener 03)
2.1 G144, G146: backbone mutations (Lu01)
KcsA W68-Y78: H-bond
2.1 E138-R148: salt bridge (Yang 97)
2.1 C122-C154 disulfide bond (Cho 00)
3.2 G156S weaver mutation (Kofuji 96, Slesinger 96)
3.4 N132 not glycosylated (Pabon 00)

3.1 Q165: gating @SF (Sadja 01)
3.2 S177: gating @SF, selectivity (Yi 01)
2.1 S165: inward rectification
1.1 N171, 2.1 D172: inward rectification
3.1 S170, 3.4 S176: proline kink (Sadja 01, Jin 02)
3.2 V188: gating @BXing (Yi 01)
3.1 C179, 3.4 C185: gating @BXing (Sadja 01)
3.1 F181: gating @BXing (Sadja 01)
3.1 I182: gating @BXing (Sadja 01)
6.2 C166: Po increased (Trapp 98, Tucker 98)
6.2 I167: Po increased (Tucker 98)
6.2 T171: ATP binding (Drain 98, Tucker 98), gating (Li00)
6.2 170-204: interacts with N-terminus (Jones 01)
3.1 181-254: binds Gbg (Ivanina 03)
1.1 Y144N can be glycosylated (Schwalbe 97)
1.1 F146N can be glycosylated (Schwalbe 97)

1.1 K186, R188, K190: PIP2 binding (Huang98, Lopes 02)
2.1 K185, K187, K188, R189 PIP2 binding (Lopes 02)
6.2 R176, R177: PIP2 binding (Shyng 00)
6.2 H175: pH sensitivity (Xu 01)
KirBac 150-153: flexible linker (Kuo 03)
6.2 I182: ATP binding (Drain 98, Tucker 98)
6.2 K185: ATP bind. (Tucker 97, Koster 99, Reimann 99, Shyng 00, Trapp 03)
2.1 202-218: peptide inhibits Gbg binding (Krapivinsky 98)
3.1 203-219: peptide has no effect on Gbg binding (Krapivinsky 98)
3.4 209-225: peptide inhibits Gbg binding (Krapivinsky 98)
3.1 S185 PKC phosphorylation (Mao 04)
3.4 S191 PKC phosphorylation (Mao 04)
6.2 T180 PKC phosphorylation => activation (Light 00)

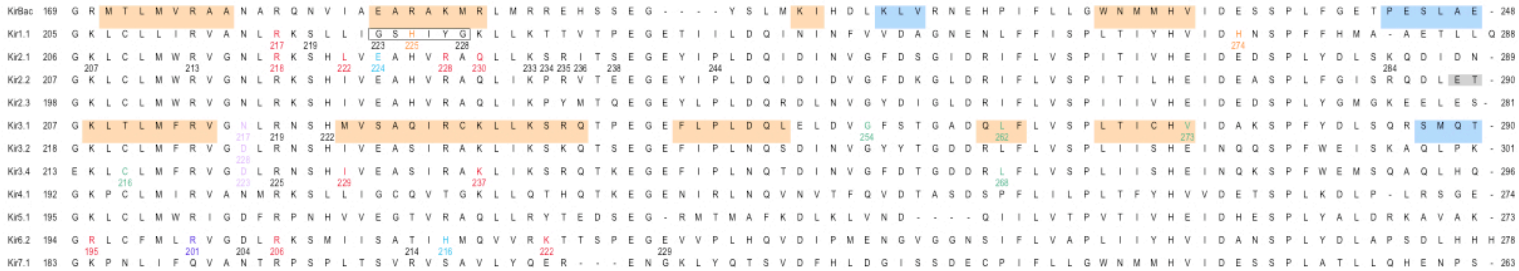

6.2 R195: PIP2 binding (Shyng 00)
6.2 R201: ATP binding (Shyng 00)
3.4 C216: Gbg binding (Krapivinsky 98)
6.2 214-222: interacts with N-terminus (Jones 01)
3.1 N217: Na+ binding (Zhang 99, Ho 99a and b)
2.1 L222I: less PIP2 binding, 3.4 I229L more PIP2 binding (Zhang 99)
2.1 R218, R228: PIP2 binding (Zhang 99, Lopes 02)
1.1 R217: PIP2 binding (Lopes 02)
2.1: K207, R213, K233, R235: not involved in PIP2 binding (Zhang 99)
3.4 K237Q: strengthens PIP2 binding, 2.1 Q230K: no effect (Zhang 99)
2.1 E224: inward rectification ()
6.2 H216: protonation weakens inward rectification ()
6.2 R206, K222: PIP2 binding (Shyng 00)

6.2 E229: interacts with R314 (Lin 03)
3.1 254-319: binds Gbg (Ivanina 03)
3.1 L262, 3.4 L268: basal Gbg binding (He 02)
1.1 H274: protonation site? ()
3.1 273-462: Gbg binding (Huang 95)
2.1 K284 (2.2 R285): forward trafficking (Kaibara 02)
1.1 H225: protonation site? ()
2.1 234-8: PYMQ motif in 2.3
2.1 207-244: can replace PIP2 b.d. in TRPV1 (Prescott 03)
3.1 217-222: disordered in structure (Nishida 02)
1.1 S219 PKA phosphorylation (Muto 01)
1.1 G223-G228 WALKER A motif, MgATP binding => inhibition (Muto 01)

6.2 279-323: interacts with N-terminus (Jones 01)
2.1 E299: inward rectification ()
3.1 303-309: disordered in structure (Nishida 02)
1.1 C308: accessible only after pH inactivation (Schulte 98)
1.1 R311: shifts K80 pKa (Schulte 99) -> no!
3.2 310-380: binds Gbg (Ivanina 03)
2.1 R312: PIP2 binding (Lopes 02)
6.2: R301, R314: PIP2 binding (Shyng 00)
6.2 R314: interacts with E229 (Lin 03)
1.1 S313 PKA phosphorylation (Muto 01)

3.1 318-374: Gbg binding (Huang 97)
3.1 320-370: Gbg binding (Ivanina 03)
3.1 L333, 3.4 L339: agonist induced Gbg binding (He 99)
3.1 336-409: Gbg binding (Ivanina 03)
1.1 H342: protonation site? ()
6.2 E308A, I309A, W311A, F315A: nonfunctional (Cukras 02)
KirBac 290-296: disordered in structure (Kuo 03)

2.1 R343, K346: PIP2 binding (Soom 01)
6.2 334-337: ATP binding, esp G334 (Drain 98, Trapp 03)
1.1 H354: protonation site? ()
3.1 358-369: a-helix, Gbg binding (Nishida 02)
3.1 364-383: peptide inhibits Gbg binding to 3.4 (Krapivinsky 98)
2.2 T354 PKC phosphorylation site (Karle 02), T353 is their paper because they use 2.2 lacking R285
6.2 L355 L356 endocytosis signal (Hu 03)

3.1 374-384: homology to adenylate cyclase? -> no (see Huang 97)
3.1 390-462: Gbg interaction (Huang 97)
2.1 F374 to E379 FCYENE ER export motif (Ma 01)
3.2 E396 to E403 ER export motif (Ma 02)
3.4 E391 to G408 post-Golgi surface trafficking (Ma 02)
6.2 R368 K369 R370 ER retention retrieval signal (Zerangue 99)

2.1, 2.2, 3.2, 3.3, 4.1: PDZ domain interaction (Cohen 96, Hibino 00)
2.2 S430 to I432 PDZ ligand (Leonoudakis 01, 04 a and b)
1.1 390-393 PDZ ligand Yoo 2004

3.1 434-462: peptide inhibits Gbg binding (Huang 95)

References

Abraham MR, Jahangir A, Alekseev AE, Terzic A (1999) Channelopathies of inwardly rectifying potassium channels. Faseb J 13:1901-1910.

Aguilar-Bryan L, Bryan J (1999) Molecular biology of adenosine triphosphate-sensitive potassium channels. Endocr Rev 20:101-135.

Albert A, Yenush L, Gil-Mascarell MR, Rodriguez PL, Patel S, Martinez-Ripoll M, Blundell TL, Serrano R (2000) X-ray structure of yeast Hal2p, a major target of lithium and sodium toxicity, and identification of framework interactions determining cation sensitivity. J Mol Biol 295:927-938.

Alder NN, Johnson AE (2004) Cotranslational membrane protein biogenesis at the endoplasmic reticulum. J Biol Chem 279:22787-22790.

Amberg DC, Burke DJ, Strathern JN (2005) Methods in Yeast Genetics. Cold Spring Harbor, NY, USA: Cold Spring Harbor Laboratory Press.

Anderson JA, Huprikar SS, Kochian LV, Lucas WJ, Gaber RF (1992) Functional expression of a probable Arabidopsis thaliana potassium channel in Saccharomyces cerevisiae. Proc Natl Acad Sci U S A 89:3736-3740.

Ashcroft SJ (2000) The beta-cell K(ATP) channel. J Membr Biol 176:187-206.

Ashfield R, Ashcroft SJ (1998) Cloning of the promoters for the beta-cell ATP-sensitive K-channel subunits Kir6.2 and SUR1. Diabetes 47:1274-1280.

Ball AJ, McCluskey JT, Flatt PR, McClenaghan NH (2004) Chronic exposure to tolbutamide and glibenclamide impairs insulin secretion but not transcription of K(ATP) channel components. Pharmacol Res 50:41-46.

Ballanyi K (2004) Protective role of neuronal KATP channels in brain hypoxia. J Exp Biol 207:3201-3212.

Belden WJ, Barlowe C (1996) Erv25p, a component of COPII-coated vesicles, forms a complex with Emp24p that is required for efficient endoplasmic reticulum to Golgi transport. J Biol Chem 271:26939-26946.

Bichet D, Haass FA, Jan LY (2003) Merging functional studies with structures of inward-rectifier K(+) channels. Nat Rev Neurosci 4:957-967.

Bichet D, Lin YF, Ibarra CA, Huang CS, Yi BA, Jan YN, Jan LY (2004) Evolving potassium channels by means of yeast selection reveals structural elements important for selectivity. Proc Natl Acad Sci U S A 101:4441-4446.

Bonifacino JS, Traub LM (2003) Signals for sorting of transmembrane proteins to endosomes and lysosomes. Annu Rev Biochem 72:395-447.

Brachmann CB, Davies A, Cost GJ, Caputo E, Li J, Hieter P, Boeke JD (1998) Designer deletion strains derived from Saccharomyces cerevisiae S288C: a useful set of strains and plasmids for PCR-mediated gene disruption and other applications. Yeast 14:115-132.

Butt AM, Kalsi A (2006) Inwardly rectifying potassium channels (Kir) in central nervous system glia: a special role for Kir4.1 in glial functions. J Cell Mol Med 10:33-44.
Carrico IS, Carlson BL, Bertozzi CR (2007) Introducing genetically encoded aldehydes into proteins. Nat Chem Biol 3:321-322.
Chatelain FC, Alagem N, Xu Q, Pancaroglu R, Reuveny E, Minor DL, Jr. (2005) The pore helix dipole has a minor role in inward rectifier channel function. Neuron 47:833-843.
Chen L, Kawano T, Bajic S, Kaziro Y, Itoh H, Art JJ, Nakajima Y, Nakajima S (2002) A glutamate residue at the C terminus regulates activity of inward rectifier K+ channels: implication for Andersen's syndrome. Proc Natl Acad Sci U S A 99:8430-8435.
Cho HC, Tsushima RG, Nguyen TT, Guy HR, Backx PH (2000) Two critical cysteine residues implicated in disulfide bond formation and proper folding of Kir2.1. Biochemistry 39:4649-4657.
Choe S, Stevens CF, Sullivan JM (1995) Three distinct structural environments of a transmembrane domain in the inwardly rectifying potassium channel ROMK1 defined by perturbation. Proc Natl Acad Sci U S A 92:12046-12049.
Clement JPt, Kunjilwar K, Gonzalez G, Schwanstecher M, Panten U, Aguilar-Bryan L, Bryan J (1997) Association and stoichiometry of K(ATP) channel subunits. Neuron 18:827-838.
Coblitz B, Shikano S, Wu M, Gabelli SB, Cockrell LM, Spieker M, Hanyu Y, Fu H, Amzel LM, Li M (2005) C-terminal recognition by 14-3-3 proteins for surface expression of membrane receptors. J Biol Chem 280:36263-36272.
Cohen NA, Brenman JE, Snyder SH, Bredt DS (1996) Binding of the inward rectifier K+ channel Kir 2.3 to PSD-95 is regulated by protein kinase A phosphorylation. Neuron 17:759-767.
Collins SR, Schuldiner M, Krogan NJ, Weissman JS (2006) A strategy for extracting and analyzing large-scale quantitative epistatic interaction data. Genome Biol 7:R63.
Conti LR, Radeke CM, Vandenberg CA (2002) Membrane targeting of ATP-sensitive potassium channel. Effects of glycosylation on surface expression. J Biol Chem 277:25416-25422.
Crane A, Aguilar-Bryan L (2004) Assembly, maturation, and turnover of K(ATP) channel subunits. J Biol Chem 279:9080-9090.
Dart C, Leyland ML (2001) Targeting of an A kinase-anchoring protein, AKAP79, to an inwardly rectifying potassium channel, Kir2.1. J Biol Chem 276:20499-20505.
Delling M, Wischmeyer E, Dityatev A, Sytnyk V, Veh RW, Karschin A, Schachner M (2002) The neural cell adhesion molecule regulates cell-surface delivery of G-protein-activated inwardly rectifying potassium channels via lipid rafts. J Neurosci 22:7154-7164.

Denzel A, Otto F, Girod A, Pepperkok R, Watson R, Rosewell I, Bergeron JJ, Solari RC, Owen MJ (2000) The p24 family member p23 is required for early embryonic development. Curr Biol 10:55-58.
Dephoure N, Howson RW, Blethrow JD, Shokat KM, O'Shea EK (2005) Combining chemical genetics and proteomics to identify protein kinase substrates. Proc Natl Acad Sci U S A 102:17940-17945.
Derst C, Karschin C, Wischmeyer E, Hirsch JR, Preisig-Muller R, Rajan S, Engel H, Grzeschik K, Daut J, Karschin A (2001) Genetic and functional linkage of Kir5.1 and Kir2.1 channel subunits. FEBS Lett 491:305-311.
Desfarges L, Durrens P, Juguelin H, Cassagne C, Bonneu M, Aigle M (1993) Yeast mutants affected in viability upon starvation have a modified phospholipid composition. Yeast 9:267-277.
Deutsch C (2002) Potassium channel ontogeny. Annu Rev Physiol 64:19-46.
Deutsch C (2003) The birth of a channel. Neuron 40:265-276.
Dickson RC, Sumanasekera C, Lester RL (2006) Functions and metabolism of sphingolipids in Saccharomyces cerevisiae. Prog Lipid Res 45:447-465.
Dupre S, Haguenauer-Tsapis R (2003) Raft partitioning of the yeast uracil permease during trafficking along the endocytic pathway. Traffic 4:83-96.
Ellgaard L, Helenius A (2003) Quality control in the endoplasmic reticulum. Nat Rev Mol Cell Biol 4:181-191.
Ellgaard L, Molinari M, Helenius A (1999) Setting the standards: quality control in the secretory pathway. Science 286:1882-1888.
Elrod-Erickson MJ, Kaiser CA (1996) Genes that control the fidelity of endoplasmic reticulum to Golgi transport identified as suppressors of vesicle budding mutations. Mol Biol Cell 7:1043-1058.
Fink M, Duprat F, Heurteaux C, Lesage F, Romey G, Barhanin J, Lazdunski M (1996) Dominant negative chimeras provide evidence for homo and heteromultimeric assembly of inward rectifier K+ channel proteins via their N-terminal end. FEBS Lett 378:64-68.
Fujita M, Yoko OT, Jigami Y (2006) Inositol deacylation by Bst1p is required for the quality control of glycosylphosphatidylinositol-anchored proteins. Mol Biol Cell 17:834-850.
Gaber RF, Styles CA, Fink GR (1988) TRK1 encodes a plasma membrane protein required for high-affinity potassium transport in Saccharomyces cerevisiae. Mol Cell Biol 8:2848-2859.
Garcia-Arranz M, Maldonado AM, Mazon MJ, Portillo F (1994) Transcriptional control of yeast plasma membrane H(+)-ATPase by glucose. Cloning and characterization of a new gene involved in this regulation. J Biol Chem 269:18076-18082.
Giaever G, Chu AM, Ni L, Connelly C, Riles L, Veronneau S, Dow S, Lucau-Danila A, Anderson K, Andre B, Arkin AP, Astromoff A, El-Bakkoury M, Bangham R, Benito R, Brachat S, Campanaro S, Curtiss M, Davis K, Deutschbauer A, Entian KD, Flaherty P, Foury F, Garfinkel DJ, Gerstein M, Gotte D, Guldener U, Hegemann JH, Hempel S, Herman Z, Jaramillo

DF, Kelly DE, Kelly SL, Kotter P, LaBonte D, Lamb DC, Lan N, Liang H, Liao H, Liu L, Luo C, Lussier M, Mao R, Menard P, Ooi SL, Revuelta JL, Roberts CJ, Rose M, Ross-Macdonald P, Scherens B, Schimmack G, Shafer B, Shoemaker DD, Sookhai-Mahadeo S, Storms RK, Strathern JN, Valle G, Voet M, Volckaert G, Wang CY, Ward TR, Wilhelmy J, Winzeler EA, Yang Y, Yen G, Youngman E, Yu K, Bussey H, Boeke JD, Snyder M, Philippsen P, Davis RW, Johnston M (2002) Functional profiling of the Saccharomyces cerevisiae genome. Nature 418:387-391.

Giebisch G (1998) Renal potassium transport: mechanisms and regulation. Am J Physiol 274:F817-833.

Gong Q, Weide M, Huntsman C, Xu Z, Jan LY, Ma D (2007) Identification and characterization of a new class of trafficking motifs for controlling clathrin-independent internalization and recycling. J Biol Chem 282:13087-13097.

Gosset P, Ghezala GA, Korn B, Yaspo ML, Poutska A, Lehrach H, Sinet PM, Creau N (1997) A new inward rectifier potassium channel gene (KCNJ15) localized on chromosome 21 in the Down syndrome chromosome region 1 (DCR1). Genomics 44:237-241.

Gross GJ, Peart JN (2003) KATP channels and myocardial preconditioning: an update. Am J Physiol Heart Circ Physiol 285:H921-930.

Haider S, Khalid S, Tucker SJ, Ashcroft FM, Sansom MS (2007) Molecular dynamics simulations of inwardly rectifying (Kir) potassium channels: a comparative study. Biochemistry 46:3643-3652.

Hancock JF (2006) Lipid rafts: contentious only from simplistic standpoints. Nat Rev Mol Cell Biol 7:456-462.

Helenius A, Aebi M (2004) Roles of N-linked glycans in the endoplasmic reticulum. Annu Rev Biochem 73:1019-1049.

Heusser K, Yuan H, Neagoe I, Tarasov AI, Ashcroft FM, Schwappach B (2006) Scavenging of 14-3-3 proteins reveals their involvement in the cell-surface transport of ATP-sensitive K+ channels. J Cell Sci 119:4353-4363.

Hibino H, Inanobe A, Tanemoto M, Fujita A, Doi K, Kubo T, Hata Y, Takai Y, Kurachi Y (2000) Anchoring proteins confer G protein sensitivity to an inward-rectifier K(+) channel through the GK domain. Embo J 19:78-83.

Hieronymus H, Silver PA (2004) A systems view of mRNP biology. Genes Dev 18:2845-2860.

Hilgemann DW, Feng S, Nasuhoglu C (2001) The complex and intriguing lives of PIP2 with ion channels and transporters. Sci STKE 2001:RE19.

Hille B (2001) Ion channels of Excitable membranes, Third Edition Edition. Sunderland, MA USA: Sinauer Associates Inc.

Ho K, Nichols CG, Lederer WJ, Lytton J, Vassilev PM, Kanazirska MV, Hebert SC (1993) Cloning and expression of an inwardly rectifying ATP-regulated potassium channel. Nature 362:31-38.

Hofherr A, Fakler B, Klocker N (2005) Selective Golgi export of Kir2.1 controls the stoichiometry of functional Kir2.x channel heteromers. J Cell Sci 118:1935-1943.

Horvath A, Sutterlin C, Manning-Krieg U, Movva NR, Riezman H (1994) Ceramide synthesis enhances transport of GPI-anchored proteins to the Golgi apparatus in yeast. Embo J 13:3687-3695.
Hu K, Huang CS, Jan YN, Jan LY (2003) ATP-sensitive potassium channel traffic regulation by adenosine and protein kinase C. Neuron 38:417-432.
Huang CL, Feng S, Hilgemann DW (1998) Direct activation of inward rectifier potassium channels by PIP2 and its stabilization by Gbetagamma. Nature 391:803-806.
Huh WK, Falvo JV, Gerke LC, Carroll AS, Howson RW, Weissman JS, O'Shea EK (2003) Global analysis of protein localization in budding yeast. Nature 425:686-691.
Inanobe A, Yoshimoto Y, Horio Y, Morishige KI, Hibino H, Matsumoto S, Tokunaga Y, Maeda T, Hata Y, Takai Y, Kurachi Y (1999) Characterization of G-protein-gated K+ channels composed of Kir3.2 subunits in dopaminergic neurons of the substantia nigra. J Neurosci 19:1006-1017.
Jacobson K, Mouritsen OG, Anderson RG (2007) Lipid rafts: at a crossroad between cell biology and physics. Nat Cell Biol 9:7-14.
Jiang K, Shui Q, Xia Z, Yu Z (2004) Changes in the gene and protein expression of K(ATP) channel subunits in the hippocampus of rats subjected to picrotoxin-induced kindling. Brain Res Mol Brain Res 128:83-89.
Kaiser C (2000) Thinking about p24 proteins and how transport vesicles select their cargo. Proc Natl Acad Sci U S A 97:3783-3785.
Keene JD, Tenenbaum SA (2002) Eukaryotic mRNPs may represent posttranscriptional operons. Mol Cell 9:1161-1167.
Keene JD, Lager PJ (2005) Post-transcriptional operons and regulons co-ordinating gene expression. Chromosome Res 13:327-337.
Kennedy ME, Nemec J, Clapham DE (1996) Localization and interaction of epitope-tagged GIRK1 and CIR inward rectifier K+ channel subunits. Neuropharmacology 35:831-839.
Kennedy ME, Nemec J, Corey S, Wickman K, Clapham DE (1999) GIRK4 confers appropriate processing and cell surface localization to G-protein-gated potassium channels. J Biol Chem 274:2571-2582.
Kleta R, Bockenhauer D (2006) Bartter syndromes and other salt-losing tubulopathies. Nephron Physiol 104:p73-80.
Ko CH, Buckley AM, Gaber RF (1990) TRK2 is required for low affinity K+ transport in Saccharomyces cerevisiae. Genetics 125:305-312.
Kofuji P, Hofer M, Millen KJ, Millonig JH, Davidson N, Lester HA, Hatten ME (1996) Functional analysis of the weaver mutant GIRK2 K+ channel and rescue of weaver granule cells. Neuron 16:941-952.
Konstas AA, Korbmacher C, Tucker SJ (2003) Identification of domains that control the heteromeric assembly of Kir5.1/Kir4.0 potassium channels. Am J Physiol Cell Physiol 284:C910-917.

Kosolapov A, Tu L, Wang J, Deutsch C (2004) Structure acquisition of the T1 domain of Kv1.3 during biogenesis. Neuron 44:295-307.
Koster JC, Permutt MA, Nichols CG (2005) Diabetes and insulin secretion: the ATP-sensitive K+ channel (K ATP) connection. Diabetes 54:3065-3072.
Koster JC, Bentle KA, Nichols CG, Ho K (1998) Assembly of ROMK1 (Kir 1.1a) inward rectifier K+ channel subunits involves multiple interaction sites. Biophys J 74:1821-1829.
Krapivinsky G, Gordon EA, Wickman K, Velimirovic B, Krapivinsky L, Clapham DE (1995) The G-protein-gated atrial K+ channel IKACh is a heteromultimer of two inwardly rectifying K(+)-channel proteins. Nature 374:135-141.
Krapivinsky G, Medina I, Eng L, Krapivinsky L, Yang Y, Clapham DE (1998) A novel inward rectifier K+ channel with unique pore properties. Neuron 20:995-1005.
Krogan NJ, others (2006) Global landscape of protein complexes in the yeast Saccharomyces cerevisiae. Nature 440:637-643.
Kubo Y, Adelman JP, Clapham DE, Jan LY, Karschin A, Kurachi Y, Lazdunski M, Nichols CG, Seino S, Vandenberg CA (2005) International Union of Pharmacology. LIV. Nomenclature and molecular relationships of inwardly rectifying potassium channels. Pharmacol Rev 57:509-526.
Kuo A, Gulbis JM, Antcliff JF, Rahman T, Lowe ED, Zimmer J, Cuthbertson J, Ashcroft FM, Ezaki T, Doyle DA (2003) Crystal structure of the potassium channel KirBac1.1 in the closed state. Science 300:1922-1926.
Kushnirov VV (2000) Rapid and reliable protein extraction from yeast. Yeast 16:857-860.
Leonoudakis D, Mailliard W, Wingerd K, Clegg D, Vandenberg C (2001) Inward rectifier potassium channel Kir2.2 is associated with synapse-associated protein SAP97. J Cell Sci 114:987-998.
Leonoudakis D, Conti LR, Radeke CM, McGuire LM, Vandenberg CA (2004a) A multiprotein trafficking complex composed of SAP97, CASK, Veli, and Mint1 is associated with inward rectifier Kir2 potassium channels. J Biol Chem 279:19051-19063.
Leonoudakis D, Conti LR, Anderson S, Radeke CM, McGuire LM, Adams ME, Froehner SC, Yates JR, 3rd, Vandenberg CA (2004b) Protein trafficking and anchoring complexes revealed by proteomic analysis of inward rectifier potassium channel (Kir2.x)-associated proteins. J Biol Chem 279:22331-22346.
Liu Y, Liu D, Heath L, Meyers DM, Krafte DS, Wagoner PK, Silvia CP, Yu W, Curran ME (2001) Direct activation of an inwardly rectifying potassium channel by arachidonic acid. Mol Pharmacol 59:1061-1068.
Logothetis DE, Jin T, Lupyan D, Rosenhouse-Dantsker A (2007) Phosphoinositide-mediated gating of inwardly rectifying K(+) channels. Pflugers Arch.

Lohberger B, Groschner K, Tritthart H, Schreibmayer W (2000) IK.ACh activation by arachidonic acid occurs via a G-protein-independent pathway mediated by the GIRK1 subunit. Pflugers Arch 441:251-256.
Lopatin AN, Nichols CG (2001) Inward rectifiers in the heart: an update on I(K1). J Mol Cell Cardiol 33:625-638.
Lopatin AN, Makhina EN, Nichols CG (1994) Potassium channel block by cytoplasmic polyamines as the mechanism of intrinsic rectification. Nature 372:366-369.
Lu J, Deutsch C (2005a) Folding zones inside the ribosomal exit tunnel. Nat Struct Mol Biol 12:1123-1129.
Lu J, Deutsch C (2005b) Secondary structure formation of a transmembrane segment in Kv channels. Biochemistry 44:8230-8243.
Lu J, Robinson JM, Edwards D, Deutsch C (2001a) T1-T1 interactions occur in ER membranes while nascent Kv peptides are still attached to ribosomes. Biochemistry 40:10934-10946.
Lu T, Hoshi T, Weintraub NL, Spector AA, Lee HC (2001b) Activation of ATP-sensitive K(+) channels by epoxyeicosatrienoic acids in rat cardiac ventricular myocytes. J Physiol 537:811-827.
Luscher C, Jan LY, Stoffel M, Malenka RC, Nicoll RA (1997) G protein-coupled inwardly rectifying K+ channels (GIRKs) mediate postsynaptic but not presynaptic transmitter actions in hippocampal neurons. Neuron 19:687-695.
Ma D, Jan LY (2002) ER transport signals and trafficking of potassium channels and receptors. Curr Opin Neurobiol 12:287-292.
Ma D, Zerangue N, Raab-Graham K, Fried SR, Jan YN, Jan LY (2002) Diverse trafficking patterns due to multiple traffic motifs in G protein-activated inwardly rectifying potassium channels from brain and heart. Neuron 33:715-729.
Ma D, Zerangue N, Lin YF, Collins A, Yu M, Jan YN, Jan LY (2001) Role of ER export signals in controlling surface potassium channel numbers. Science 291:316-319.
Macica CM, Yang Y, Lerea K, Hebert SC, Wang W (1998) Role of the NH2 terminus of the cloned renal K+ channel, ROMK1, in arachidonic acid-mediated inhibition. Am J Physiol 274:F175-181.
Mager WH, Siderius M (2002) Novel insights into the osmotic stress response of yeast. FEMS Yeast Res 2:251-257.
Makhina EN, Kelly AJ, Lopatin AN, Mercer RW, Nichols CG (1994) Cloning and expression of a novel human brain inward rectifier potassium channel. J Biol Chem 269:20468-20474.
Mark MD, Herlitze S (2000) G-protein mediated gating of inward-rectifier K+ channels. Eur J Biochem 267:5830-5836.
Martens JR, O'Connell K, Tamkun M (2004) Targeting of ion channels to membrane microdomains: localization of KV channels to lipid rafts. Trends Pharmacol Sci 25:16-21.

Marzioch M, Henthorn DC, Herrmann JM, Wilson R, Thomas DY, Bergeron JJ, Solari RC, Rowley A (1999) Erp1p and Erp2p, partners for Emp24p and Erv25p in a yeast p24 complex. Mol Biol Cell 10:1923-1938.
McCusker JH, Perlin DS, Haber JE (1987) Pleiotropic plasma membrane ATPase mutations of Saccharomyces cerevisiae. Mol Cell Biol 7:4082-4088.
Michelsen K, Yuan H, Schwappach B (2005) Hide and run. Arginine-based endoplasmic-reticulum-sorting motifs in the assembly of heteromultimeric membrane proteins. EMBO Rep 6:717-722.
Miki T, Suzuki M, Shibasaki T, Uemura H, Sato T, Yamaguchi K, Koseki H, Iwanaga T, Nakaya H, Seino S (2002) Mouse model of Prinzmetal angina by disruption of the inward rectifier Kir6.1. Nat Med 8:466-472.
Miller JP, Lo RS, Ben-Hur A, Desmarais C, Stagljar I, Noble WS, Fields S (2005) Large-scale identification of yeast integral membrane protein interactions. Proc Natl Acad Sci U S A 102:12123-12128.
Minor DL, Jr., Masseling SJ, Jan YN, Jan LY (1999) Transmembrane structure of an inwardly rectifying potassium channel. Cell 96:879-891.
Mirshahi T, Logothetis DE (2002) GIRK Channel Trafficking: Different Paths for Different Family Members. Mol Interv 2:289-291.
Mirshahi T, Logothetis DE (2004) Molecular determinants responsible for differential cellular distribution of G protein-gated inwardly rectifying K+ channels. J Biol Chem 279:11890-11897.
Moritz W, Leech CA, Ferrer J, Habener JF (2001) Regulated expression of adenosine triphosphate-sensitive potassium channel subunits in pancreatic beta-cells. Endocrinology 142:129-138.
Murguia JR, Belles JM, Serrano R (1995) A salt-sensitive 3'(2'),5'-bisphosphate nucleotidase involved in sulfate activation. Science 267:232-234.
Nakamura N, Suzuki Y, Sakuta H, Ookata K, Kawahara K, Hirose S (1999) Inwardly rectifying K+ channel Kir7.1 is highly expressed in thyroid follicular cells, intestinal epithelial cells and choroid plexus epithelial cells: implication for a functional coupling with Na+,K+-ATPase. Biochem J 342 (Pt 2):329-336.
Nakamura RL, Gaber RF (1998) Studying ion channels using yeast genetics. Methods Enzymol 293:89-104.
Nakamura RL, Anderson JA, Gaber RF (1997) Determination of key structural requirements of a K+ channel pore. J Biol Chem 272:1011-1018.
Nakanishi H, Suda Y, Neiman AM (2007) Erv14 family cargo receptors are necessary for ER exit during sporulation in Saccharomyces cerevisiae. J Cell Sci 120:908-916.
Neagoe I, Schwappach B (2005) Pas de deux in groups of four--the biogenesis of KATP channels. J Mol Cell Cardiol 38:887-894.
Nehring RB, Wischmeyer E, Doring F, Veh RW, Sheng M, Karschin A (2000) Neuronal inwardly rectifying K(+) channels differentially couple to PDZ proteins of the PSD-95/SAP90 family. J Neurosci 20:156-162.

Neusch C, Weishaupt JH, Bahr M (2003) Kir channels in the CNS: emerging new roles and implications for neurological diseases. Cell Tissue Res 311:131-138.
Newman JR, Ghaemmaghami S, Ihmels J, Breslow DK, Noble M, DeRisi JL, Weissman JS (2006) Single-cell proteomic analysis of S. cerevisiae reveals the architecture of biological noise. Nature 441:840-846.
Nicchitta CV (2002) A platform for compartmentalized protein synthesis: protein translation and translocation in the ER. Curr Opin Cell Biol 14:412-416.
O'Connell AD, Leng Q, Dong K, MacGregor GG, Giebisch G, Hebert SC (2005) Phosphorylation-regulated endoplasmic reticulum retention signal in the renal outer-medullary K+ channel (ROMK). Proc Natl Acad Sci U S A 102:9954-9959.
Ogino T, den Hollander JA, Shulman RG (1983) 39K, 23Na, and 31P NMR studies of ion transport in Saccharomyces cerevisiae. Proc Natl Acad Sci U S A 80:5185-5189.
Oh CS, Toke DA, Mandala S, Martin CE (1997) ELO2 and ELO3, homologues of the Saccharomyces cerevisiae ELO1 gene, function in fatty acid elongation and are required for sphingolipid formation. J Biol Chem 272:17376-17384.
Okamoto M, Yoko-o T, Umemura M, Nakayama K, Jigami Y (2006) Glycosylphosphatidylinositol-anchored proteins are required for the transport of detergent-resistant microdomain-associated membrane proteins Tat2p and Fur4p. J Biol Chem 281:4013-4023.
Olkkonen VM, Ikonen E (2006) When intracellular logistics fails--genetic defects in membrane trafficking. J Cell Sci 119:5031-5045.
Pabon A, Chan KW, Sui JL, Wu X, Logothetis DE, Thornhill WB (2000) Glycosylation of GIRK1 at Asn119 and ROMK1 at Asn117 has different consequences in potassium channel function. J Biol Chem 275:30677-30682.
Patil N, Cox DR, Bhat D, Faham M, Myers RM, Peterson AS (1995) A potassium channel mutation in weaver mice implicates membrane excitability in granule cell differentiation. Nat Genet 11:126-129.
Pei Q, Lewis L, Grahame-Smith DG, Zetterstrom TS (1999) Alteration in expression of G-protein-activated inward rectifier K+-channel subunits GIRK1 and GIRK2 in the rat brain following electroconvulsive shock. Neuroscience 90:621-627.
Perier F, Radeke CM, Vandenberg CA (1994) Primary structure and characterization of a small-conductance inwardly rectifying potassium channel from human hippocampus. Proc Natl Acad Sci U S A 91:6240-6244.
Perlin DS, Brown CL, Haber JE (1988) Membrane potential defect in hygromycin B-resistant pma1 mutants of Saccharomyces cerevisiae. J Biol Chem 263:18118-18122.

Pessia M, Imbrici P, D'Adamo MC, Salvatore L, Tucker SJ (2001) Differential pH sensitivity of Kir4.1 and Kir4.2 potassium channels and their modulation by heteropolymerisation with Kir5.1. J Physiol 532:359-367.
Pike LJ (2006) Rafts defined: a report on the Keystone Symposium on Lipid Rafts and Cell Function. J Lipid Res 47:1597-1598.
Pittet M, Conzelmann A (2007) Biosynthesis and function of GPI proteins in the yeast Saccharomyces cerevisiae. Biochim Biophys Acta 1771:405-420.
Plaster NM, Tawil R, Tristani-Firouzi M, Canun S, Bendahhou S, Tsunoda A, Donaldson MR, Iannaccone ST, Brunt E, Barohn R, Clark J, Deymeer F, George AL, Jr., Fish FA, Hahn A, Nitu A, Ozdemir C, Serdaroglu P, Subramony SH, Wolfe G, Fu YH, Ptacek LJ (2001) Mutations in Kir2.1 cause the developmental and episodic electrical phenotypes of Andersen's syndrome. Cell 105:511-519.
Powers J, Barlowe C (1998) Transport of axl2p depends on erv14p, an ER-vesicle protein related to the Drosophila cornichon gene product. J Cell Biol 142:1209-1222.
Raab-Graham KF, Vandenberg CA (1998) Tetrameric subunit structure of the native brain inwardly rectifying potassium channel Kir 2.2. J Biol Chem 273:19699-19707.
Robinson JM, Deutsch C (2005) Coupled tertiary folding and oligomerization of the T1 domain of Kv channels. Neuron 45:223-232.
Rodriguez-Navarro A (2000) Potassium transport in fungi and plants. Biochim Biophys Acta 1469:1-30.
Rodriguez-Navarro A, Ramos J (1984) Dual system for potassium transport in Saccharomyces cerevisiae. J Bacteriol 159:940-945.
Romanenko VG, Rothblat GH, Levitan I (2002) Modulation of endothelial inward-rectifier K+ current by optical isomers of cholesterol. Biophys J 83:3211-3222.
Romanenko VG, Fang Y, Byfield F, Travis AJ, Vandenberg CA, Rothblat GH, Levitan I (2004) Cholesterol sensitivity and lipid raft targeting of Kir2.1 channels. Biophys J 87:3850-3861.
Rossler H, Rieck C, Delong T, Hoja U, Schweizer E (2003) Functional differentiation and selective inactivation of multiple Saccharomyces cerevisiae genes involved in very-long-chain fatty acid synthesis. Mol Genet Genomics 269:290-298.
Ruppersberg JP (2000) Intracellular regulation of inward rectifier K+ channels. Pflugers Arch 441:1-11.
Sadja R, Alagem N, Reuveny E (2003) Gating of GIRK channels: details of an intricate, membrane-delimited signaling complex. Neuron 39:9-12.
Sadja R, Smadja K, Alagem N, Reuveny E (2001) Coupling Gbetagamma-dependent activation to channel opening via pore elements in inwardly rectifying potassium channels. Neuron 29:669-680.

Salama NR, Chuang JS, Schekman RW (1997) Sec31 encodes an essential component of the COPII coat required for transport vesicle budding from the endoplasmic reticulum. Mol Biol Cell 8:205-217.
Sato Y, Sakaguchi M, Goshima S, Nakamura T, Uozumi N (2002) Integration of Shaker-type K+ channel, KAT1, into the endoplasmic reticulum membrane: synergistic insertion of voltage-sensing segments, S3-S4, and independent insertion of pore-forming segments, S5-P-S6. Proc Natl Acad Sci U S A 99:60-65.
Schoots O, Voskoglou T, Van Tol HH (1997) Genomic organization and promoter analysis of the human G-protein-coupled K+ channel Kir3.1 (KCNJ3/HGIRK1). Genomics 39:279-288.
Schuldiner M, Collins SR, Weissman JS, Krogan NJ (2006) Quantitative genetic analysis in Saccharomyces cerevisiae using epistatic miniarray profiles (E-MAPs) and its application to chromatin functions. Methods 40:344-352.
Schuldiner M, Collins SR, Thompson NJ, Denic V, Bhamidipati A, Punna T, Ihmels J, Andrews B, Boone C, Greenblatt JF, Weissman JS, Krogan NJ (2005) Exploration of the function and organization of the yeast early secretory pathway through an epistatic miniarray profile. Cell 123:507-519.
Schwalbe RA, Bianchi L, Brown AM (1997) Mapping the kidney potassium channel ROMK1. Glycosylation of the pore signature sequence and the COOH terminus. J Biol Chem 272:25217-25223.
Schwalbe RA, Wang Z, Wible BA, Brown AM (1995) Potassium channel structure and function as reported by a single glycosylation sequon. J Biol Chem 270:15336-15340.
Schwalbe RA, Rudin A, Xia SL, Wingo CS (2002) Site-directed glycosylation tagging of functional Kir2.1 reveals that the putative pore-forming segment is extracellular. J Biol Chem 277:24382-24389.
Schwanstecher C, Meyer U, Schwanstecher M (2002) K(IR)6.2 polymorphism predisposes to type 2 diabetes by inducing overactivity of pancreatic beta-cell ATP-sensitive K(+) channels. Diabetes 51:875-879.
Schwappach B, Zerangue N, Jan YN, Jan LY (2000) Molecular basis for K(ATP) assembly: transmembrane interactions mediate association of a K+ channel with an ABC transporter. Neuron 26:155-167.
Sentenac H, Bonneaud N, Minet M, Lacroute F, Salmon JM, Gaymard F, Grignon C (1992) Cloning and expression in yeast of a plant potassium ion transport system. Science 256:663-665.
Serrano R, Rodriguez-Navarro A (2001) Ion homeostasis during salt stress in plants. Curr Opin Cell Biol 13:399-404.
Shikano S, Coblitz B, Sun H, Li M (2005) Genetic isolation of transport signals directing cell surface expression. Nat Cell Biol 7:985-992.
Shimoni Y, Schekman R (2002) Vesicle budding from endoplasmic reticulum. Methods Enzymol 351:258-278.

Shuck ME, Bock JH, Benjamin CW, Tsai TD, Lee KS, Slightom JL, Bienkowski MJ (1994) Cloning and characterization of multiple forms of the human kidney ROM-K potassium channel. J Biol Chem 269:24261-24270.
Simons K, Ikonen E (1997) Functional rafts in cell membranes. Nature 387:569-572.
Simons K, Vaz WL (2004) Model systems, lipid rafts, and cell membranes. Annu Rev Biophys Biomol Struct 33:269-295.
Slesinger PA, Patil N, Liao YJ, Jan YN, Jan LY, Cox DR (1996) Functional effects of the mouse weaver mutation on G protein-gated inwardly rectifying K+ channels. Neuron 16:321-331.
Springer S, Chen E, Duden R, Marzioch M, Rowley A, Hamamoto S, Merchant S, Schekman R (2000) The p24 proteins are not essential for vesicular transport in Saccharomyces cerevisiae. Proc Natl Acad Sci U S A 97:4034-4039.
Stevens EB, Woodward R, Ho IH, Murrell-Lagnado R (1997) Identification of regions that regulate the expression and activity of G protein-gated inward rectifier K+ channels in Xenopus oocytes. J Physiol 503 (Pt 3):547-562.
Stockklausner C, Klocker N (2003) Surface expression of inward rectifier potassium channels is controlled by selective Golgi export. J Biol Chem 278:17000-17005.
Stockklausner C, Ludwig J, Ruppersberg JP, Klocker N (2001) A sequence motif responsible for ER export and surface expression of Kir2.0 inward rectifier K(+) channels. FEBS Lett 493:129-133.
Sun H, Shikano S, Xiong Q, Li M (2004) Function recovery after chemobleaching (FRAC): evidence for activity silent membrane receptors on cell surface. Proc Natl Acad Sci U S A 101:16964-16969.
Tanaka S, Maeda Y, Tashima Y, Kinoshita T (2004) Inositol deacylation of glycosylphosphatidylinositol-anchored proteins is mediated by mammalian PGAP1 and yeast Bst1p. J Biol Chem 279:14256-14263.
Tanemoto M, Fujita A, Higashi K, Kurachi Y (2002) PSD-95 mediates formation of a functional homomeric Kir5.1 channel in the brain. Neuron 34:387-397.
Tang W, Ruknudin A, Yang WP, Shaw SY, Knickerbocker A, Kurtz S (1995) Functional expression of a vertebrate inwardly rectifying K+ channel in yeast. Mol Biol Cell 6:1231-1240.
Tang XD, Santarelli LC, Heinemann SH, Hoshi T (2004) Metabolic regulation of potassium channels. Annu Rev Physiol 66:131-159.
Tikku S, Epshtein Y, Collins H, Travis AJ, Rothblat GH, Levitan I (2007) Relationship between Kir2.1/Kir2.3 activity and their distributions between cholesterol-rich and cholesterol-poor membrane domains. Am J Physiol Cell Physiol 293:C440-450.
Tinker A (2002) The assembly and targeting of potassium channels. In: Receptor and Ion-Channel Trafficking: Cell Biology of Ligand-Gated and Voltage-Sensitive Ion Channels (Moss S, Henley J, eds), pp 28-57. Oxford: Oxford University Press.

Tinker A, Jan LY (1999) Chapter 9: The Assembly of Inwardly Rectifying Potassium Channels. Current Topics in Membranes 46:143-158.
Tinker A, Jan YN, Jan LY (1996) Regions responsible for the assembly of inwardly rectifying potassium channels. Cell 87:857-868.
Tong AH, Evangelista M, Parsons AB, Xu H, Bader GD, Page N, Robinson M, Raghibizadeh S, Hogue CW, Bussey H, Andrews B, Tyers M, Boone C (2001) Systematic genetic analysis with ordered arrays of yeast deletion mutants. Science 294:2364-2368.
Tong AH, Lesage G, Bader GD, Ding H, Xu H, Xin X, Young J, Berriz GF, Brost RL, Chang M, Chen Y, Cheng X, Chua G, Friesen H, Goldberg DS, Haynes J, Humphries C, He G, Hussein S, Ke L, Krogan N, Li Z, Levinson JN, Lu H, Menard P, Munyana C, Parsons AB, Ryan O, Tonikian R, Roberts T, Sdicu AM, Shapiro J, Sheikh B, Suter B, Wong SL, Zhang LV, Zhu H, Burd CG, Munro S, Sander C, Rine J, Greenblatt J, Peter M, Bretscher A, Bell G, Roth FP, Brown GW, Andrews B, Bussey H, Boone C (2004) Global mapping of the yeast genetic interaction network. Science 303:808-813.
Topert C, Doring F, Wischmeyer E, Karschin C, Brockhaus J, Ballanyi K, Derst C, Karschin A (1998) Kir2.4: a novel K+ inward rectifier channel associated with motoneurons of cranial nerve nuclei. J Neurosci 18:4096-4105.
Toulmay A, Schneiter R (2007) Lipid-dependent surface transport of the proton pumping ATPase: a model to study plasma membrane biogenesis in yeast. Biochimie 89:249-254.
Treco DA, Lundblad V (1993) Basic techniques of yeast genetics. Current Protocols in Molecular Biolog, 1311-1317.
Tu L, Wang J, Helm A, Skach WR, Deutsch C (2000) Transmembrane biogenesis of Kv1.3. Biochemistry 39:824-836.
Tucker SJ, Bond CT, Herson P, Pessia M, Adelman JP (1996) Inhibitory interactions between two inward rectifier K+ channel subunits mediated by the transmembrane domains. J Biol Chem 271:5866-5870.
Uemura S, Kihara A, Inokuchi J, Igarashi Y (2003) Csg1p and newly identified Csh1p function in mannosylinositol phosphorylceramide synthesis by interacting with Csg2p. J Biol Chem 278:45049-45055.
Uemura S, Kihara A, Iwaki S, Inokuchi J, Igarashi Y (2007) Regulation of the transport and protein levels of the inositol phosphorylceramide mannosyltransferases Csg1 and Csh1 by the Ca2+-binding protein Csg2. J Biol Chem 282:8613-8621.
Umigai N, Sato Y, Mizutani A, Utsumi T, Sakaguchi M, Uozumi N (2003) Topogenesis of two transmembrane type K+ channels, Kir 2.1 and KcsA. J Biol Chem 278:40373-40384.
Uozumi N, Gassmann W, Cao Y, Schroeder JI (1995) Identification of strong modifications in cation selectivity in an Arabidopsis inward rectifying

potassium channel by mutant selection in yeast. J Biol Chem 270:24276-24281.
Valiyaveetil FI, Zhou Y, MacKinnon R (2002) Lipids in the structure, folding, and function of the KcsA K+ channel. Biochemistry 41:10771-10777.
Vallejo CG, Serrano R (1989) Physiology of mutants with reduced expression of plasma membrane H+-ATPase. Yeast 5:307-319.
Vashist S, Kim W, Belden WJ, Spear ED, Barlowe C, Ng DT (2001) Distinct retrieval and retention mechanisms are required for the quality control of endoplasmic reticulum protein folding. J Cell Biol 155:355-368.
Warringer J, Ericson E, Fernandez L, Nerman O, Blomberg A (2003) High-resolution yeast phenomics resolves different physiological features in the saline response. Proc Natl Acad Sci U S A 100:15724-15729.
Wei J, Hodes ME, Piva R, Feng Y, Wang Y, Ghetti B, Dlouhy SR (1998) Characterization of murine Girk2 transcript isoforms: structure and differential expression. Genomics 51:379-390.
Wickman K, Nemec J, Gendler SJ, Clapham DE (1998) Abnormal heart rate regulation in GIRK4 knockout mice. Neuron 20:103-114.
Woodward R, Stevens EB, Murrell-Lagnado RD (1997) Molecular determinants for assembly of G-protein-activated inwardly rectifying K+ channels. J Biol Chem 272:10823-10830.
Yang J, Yu M, Jan YN, Jan LY (1997) Stabilization of ion selectivity filter by pore loop ion pairs in an inwardly rectifying potassium channel. Proc Natl Acad Sci U S A 94:1568-1572.
Yi BA, Lin YF, Jan YN, Jan LY (2001) Yeast screen for constitutively active mutant G protein-activated potassium channels. Neuron 29:657-667.
Yoo D, Fang L, Mason A, Kim BY, Welling PA (2005) A phosphorylation-dependent export structure in ROMK (Kir 1.1) channel overrides an endoplasmic reticulum localization signal. J Biol Chem 280:35281-35289.
Yoo D, Flagg TP, Olsen O, Raghuram V, Foskett JK, Welling PA (2004) Assembly and trafficking of a multiprotein ROMK (Kir 1.1) channel complex by PDZ interactions. J Biol Chem 279:6863-6873.
Yoo D, Kim BY, Campo C, Nance L, King A, Maouyo D, Welling PA (2003) Cell surface expression of the ROMK (Kir 1.1) channel is regulated by the aldosterone-induced kinase, SGK-1, and protein kinase A. J Biol Chem 278:23066-23075.
Yuan H, Michelsen K, Schwappach B (2003) 14-3-3 dimers probe the assembly status of multimeric membrane proteins. Curr Biol 13:638-646.
Zaritsky JJ, Eckman DM, Wellman GC, Nelson MT, Schwarz TL (2000) Targeted disruption of Kir2.1 and Kir2.2 genes reveals the essential role of the inwardly rectifying K(+) current in K(+)-mediated vasodilation. Circ Res 87:160-166.
Zerangue N, Schwappach B, Jan YN, Jan LY (1999) A new ER trafficking signal regulates the subunit stoichiometry of plasma membrane K(ATP) channels. Neuron 22:537-548.

Zerangue N, Malan MJ, Fried SR, Dazin PF, Jan YN, Jan LY, Schwappach B (2001) Analysis of endoplasmic reticulum trafficking signals by combinatorial screening in mammalian cells. Proc Natl Acad Sci U S A 98:2431-2436.

Publishing Agreement

It is the policy of the University to encourage the distribution of all theses and dissertations. Copies of all UCSF theses and dissertations will be routed to the library via the Graduate Division. The library will make all theses and dissertations accessible to the public and will preserve these to the best of their abilities, in perpetuity.

Please sign the following statement:

I hereby grant permission to the Graduate Division of the University of California, San Francisco to release copies of my thesis or dissertation to the Campus Library to provide access and preservation, in whole or in part, in perpetuity.

9/27/07

Author Signature | Date